HEATING AND DRYING PEANUTS WITH
RADIO-FREQUENCY ENERGY

By

MALCOLM E. WRIGHT

Bachelor of Science
Louisiana State University
Baton Rouge, Louisiana
1957

Master of Science
Louisiana State University
Baton Rouge, Louisiana
1966

Submitted to the Faculty of the Graduate College
of the Oklahoma State University
in partial fulfillment of the requirements
for the Degree of
DOCTOR OF PHILOSOPHY
May, 1970

HEATING AND DRYING PEANUTS WITH

RADIO-FREQUENCY ENERGY

Thesis Approved:

Jay G Porterfield

Thesis Adviser

Ralph S. Matlock

J. A. Wiebelt

N. Durham

Dean of the Graduate College

ACKNOWLEDGMENTS

The research reported in this study was partially supported by funds from the Oklahoma Peanut Research Foundation. This support is appreciated.

I am grateful to my major adviser, Professor Jay Porterfield, for his guidance and encouragement, but more especially for giving me a new appreciation of originality in problem solving.

I would like to thank the other members of my advisory committee, Dr. Gordon Nelson who is now Head of the Agricultural Engineering Department at the Ohio State University; Dr. John Wiebelt of the Mechanical Engineering Department; and Dr. Ralph Matlock of the Agronomy Department for their advice, criticism and instruction.

Appreciation is extended to Professor E. W. Schroeder, Head of the Agricultural Engineering Department, for providing facilities, personal financial support and a working atmosphere most conducive to research and study.

The skill and patience of Mr. Clyde Skoch, Mr. Norvil Cole, and Mr. Jesse Hoisington of the Agricultural Engineering Laboratory, Mr. Jack Fryrear and Mr. Don McCracken, draftsmen, is to be commended.

Finally, very special thanks to my wife, Martha, for her encouragement and patience throughout this course of study.

TABLE OF CONTENTS

LIST OF TABLES

LIST OF FIGURES

Figure | Page

CHAPTER I

INTRODUCTION

Background Information

Food producers in the United States have been forced to mechanize many phases of their operations in recent years due to a declining labor force in agricultural areas. Mechanization has assured a continuing abundance of food, but has also introduced many problems. These include quality control, overloading of processing facilities, higher costs, and others. Bulk handling, for instance, has enabled a relatively small number of workers to process large quantities of food materials, but has also introduced the potential of bulk spoilage. The amount of labor available for food processing is not likely to increase in the future. The alternative, then, is to refine our mechanization processes without losing production capability.

The initial processing or "curing" of peanuts after harvest is an example of the changes brought about by mechanization of a food producing process. Formerly, when time and labor were not at a premium, this process was accomplished by stacking the freshly dug vines with peanuts attached around upright poles in the field and allowing time to dry or "cure" naturally over a period of weeks. The peanuts were then removed from the vines and stored or further processed.

Today the curing process consists of digging the peanuts, shaking the soil from them and placing them in windrows where some curing and drying take place in a three to seven day period. At the end of this period the peanuts are removed from the vines by combines and the curing process completed in batch type, forced air dryers that provide heat as needed. This system eliminates some obvious weather hazards, but introduces new problems in maintaining quality during the artificial drying period.

The quality of the peanut that finally reaches the consumer is the result of many factors. These include varietal characteristics, growing conditions, processing beyond the curing stage and others. The quality characteristics most influenced by curing methods are: taste, texture (hardness) and milling quality (amount of skin slippage, splits and cracks). Following is a partial list of researchers who have studied the effect of curing techniques on the above qualities and associated problems: L. Aristizabal, E. E. Burns and O. R. Kunze (2), E. O. Beasley (4) (5) (36), J. W. Dickens (4) (5) (29) (50), S. R. Cecil (12), H. A. Kramer (25), H. E. Pattee and J. A. Singleton (36), D. Sharon (42), W. Chaffin (13), R. S. Hutchinson (21) (55), W. T. Mills (29), T. B. Whitaker (50), J. D. Woodward and J. I. Davidson (55), and R. U. Schenk (38), (39). A brief summary of this work is itemized below:

1. Off-flavor increases as temperature in the drying process increases and as the length of exposure to high temperatures increases.
2. Off-flavor as a result of elevated drying temperatures is more pronounced in immature kernels than mature ones.
3. The chemical compounds that produce off-flavor are present in all kernels but appear in increased

quantities in those dryed at elevated temperatures.

4. Very low drying temperatures, (freeze-drying), tend to produce bland flavors.
5. The effect of drying rate on flavor has not yet been clearly separated from temperature effects. Some investigators have reported bland flavors resulting from rapid drying rates; others have reported no effects on flavor due to drying rate.
6. Rapid drying rates tend to produce kernels with hardened outer layers, an increase in skin slippage and an increase in split or cracked kernels.
7. The gas exchange rate for several gases is decreased in kernels having a hardened outer layer. One exception to this is water vapor which does not appear to be affected.
8. Overdrying tends to increase milling damage, i.e. skin slippage, split and cracked kernels.

Flavor and maturity evaluations in the above research were results of subjective tests, but the preponderance of data indicates that they are fairly consistent. Flavor was evaluated by organoleptic panels and maturity by the color of the inside of the peanut hull. Mature peanuts usually have a dark brown inner hull color the source of which is described by Schenk (39).

The results noted above have led to recommended practices for drying peanuts in batches with forced air. These recommendations are:

1. Air temperature should not exceed 95°F.
2. Heat should be added to the drying air only if the relative humidity is above 65%.
3. Maximum air flow rates should be about 24 cfm per square foot of bin crossectional area perpendicular to the air flow. Flow rates above this amount have little effect on drying rates.
4. Peanuts should be dried to a minimum moisture content of about 9%, wet basis.

Three disadvantages of a forced air system operated according to the above recommendations are:

1. The maximum rate of moisture removal is limited.
2. Drying must proceed from the surface of the peanut inward resulting in uneven drying and increased chances for kernel surface hardening, splits and cracks.
3. All peanuts in a batch are subjected to the same environment regardless of their individual needs.

The use of radio-frequency or dielectric heating could be a means of overcoming these disadvantages. An object of dielectric material placed in a radio-frequency field tends to absorb power throughout and this power is converted to heat. This internal energy generation establishes positive temperature gradients from the surface inward that tend to produce similar moisture driving potentials in moist, hygroscopic materials. It is hypothesized that a peanut heated internally by a radio-frequency field and surrounded by a flowing air stream would dry more rapidly and evenly than one subjected only to heated air. Evenness of drying within the peanut kernel might alleviate some problems due to surface hardening. These include stress buildups that result in skin slippage, splits and cracks and unfavorable gas exchange rates.

S. O. Nelson (31), Solderholm (45), Wratten (56), Whitney and Porterfield (52) (53), and others who have determined the dielectric characteristics of many agricultural products, including peanuts, show that the potential for power absorption increases with increasing moisture content. This implies that the wettest peanuts in a batch at the initiation of drying in a radio-frequency field would absorb the most power. This would result in a more uniform distribution of moisture in the batch at the end of the drying period. Conceivably, a forced air system using a radio-frequency field as an energy source could be designed that would increase the drying rate of peanuts over the conventional warm air system with the added possibility of improving the quality of the final product.

Statement of Objectives

The preceding background information indicates a number of specific areas that could be studied. The following two objectives were selected for this study based on the overall problem, the review of literature in the following chapter, and available equipment.

1. Determine the power absorption of peanuts in a radio-frequency field of fixed frequency as a function of moisture content, volume of peanuts per volume of heating chamber, an average characteristic

length of the peanuts parallel to the electric field and the electric field strength.

2. Develop a prediction equation for the rate of drying peanuts in a model of a conventional, batch-type, forced air drying system based on the initial moisture content of the peanuts, the conditions of the incoming air and the power absorption from a radio-frequency field impressed on the sample.

CHAPTER II

LITERATURE REVIEW

Two major areas of literature review are suggested by an overall view of the problem and the specific objectives. They are: power absorption by non-conductors in a radio-frequency field, and simultaneous heat and mass transfer in hygroscopic materials. A massive amount of literature is available in both of these areas. Sufficient material in each area is reviewed here to demonstrate the method of selecting the pertinent quantities needed to achieve the problem objectives.

Power Absorption by Non-Conductors in a Radio-Frequency Field

Theoretical Considerations

The micro-physics of power absorption, (dielectric heating), of a biological material in a radio-frequency field is very complicated. Solderholm (45) and Thompson and Zachariah (49) discuss the factors believed to contribute to heat generation in a biological dielectric material. These include electronic, atomic, ionic and molecular polarizations. Each of these types of polarizations occur as the result of a changed particle attempting to align itself with an alternating electric field.

Relaxation time for a particle is defined as the time required for its polarization to reach 1/e times its original value. The amount of energy appearing in the form of heat is a function of the resistance to particle rotation. Since the relaxation times for electrons and atoms are very small compared to typical radio-frequencies the contribution to the dielectric properties of the material from this source is fairly constant up to frequencies approaching the infrared region. The major contributions to dielectric properties of a material subjected to radio-frequencies comes from the ionic and molecular polarizations whose relaxation times are on the order of these frequencies. Ionic polarizations occur at the interfaces of components having dissimilar dielectric properties in a heterogeneous material.

Thompson and Zachariah also discuss the effects of directional current flow in biological cells and bound and free water on dielectric properties.

The discussion so far points up the importance moisture content and frequency would have on dielectric heating. The following discussion, based on classical macro-dielectric theory, is intended to show the necessity for considering bulk dielectric properties, size, shape, and packing density. The material is drawn from an excellent text by Brown, Hoyler and Bierwirth (9) and a concise review of elementary dielectric theory by S. O. Nelson (31).

The model taken for a centimeter cube of dielectric material in a radio-frequency field is shown in Figure 1. The cube is assumed to have a good electrical conductor on the faces to which the electrodes are attached and edge effects are negligible. A model for the complex admittance for this cube is shown in Figure 2.

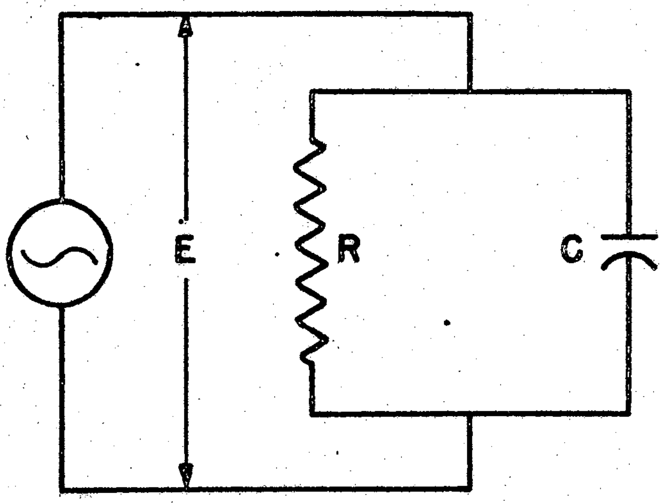

Figure 1. Model of a Centimeter Cube of Dielectric Material

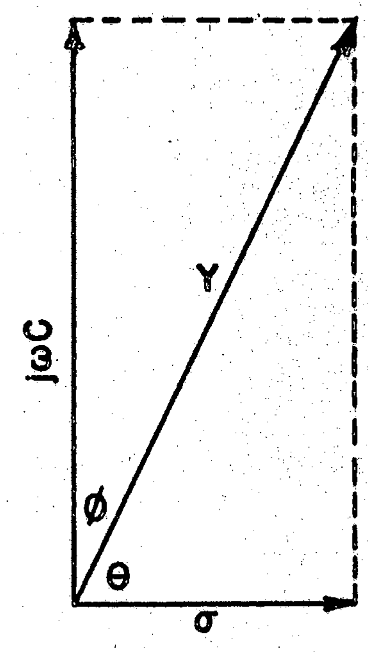

Figure 2. Complex Admittance of Dielectric Cube

In Figures 1 and 2:

E = Field strength, volts/cm.

R = Resistance, ohms.

C = Capacitance, farads.

$\omega = 2\Pi f$.

f = Frequency, cycles/sec.

$\sigma = 1/R$, conductivity, mhos/cm.

The complex admittance may be expressed as:

$$Y = \sigma + j\omega C \tag{1}$$

but:

$$C = \varepsilon\varepsilon_o \tag{2}$$

where:

ε = The dielectric constant of the material, dimensionless.

ε_o = The dielectric constant of free space, 8.85 X 10^{-14} farads/cm.

Substituting:

$$Y = \sigma + j\omega\varepsilon\varepsilon_o \tag{3}$$

Now the total current flow is:

$$I_t = EY = E(\sigma + j\omega\varepsilon\varepsilon_o) \tag{4}$$

The power loss in the material is:

$$P = E\ I_t \cos\Theta \tag{5}$$

or:

$$P = E\ I_R = E\ \frac{E}{R} = E^2\sigma \tag{6}$$

where:

I_R = Current flow through resistor, amps.

P = Power loss in watts/cm^3.

Now $\cos\Theta$ is the power factor, p , for the material and:

$$\cos\Theta = p = \frac{\sigma}{\sqrt{\sigma^2 + |j^{\omega\varepsilon\varepsilon_o}|^2}} = \frac{\sigma}{\sqrt{\sigma^2 + (\omega\varepsilon\varepsilon_o)^2}} \tag{7}$$

And if σ is very small:

$$p \simeq \frac{\sigma}{\omega\varepsilon\varepsilon_o} = \tan\Phi \tag{8}$$

The $\tan\phi$ is often reported in the literature as the "loss tangent" of a dielectric material.

Finally by rearranging equation (8) and substituting for in equation (6) power loss may be expressed as:

$$P = \omega\varepsilon\varepsilon_o\, pE^2 = 2\Pi f\varepsilon\varepsilon_o\, pE^2 \tag{9}$$

Equation (9) may be used to calculate the power loss in a homogeneous dielectric if the dielectric constant ε, the power factor, p, and the field strength E are known.

Brown, Hoyler and Bierwirth present two other developments that will demonstrate the need to consider the size, shape and packing arrangements of particles in a radio-frequency field. The first is concerned with the radial distribution of the electrical field intensity, E, in a cylinder of dielectric material whose ends are placed between two conducting electrodes. The relationship they develop is:

$$\frac{d^2E}{dr^2} + \frac{1}{r}\frac{dE}{dr} + E(\,j\omega\mu(\sigma + j\omega\varepsilon\varepsilon_o)) = 0 \tag{10}$$

where:

r = Any radius of the cylinder, cm.

μ = Permeability of the cylinder material, newtons/ amp^2.

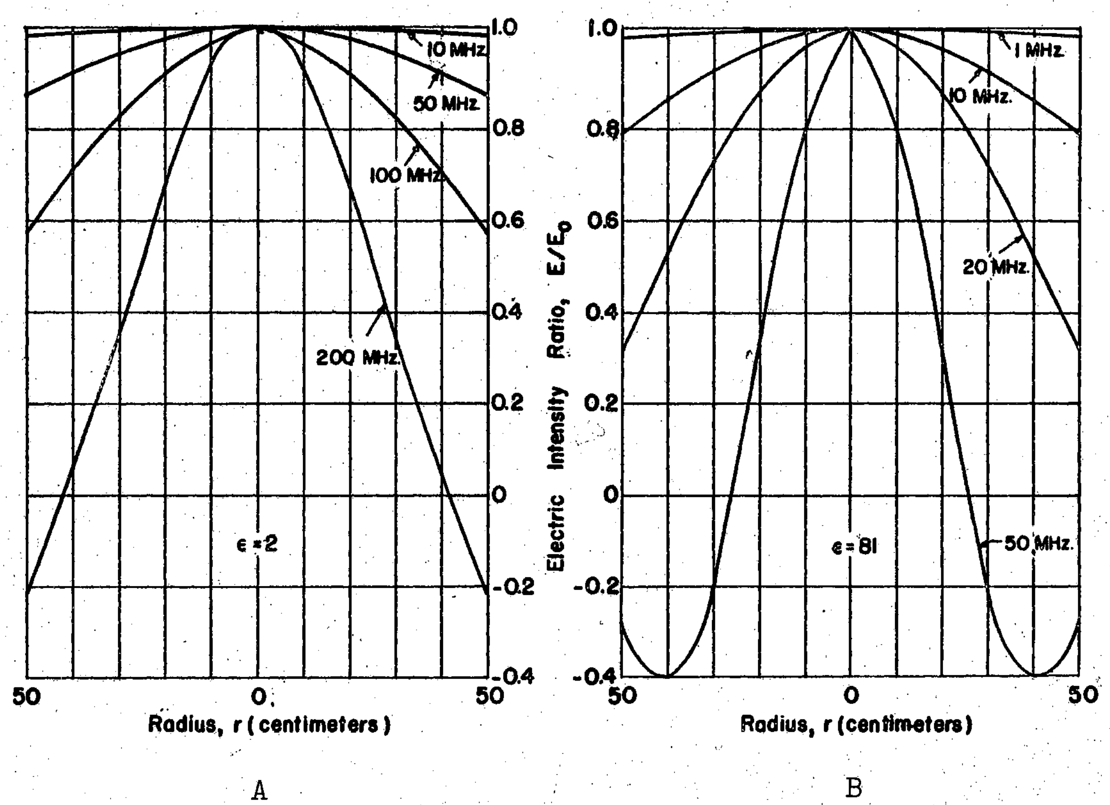

Figure 3. Electric Field Strength Distribution in Dielectric Cylinders at Several Frequencies. (Taken from Brown, Hoyler and Bierwirth (9)).

Figures 3A and 3B show the solution of equation (10) in vertical crossection for cylinders with respective dielectric constants of 2 and 81. E_o in these solutions represents the electric field intensity along the cylinder centerline.

The second development is concerned with the distortion of an initially uniform electric field by a dielectric cylinder placed in it with its axis perpendicular to the field. Figure 4 pictures the situation described by the following two equations:

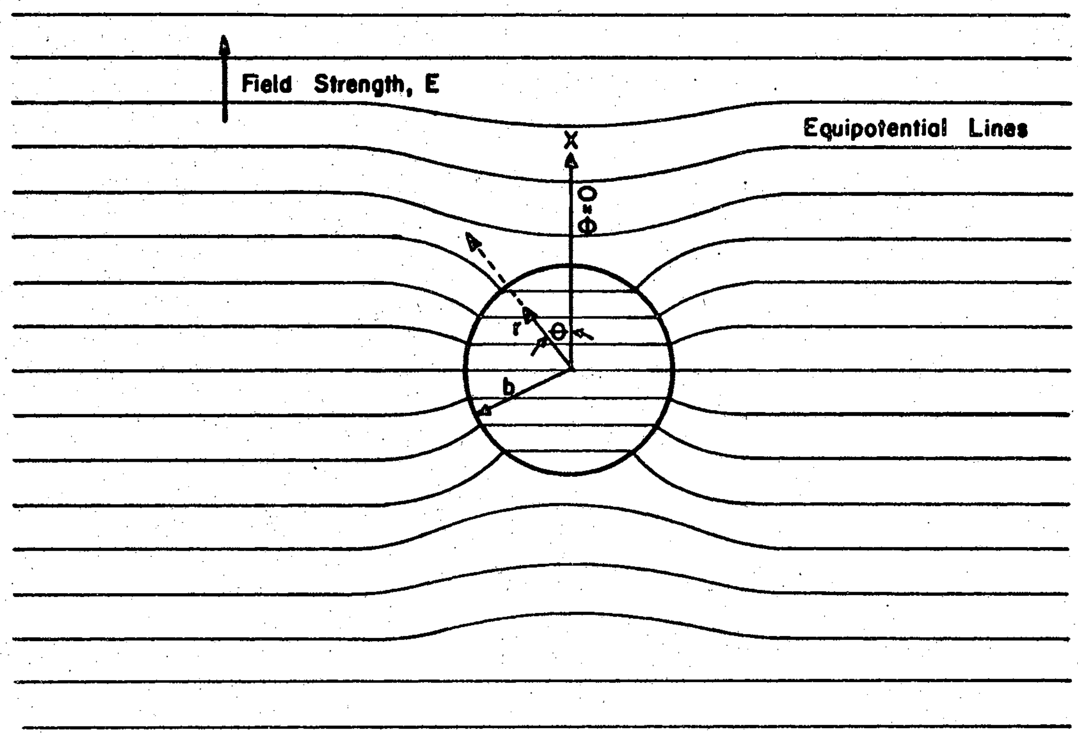

Figure 4. Distortion of an Initially Uniform Electric Field by a Cylindrical Dielectric.

$$V_o = E\left(r - \frac{\varepsilon - 1}{\varepsilon + 1}\frac{b^2}{r}\right)\cos\theta \qquad (11)$$

$$V_i = \frac{2E}{\varepsilon + 1}\, r\cos\theta \qquad (12)$$

where:

V_o = Potential outside the cylinder with respect to the cylinder axis, volts.

V_i = Potential inside the cylinder with respect to the axis, volts.

E = Field intensity, volts/cm.

θ = Angle of direction.

b = Radius of cylinder, cm.

r = Distance from origin, cm.

ε = Dielectric constant of the cylinder.

Equations (11) and (12) are solutions to the differential equation for the electric field when the electrode spacing is large compared to the radius, b, of the cylinder. Note that the field strength within the dielectric is constant since from equation (12):

$r \cos\Theta = x$

So:

$$V_i = \frac{2E}{\varepsilon + 1} x$$

and:

$$\frac{dV_i}{dx} = \frac{2E}{\varepsilon + 1}$$

An electrode near the cylinder would form a flat equipotential surface resulting in a distorted field within the cylinder and uneven power absorption. The effect of multiple cylinders in the same field can be visualized assuming that superposition holds. The field strength within each cylinder would be affected by the size and spacing of adjacent ones.

Some Dielectric Experiments

A good example of the dielectric heating of a homogeneous solid is provided by Buckham and Stuelpnagel (10). They studied the heating rate of lucite plastic in a radio-frequency field and found good correlation between the power absorbed as calculated by the dielectric properties and the heating rate calculated from the thermal properties of the material.

Research with non-hygroscopic granular materials has produced some insight into the effects of particle size on rate of heating and the effect of air velocities on rate of drying in a radio-frequency field. Schutz and McMahon (41) determined that the loss factor, p, and the heating rate of sand grains increased in proportion to particle size. Mann, Ceaglske and Olson (27) obtained similar increases in the rate of drying of wet sands as a function of particle size. They further determined that increasing the air velocity over the heated sample above a certain value decreased the drying rate if the air temperature was below that of the sample. They attributed this to the breakdown of the surface heat transfer film as velocity increased. This resulted in a heat loss from the sample to the air that would have otherwise been absorbed by evaporation of the moisture.

Brown, Hoyler and Bierwirth (9) developed a method for determining the dielectric properties of liquids. They built a coaxial capacitor in which the top end was open and the bottom sealed by an annulus of polystyrene plastic between the inner and outer electrodes. This capacitor was used with a coil in a series resonant circuit attached to a Q-meter. The technique consisted of first measuring the capacity and Q, (quality), of the circuit with a small amount of liquid in the capacitor to minimize edge effects. Next, a known volume of liquid was added and the measurements repeated. The differences in capacity, Q, and filled depth were then used in the equations for coaxial capacitors to obtain dielectric constants and loss factors.

Wratten (57) was apparently the first to apply this method to determine the dielectric properties of a granular hygroscopic material, (rice). He found that the dielectric constant and power factor generally increased with increasing moisture content, but were only slightly affected by frequency in the 5 to 40 megahertz range. Conductivity, however, increased with both increasing moisture content and frequency. He observed in subsequent heating tests that the temperature measured by an alcohol thermometer of a sample of rice subjected to a radio-frequency field continued to increase for approximately two minutes after the power had been turned off. This indicates that positive temperature gradients from the surface of the individual grains inward were developed during the heating process.

S. O. Nelson (31) improved Brown, Hoyler and Bierwirth's method of making dielectric measurements by adding a small variable vernier capacitor in parallel with the coaxial test cylinder and describing a technique for its use. Nelson and his associates have contributed the bulk of the available dielectric property data for agricultural products. Evidence of this is contained in the Agricultural Engineers Yearbook, 1969 (1). Their results are similar to those observed by Wratten for rice. Typical dielectric constants for agricultural products will range from 2.0 to 8.0 increasing with moisture content and decreasing slightly with frequency. Loss tangents behave similarly with values in the range of 0.05 to 0.30. Conductivity increases with both moisture content and frequency. Typical values are in the range of 2.0 to 30.0 micro-mhos/cm.

A few references indicating the scope and accomplishments of S. O. Nelson and researchers who have been associated with him are listed in the bibliography, (31) (32) (33) (34) (48). These include work by Solderholm (45) (46) and Nelson and Whitney (34) on controlling insect infestation in stored grain. They showed that 100% mortality of certain weevils and beetles in wheat could be obtained by the differential heating effect of dissimilar dielectrics in a radio-frequency field without reducing the germination of the wheat.

Whitney and Porterfield (52) (53) determined the dielectric properties of whole peanuts, kernels and shells using the methods developed by S. O. Nelson. Following is a list of expressions they developed for dielectric properties:

Whole Peanuts:

$$\varepsilon = 1.025 - 0.008\ f + 0.086\ m \tag{13}$$

Kernels:

$$\varepsilon = 3.153 - 0.049\ f + 0.136\ m \tag{14}$$

$$\tan\Phi = 0.185 + 0.0016\ f + 0.0024\ m \tag{15}$$

Layers of kernels separated by paper disks to simulate kernel distribution in whole peanuts:

$$\varepsilon = 1.419 = 0.005\ f + 0.045\ m \tag{16}$$

$$\tan\phi = 0.138 + 0.0012\ f + 0.0011\ m \tag{17}$$

Shells:

$$\varepsilon = 0.501 - 0.003\ f + 0.063\ m \tag{18}$$

$$\tan\phi = 0.030 - 0.034\ f + 0.023\ m \tag{19}$$

where:

f = Frequency, MHz.

m = Moisture content, % wet basis.

No expression for loss tangent of whole peanuts was presented due to low correlation of the data. Correlation coefficients were low for the loss tangents of kernels and shells. This may be due in part to the small slopes of the loss tangent curves. High correlation coefficients are inherently difficult to obtain for "flat" curves.

Unpublished data for whole peanuts at 25 MHz is presented below:

Moisture Content % Wet Basis	Dielectric Constant ε	Loss Tangent $\tan\Phi$
12.0	1.84	0.13
14.6	1.93	0.16
19.2	2.08	0.17
24.5	2.58	0.17
30.9	2.92	0.27

Simultaneous Heat and Mass Transfer in Porous Hygroscopic Solids

Theoretical Considerations

The mechanism for heat or mass movement in a body is generally accepted to be diffusion. Derivations and solutions of the generalized heat and mass transfer equations (22) and (23), from Fourier's law, equation (20), and Fick's law, equation (21), are presented in many texts including Arpaci (3), Schneider (40), Carslaw and Jaeger (11).

$$\mathring{q} = -KA\,\frac{dT}{dr} \tag{20}$$

$$\mathring{m} = -\beta\frac{dC}{dr} \tag{21}$$

$$\frac{\partial T}{\partial t} = \alpha\nabla^2 T + \frac{\mathring{Q}}{\rho c} \tag{22}$$

$$\frac{\partial C}{\partial t} = \beta\nabla^2 C \tag{23}$$

where:

$\mathring{q}$ = Rate of heat transfer.

K = Thermal conductivity.

A = Crossectional area.

T = Temperature.

r = Space coordinate.

$\mathring{m}$ = Rate of mass transfer.

β = Mass diffusion coefficient.

C = Mass concentration.

$\alpha = \frac{K}{\rho c}$ = Heat diffusion coefficient.

t = Time.

$\mathring{Q}$ = Rate of internal energy generation per unit volume.

ρ = Mass density.

c = Material specific heat.

Typical boundary and initial conditions for equations (22) and (23) are:

$$T_i \text{ or } C_i = f(r) \tag{24}$$

$$\mathring{q}_s = -KA\frac{\partial T_s}{\partial r} = -h_t A(T_s - T_\infty) \tag{25}$$

$$\mathring{m}_s = -\beta\frac{\partial C_s}{\partial r} = -h_m A(C_s - C_\infty) \tag{26}$$

where:

Subscript i = Initial conditions.

Subscript s = Surface conditions.

Subscript ∞ = Conditions at some distance away from the surface.

$f(r)$ = A function of the space coordinates.

h_t, h_m = Heat and mass transfer coefficients, respectively, at the surface.

The solutions for equations (22) and (23) for standard shapes made of homogeneous materials are tabulated in many references. Various methods have been devised to overcome the problem of irregular shapes. For example, Kinch and Stoutenberg (24) assumed cylindrical or spherical shapes in determining the thermal diffusivity of large fruits. Smith, G. L. Nelson and Henrickson (43) (44) recognized the similarity in the solutions of equation (22) for spheres, infinite sylinders and infinite slabs. They developed a method of obtaining a geometry index to use in a simplified solution of transient heat flow in ellipsoids based on this similarity. Consistent results were obtained in determining the thermal diffusivity of hams by using this approach and estimating their shape to be ellipsoids with orthogonal crossectional areas equivalent to the hams. Solutions for irregular shapes could, of course, be obtained by numerical methods with the other parameters known. No such work on agricultural products, however, was discovered in making this review.

A more important problem than consideration of shape is that of the interaction of temperature and moisture gradients. Whitney (51) and Matthes and Bowen (28) present ample evidence in their literature reviews that moisture transfer is influenced by thermal gradients. The amount of moisture transferred in a porous system under a thermal gradient is more than can accounted for by diffusion operating alone. Matthes and Bowen present a theoretical development followed by experimental evidence that results in the following equation:

$$J_v = -\beta \frac{dC}{dx} - L_{ve} \frac{d(\ln T)}{dx} \qquad (27)$$

where:

J_v = Water vapor flux in a soil sample.

β = Water vapor diffusivity under isothermal conditions.

T = Temperature.

C = Water vapor concentration.

L_{ve} = A coefficient describing the effect of a thermal gradient on the vapor flux.

The quantity, L_{ve}, is called a coupling coefficient. Experimental results of this work showed that the second term in equation (27) contributed more to the total water vapor flux, J_v, than the diffusivity term.

A porous system that is also hygroscopic presents additional problems. Many models based on variations of the diffusion equations have been presented. Henderson and Perry (20) state that moisture movement is by liquid diffusion only, but admit that the diffusion coefficient for many agricultural products is not a constant. Whitney (51), Whitney and Porterfield (54) and Young (59) assumed that liquid moisture movement was negligible in their models of an hygroscopic system. Chen and Johnson (15) (16) developed a quasi-analytical approach that lumped vapor and liquid flows and accounted for the effects of temperature and shrinkage.

The models of Whitney, Whitney and Porterfield, (equations (28), (29), and (30)), and Young are of particular importance here. Their solutions include the effects of internal energy generation and the coupling of the heat and mass diffusion equations by making use of the hygroscopic characteristics of the material.

For one-dimensional mass transfer:

$$\beta \frac{\partial^2 C}{\partial x^2} = \nu \frac{\partial C}{\partial t} + (1 - \nu)\, d_s \frac{\partial M}{\partial t} \qquad (28)$$

For one-dimensional heat transfer:

$$K \frac{\partial^2 T}{\partial x^2} = C_s \frac{d\,\partial T}{\partial t} - hd \frac{\partial M}{\partial t} - \overset{\circ}{Q} \qquad (29)$$

To describe the hygroscopic character of the material:

$$M = a + bC - cT \tag{30}$$

where:

ν = Void fraction.

d_s = Density of the soild material.

d = Bulk density.

M = Moisture content, lb H_2O per lb dry matter.

C_s = Specific heat of the solid.

h = Heat required to evaporate water into pore spaces.

a, b, c = Constants.

Young's equations differed slightly in that he separated the first term on the right hand side of equation (29) into two parts — one to account for the heat content of the water and the other to account for the heat content of the solid. Previous work by Young (60) and Young and Nelson (61) showed that the equilibrium moisture content of an hygroscopic material was not linear with moisture content and temperature. Equation (30), however, was assumed to be representative over much of the moisture content range. Young also assumed that diffusivity was a linear function of moisture content and temperature, and thermal conductivity a linear function of moisture content.

The simultaneous solutions of equations (28), (29), and (30) and Young's solutions demonstrated that for given initial and boundary conditions the rate of drying for an hygroscopic material is greater with internal energy generation than without. The moisture distribution after a given elapsed drying time is more uniform for the case of internal energy generation.

The solutions for the heat and mass transfer equations above were made by using arbitrary values for the moisture diffusivity and thermal conductivity and estimating the remaining constants from available data for peanuts.

Kazarain and Hall (23), Parker and Friesen (35), Wratten, et. al. (57), and others have used diffusion theory to determine the bulk thermal conductivity of several types of seeds. The analytical approach to internal heat and mass transfer in porous, hygroscopic solids, though not complete, seems to be well on its way to a universally acceptable solution. The major practical problem remaining appears to be the development of techniques to measure the heat and moisture diffusivities in undisturbed samples as small as a peanut or wheat grain.

Some Practical Drying Experiments

Three major models have been proposed for drying of granular hygroscopic materials with forced air in batches. These include the "thin layer" model, the "deep layer" model and a general model independent of the depth of the batch in the direction of air flow.

Henderson and Perry (20) described the thin layer model by equations (31) and (32), and a numerical method of extending it to deep layers.

$$\frac{dM}{dt} = a' \, (M - M_e) \qquad (31)$$

$$a' = V^n P_s \qquad (32)$$

where:

M = Average moisture content at any time, t.

M_e = Equilibrium moisture content for the material at the relative humidity of the incoming air.

V = Air flow rate.

P_s = Saturated vapor pressure at the temperature of the drying air.

a, n = Constants.

G. L. Nelson, Mahoney and Fryrear (30) used a generalized model developed by Nelson. This model is based on the variables affecting drying correlated by the Buckingham Pi theorem (26) into dimensionless parameters. The variables deemed pertinent for a batch grain dryer were:

E_a = Average drying effect in time, t, lbs. moisture removed per lb. of air circulated.

ΔM = Initial grain moisture content minus the equilibrium moisture content of the grain with the entering air.

T_e = Entering air temperature.

ΔT = $(T_e - T_1)$, Entering air temperature minus the leaving air temperature assuming a constant wet bulb drying process (See Figure 5).

t = Elapsed drying time.

V = Air circulation rate.

λ = Grain depth in the direction of air flow.

R = Hydraulic radius of grain bin perpendicular to the direction of air flow.

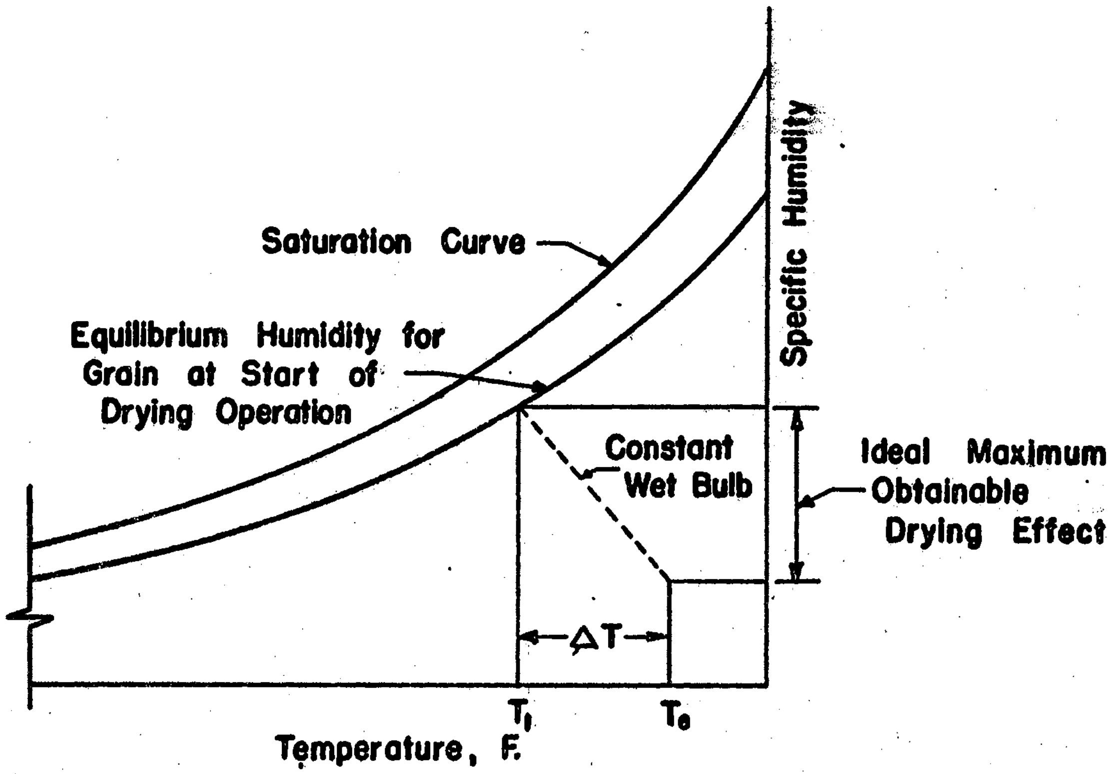

Figure 5. Skeleton Psychrometric Chart Showing Method of Obtaining the Variable, ΔT. (Taken from Nelson, Mahoney and Fryrear (30)).

ΔM and ΔT are indices of the maximum drying potential of the grain. ΔT also serves as an index of the temperature difference that will develop between the air and grain and affect the heat transfer at the surface of the grain particles. The air velocity, V, is also an index of the heat transfer from the grain to the air and is similarly an index of the moisture convection from the grain. The bed depth, λ, establishes the time that the air will be in contact with the grain and the hydraulic radius, R, accounts for edge effects.

These variables were combined into dimensionless quantities, (Π terms), as follows:

$\Pi_1 = E_a$, (dependent) $\Pi_4 = \lambda/Vt$

$\Pi_2 = \Delta M$ $\Pi_5 = R/\lambda$

$\Pi_3 = \Delta T/T_e$

The relationship developed among these Π terms for a constant size bin and grain depth, i.e. Π_5 held constant, was:

$$\Pi_1 = C_1\ (\Pi_2\Pi_3)^{C_2}\ (1.0 - e^{-C_3\Pi_4}) \tag{33}$$

This equation form was obtained by observing that Π_1 vs $\Pi_2\Pi_3$ with Π_4 held constant plotted as a straight line on log-log coordinates. The term containing Π_4 was assumed to fit the two limiting cases of first zero moisture removal per pound of air as the bed depth decreased to zero or the velocity and/or time became large and secondly the approach to a maximum moisture removal as bed depth increased or time and/or velocity approached zero.

Values of the constants obtained from data on wheat, sorghum, and rye for a small model dryer were:

$C_1 = 0.122$

$C_2 = 0.774$

$C_3 = 12{,}420.0$

Data from batch dryers in the field resulted in the following values for the constants.

$C_1 = 0.308$

$C_2 = 0.774$

$C_3 = 10{,}620.0$

The authors attributed the differences in the field and laboratory results to differences in the hydraulic radius term, Π_5. The model dryer was not insulated on its periphery. For this reason the heat loss was assumed to be larger in proportion to the crossectional area than it was in the larger batch dryers used in the field experiments.

Day (17) used the approach of Nelson, Mahoney and Fryrear in studying grain drying in cross-flow systems of deep cylindrical bins. His model included two additional dimensionless parameters as coefficients of the velocity term, Π_4, in equation (33). These were:

$\Pi_6 = T_e/T_g$

$\Pi_7 = \dfrac{R^2}{\alpha t}$

where:

Tg = Initial grain temperature.

α = Bulk thermal diffusivity.

The temperature ratio, Π_6, was an index of the amount of heat to be transferred during initial transient conditions and Π_7 apparently a measure of the rate of heating of the grain.

RamaRao, Wratten and Faulkner (37) also used a similar form of the generalized drying equation to those above. Their equation was developed for a continuous flow intermittent drying system for rice. Their equation contained three terms not previously used. These are:

$\Pi_8 = T_e/T_w$

$\Pi_9 = T_g/T_w$

$\Pi_{10} = Re$

where:

T_w = Wet bulb temperature of the entering air.

R_e = A modified form of the Reynolds Number.

No reasons were given nor were they obvious for the use of the terms. It would appear that the drying potential is adequately described by the terms $\Delta T/T_e$ and ΔM which were also in the equation. A velocity term Vt/X, where X was a length parameter of the system, was used as well as R_e. One of these terms would also appear to be redundant.

CHAPTER III

DEVELOPMENT OF THE PROBLEM

Power Absorption of Peanuts in a Radio-Frequency Field

The power absorption of a homogeneous dielectric material of low power factor exposed to a radio-frequency field between parallel electrodes was previously given as:

$$P = 2\Pi f \varepsilon \varepsilon_o p\, E^2 \tag{9}$$

where:

P = Power absorbed per unit volume, watts/cm^3.

f = Frequency of the electric field, MH_z.

ε = Dielectric constant for the material, dimensionless.

ε_o = Dielectric constant or permittivity of air, 8.85×10^{-14} farads/cm.

p = Power factor of the material, dimensionless.

E = Electric field strength, volts/cm.

or for materials of any power factor:

$$P = EI_t \cos\Theta \tag{5}$$

where:

I_t = Total current flow in sample, amps/cm^2.

$\cos\Theta$ = Power factor, p.

Power absorption of a dielectric may also be expressed in terms of the amount of heat generated in a sample exposed to a radio-frequency field:

$$P = (C_p W_w \Delta T + Q_c)/ v t \tag{34}$$

where:

P = Power absorbed per unit volume, Btu/in.^{3}-min.

C_p = Specific heat of the material, Btu/lb. °F.

W_w = Wet weight of the material, lbs.

Q_c = Heat required to raise the temperature of the container ΔT degrees, Btu.

ΔT = Change in temperature, °F, of material and container during heating time, t.

v = Volume of container, in.^{3}.

t = Time, min.

Using appropriate constants and equating (5) and (34) yields:

$$K_1 E I_t \cos\Theta = K_2 (C_p W_w \Delta T + Q_c) / v t \tag{35}$$

where:

K_1 = A constant, 16.93 cm^3/in^3.

K_2 = A constant, 17.57 watt - min/Btu.

A granular dielectric could be expected to absorb power according to equation (9) if the dielectric constant and power factor were measured under the same conditions of particle size, particle spacing and electrode spacing as the rate of heating. The literature review, however, pointed out that variations in the bulk dielectric properties of a sample of granular material could be expected due to these three variables. Dielectric properties of biological materials have also been shown to be functions of moisture content and frequency (1). Equation (5) describes the power absorption by a dielectric for a circuit in which the field strength and total current flow can be measured. $\cos\Theta$ in this equation is a function of the dielectric properties, therefore:

$$\cos\Theta = f(m, d/\zeta, \nu, f) \tag{36}$$

where:

m = Moisture content, decimal % dry basis.

d/ζ = Ratio of distance between electrodes to a characteristic length of the particles parallel to the electric field.

ν = Ratio of the volume material in the heating chamber to the total volume of the chamber.

f = Frequency, MHz.

Solving equation (35) for $\cos\Theta$ yields:

$$\cos\Theta = \frac{K_2 \, (C_p \, W_w \, \Delta T + Q_c)}{K_1 \, E \, I_t \, v \, t} \tag{37}$$

Now:

$$I_R = \cos\Theta \, I_t = \sigma E \tag{38}$$

and therefore:

$$P = \sigma E^2 \tag{39}$$

where:

I_R = The current flow in phase with the voltage, amps/in^2.

σ = Conductivity, mhos/in.

The conductivity, σ, is also a function of the dielectric properties and therefore:

$$\sigma = f(m, d/\zeta, \nu, f) \tag{40}$$

The specific heat, C_p, and the characteristic length, ζ, of the particles are the two quantities in equations (36), (37), and (40) that cannot be measured conventiently in a heating test. Wright and Porterfield (58) developed a quadratic expression for the specific heat of peanuts as a function of moisture content. The data from their tests was used to develop the following more convenient expression:

$$C_p = 0.402630 + 0.424561 \quad m^{0.880457} \tag{41}$$

R_a = Range of C_p in the tests, Btu/lb °F.

S, R^2 = Standard deviation and goodness of fit ratio, respectively, for the regression of the observed values of C_p versus the values calculated by equation (41).

Equation (41) and all equations developed from experimental data following this were obtained with the aid of a computer program written by J. Z. Borg (7) and based on a algorithm by H. Spath (47).

Additional equations and graphs of specific heat of peanuts versus moisture content and temperature are presented in Appendix A.

Beavers (6) measured the dimensions of Spanish peanuts with a micrometer. A more definitive measure of peanut size was desired, however, so a test was designed to determine it. Dimensions were taken from photographs of magnified cut sections of whole peanuts and expressed as ratios to the longest dimension of each peanut. The characteristic length for the power absorption and drying tests could then be determined relative to the average maximum lengths of the peanuts used in the tests.

Characteristic length is defined for the power absorption tests as the average maximum dimension parallel to the electric field and is an index of the field distortion. It is defined as the average maximum dimension parallel to the air flow in the drying tests, (described in the following section), and is an index of the heat and mass transfer at the surface of the peanuts.

The heating tests required a thermally insulated chamber that would be large enough to minimize edge effects and contain several layers of peanuts, but not so large that the available radio-frequency generator could not produce a reasonably rapid temperature rise in the peanuts. A circular chamber 11.75 inches in diameter and 1.656 inches deep, (four layers of peanuts), was selected from preliminary tests as the maximum size that would meet these requirements. Flat circular electrodes formed the top and bottom of the chamber. Minimum chamber depth, (electrode spacing), was 0.531 inches — that spacing that would just clear one layer of peanuts. The frequency to be used in tests was fixed by the available radio-frequency generator at 13.56 MHz.

The moisture contents to be tested were 56.25, 31.68, 13.64, and 0.0 percent dry basis. These correspond to 36.0, 24.0, 12.0 and 0.0 percent wet basis.

The volume of peanuts per unit volume of chamber could not be controlled conveniently without introducing some other material into the chamber — for example sheets of paper to separate layers of peanuts. Therefore, this quantity was allowed to vary with individual samples and peanut arrangement within the chamber.

The levels of the various factors in the test plan for the power absorption of peanuts in a radio-frequency field are shown in Table I. The basic plan required that the rate of heating of peanuts be determined for four moisture contents and three electrode spacings to vary the d/ζ ratio. One field strength was to be used. Peanuts were to be oriented in the chamber such that their long axes were

TABLE I

LEVELS OF FACTORS FOR POWER ABSORPTION BY

PEANUTS IN A RADIO-FREQUENCY FIELD

Orientation of Long Axis of Peanut to Electric Field	Moisture Content, % Dry Basis	Nominal Field Strength, Volts/Inch.	Electrode Spacing, Inches
	56.25	150.0	1.656
Perpendicular	31.58	150.0	1.656
	13.64	150.0	1.656
	0.00	150.0	1.656
	56.25	150.0	0.828
Perpendicular	31.58	150.0	0.828
	13.64	150.0	0.828
	0.00	150.0	0.828
	56.25	150.0	0.531
Perpendicular	31.58	150.0	0.531
	13.64	150.0	0.531
	0.00	150.0	0.531
	56.25	130.0	1.656
Perpendicular	31.58	130.0	1.656
	13.64	130.0	1.656
	0.00	130.0	1.656
	56.25	90.0	1.656
Perpendicular	31.58	90.0	1.656
	13.64	90.0	1.656
	0.00	90.0	1.656
	56.25	150.0	1.656
Random	31.58	150.0	1.656
	13.64	150.0	1.656
	0.00	150.0	1.656
	56.25	150.0	1.094
Parallel	31.58	150.0	1.094
	13.64	150.0	1.094
	0.00	150.0	1.094

perpendicular to the electric field. Electrical field strength was set by the voltage drop across the electrodes at 2/3 of the maximum output of the radio-frequency generator when heating the highest moisture samples.

Other tests were added to the basic plan. In one series peanuts were to be randomly oriented in the chamber. In another series the long axes of the peanuts were to be oriented parallel to the electric field with the electrode spacing just large enough to clear the peanuts. Two more series using the maximum electrode spacing and with the peanuts oriented perpendicular to the field were to be run at lower field strengths. These last two series were included to determine the effect of field strength on the dielectric properties, if any — a possibility observed by Whitney and Porterfield (52). All tests were to be replicated.

Rate of Drying of Peanuts by Forced Convection in a Radio-Frequency Field

Table II contains a list of variables considered to be the pertinent quantities affecting the forced air drying rate of peanuts heated by radio-frequency energy in a batch type dryer. These quantities were developed from subjects in the literature review, namely: heat and mass transfer in porous hygroscopic media, previous drying studies and power absorption by biological materials in a radio-frequency field. The particular system to be described by these quantities had the following characteristics: (a) peanuts to be dried would be contained between flat, parallel electrodes with their long axes perpendicular to the electric field, (b) the electrodes

TABLE II

LIST OF PERTINENT QUANTITIES FOR FORCED CONVECTIVE DRYING OF PEANUTS HEATED BY RADIO-FREQUENCY ENERGY

Quantity and Description		Units	Dimensions*
M_R,	Moisture loss in drying time, t, % dry basis, decimal	0	0
ΔM,	Initial moisture content of peanuts minus moisture content of peanuts at equilibrium with incoming air, % dry basis, decimal	0	0
T_e,	Entering dry bulb air temperature	°F	Θ
ΔT,	$T_e - T_1$, where T_1 is an ideal leaving air temperature following a wet bulb drying process, (See Figure 5)	°F	Θ
T_n,	Initial batch temperature	°F	Θ
t,	Drying time	min.	T
A_v,	Air flow rate, cfm per square foot of crossectional area perpendicular to air flow	ft/min.	LT^{-1}
d,	Depth of peanuts in direction of air flow	ft.	L
ζ,	Characteristic length of peanut perpendicular to air flow direction	ft.	L
α,	Average thermal diffusivity of peanut hulls and kernels	ft^2/min.	L^2T^{-1}
β,	Average moisture diffusivity of peanut hulls and kernels	ft^2/min.	L^2T^{-1}

TABLE II (Continued)

Quantity and Description		Units	Dimensions*
ΔP,	Power input per unit volume to wet peanuts from the electric field at a constant field strength minus the power input to dry peanuts at the same field strength	Btu/min-ft^3	$HL^{-3}T^{-1}$
C_a,	Volumetric heat capacity of incoming air	Btu/ft^3°F	$HL^{-3}\theta^{-1}$
f,	Frequency of electric field	1/min.	T^{-1}
R,	Hydraulic radius of the batch chamber	ft.	L
D,	Diameter of perforations in the electrode plates	ft.	L
O_p,	Percentage of open area in the electrode plates	0	0

*Dimensions are: 0 - dimensionless, Θ - temperature,
L - length, T - time,
H - heat

would be oriented perpendicular to the air stream and perforated to allow air to flow through the batch, (c) the periphery of the chamber would be thermally insulated.

Table II contains 17 pertinent quantities in four fundamental dimensions. According to the Buckingham Π theorem (26), these may be arranged into 17 - 4 = 13 independent dimensionless terms. The following 13 dimensionless or Π terms were determined by inspection similarly to those used by Nelson, Mahony and Fryrear (30) and Day (17).

$$\Pi_1 = M_R \qquad \Pi_8 = R/\zeta$$

$$\Pi_2 = \Delta M \qquad \Pi_9 = f\ t$$

$$\Pi_3 = \Delta T/T_e \qquad \Pi_{10} = D/\zeta$$

$$\Pi_4 = A_v\ t/\zeta \qquad \Pi_{11} = O_p$$

$$\Pi_5 = \Delta P\ t/C_a T_e \qquad \Pi_{12} = \frac{\alpha t}{\zeta^2}$$

$$\Pi_6 = T_e/T_n \qquad \Pi_{13} = \frac{\beta t}{\zeta^2}$$

$$\Pi_7 = d/\zeta$$

Π_1 or M_R is the dependent variable in the set of dimensionless parameters.

The terms Π_2, Π_3, Π_4, and Π_5 represent the minimum number of terms necessary to establish a relationship between drying rate, Π_1, the incoming air conditions and the electric power absorbed. The initial moisture content minus an equilibrium moisture content, Π_2, and the incoming air temperature minus an "ideal" or wet bulb leaving air temperature, Π_3, are indices of the maximum drying potential. The air velocity term, Π_4, is a modified Reynolds number and serves as an index of the rates of heat and mass transfer at the surface of each peanut. The temperature term, Π_3, may also be considered an index of the surface heat transfer. The power term, Π_5, is an index of the effect on drying rate of adding energy by internal generation.

The ratio of the temperature of the entering air to the initial temperature of the peanuts, Π_6, is an index of the transient conditions at the initiation of drying. This term, of course, should be included in a study aimed toward complete generality but its effect would probably be short-lived for a system where small particles were being dryed.

The terms Π_7, Π_8, Π_9, Π_{10}, and Π_{11} are related to the particular system being studied. The ratio of the depth of the sample to the characteristic length, Π_7, is an index of the effect of the changing conditions of the air as it flows through the peanuts. Overall drying effectiveness should decrease as sample depth increases due to increasing relative humidity and decreasing temperature of the air proceding through the sample.

The ratio of the hydraulic radius of the sample container to the peanut characteristic length, Π_8, can be considered an index of electrical edge effects in a system where the periphery of the sample is thermally insulated. These effects would probably be negligible in systems of large crossectional area perpendicular to the electric field.

The frequency-time term, Π_9, would be an index to the electrical power distribution within individual peanuts. As frequency increases the electric field and hence the power absorption would become more distorted, (See Figure 3). The effects of this term would appear to be negligible for the frequency used in these tests, 13.56 MHz.

The ratio of the diameter of the openings in the perforated plates to the peanut characteristic length, Π_{10}, and the percentage of open area in the plates, Π_{11}, are indices of the entrance effects on the air flow. Those terms would probably have little effect on the drying rate unless they represented severe restriction or channelization of the air flow.

The terms Π_{12} and Π_{13} are modified Fourier numbers and are indices of the internal heat and mass transfer rates, respectively, within individual peanuts. They contain α and β the thermal and moisture diffusivities and, as was pointed out in the literature review, no means have yet been established to obtain these quantities for small hygroscopic objects. This situation forces the assumption that the effects of Π_{12} and Π_{13} are negligible, even though α and β may vary considerably with moisture content. This assumption may not be too harsh for systems where the moisture and temperature gradients within each peanut are small. For cases in which these gradients are large — for instance, high rates of internal energy generation — Π_{12} and Π_{13} would have considerable effect.

The terms, Π_2, Π_3, Π_4, and Π_5 then were considered to have the most effect on the dependent term, Π_1. A plan was devised to test these effects for the initial conditions term $\Pi_6 = 1.0$. The terms describing the system, Π_7 through Π_{11}, were to be held constant.

The plan was divided into two parts. The first part was to test the effects of Π_2, Π_3, and Π_4 on Π_1 and develop a prediction equation for forced air drying alone. The second part of the plan was to test the effects of adding energy by dielectric heating, (Π_5), on the equation for forced air drying.

The drying potential terms, Π_2 and Π_3, are determined from the initial moisture content of the peanuts, the equilibrium moisture content of the peanuts, the dry bulb temperature and relative humidity of the entering air. The range of conditions for the tests was selected from those conditions commonly found in practice in drying peanuts. They are: peanut moisture contents — 56.25 to 13.64 % dry basis, (36.0 to 12.0 % wet basis), and air conditions of 66 °F at 60% relative humidity and 95 °F at 23 % relative humidity. Air at 66 °F and 60 % relative humidity represents the mean daily average for the months of August through November in the Oklahoma peanut producing areas (1). Air under these conditions will have a relative humidity of 23 % if heated to 95 °F, the highest recommended temperature for peanut drying.

The equilibrium moisture contents required for computing Π_2 and Π_3 were taken from Figure 6. The data to construct Figure 6 is from Karon and Hillery (22). The lack of variation in these data due to temperature and varietal differences is noteworthy.

The work of Beasley and Dickens (4) showed that rate of drying of peanuts was not increased materially at air flow rates above 24 cfm per ft^2 of bin crossectional area perpendicular to the air flow. The range of air flow rates was picked to include this value — 12 to 48 cfm/ft^2. The time limit for all tests was arbitrarily set at 60 minutes.

Part I of the experimental plan called for Π_1 to be observed for three levels of Π_2 and four levels of Π_4. The levels of Π_2, the moisture term, could be adjusted by manipulating the initial moisture content of the peanuts to obtain constant values for the two conditions used for the incoming air. The temperature term, Π_3, could not be held at constant values for constant values of Π_2 so it was allowed

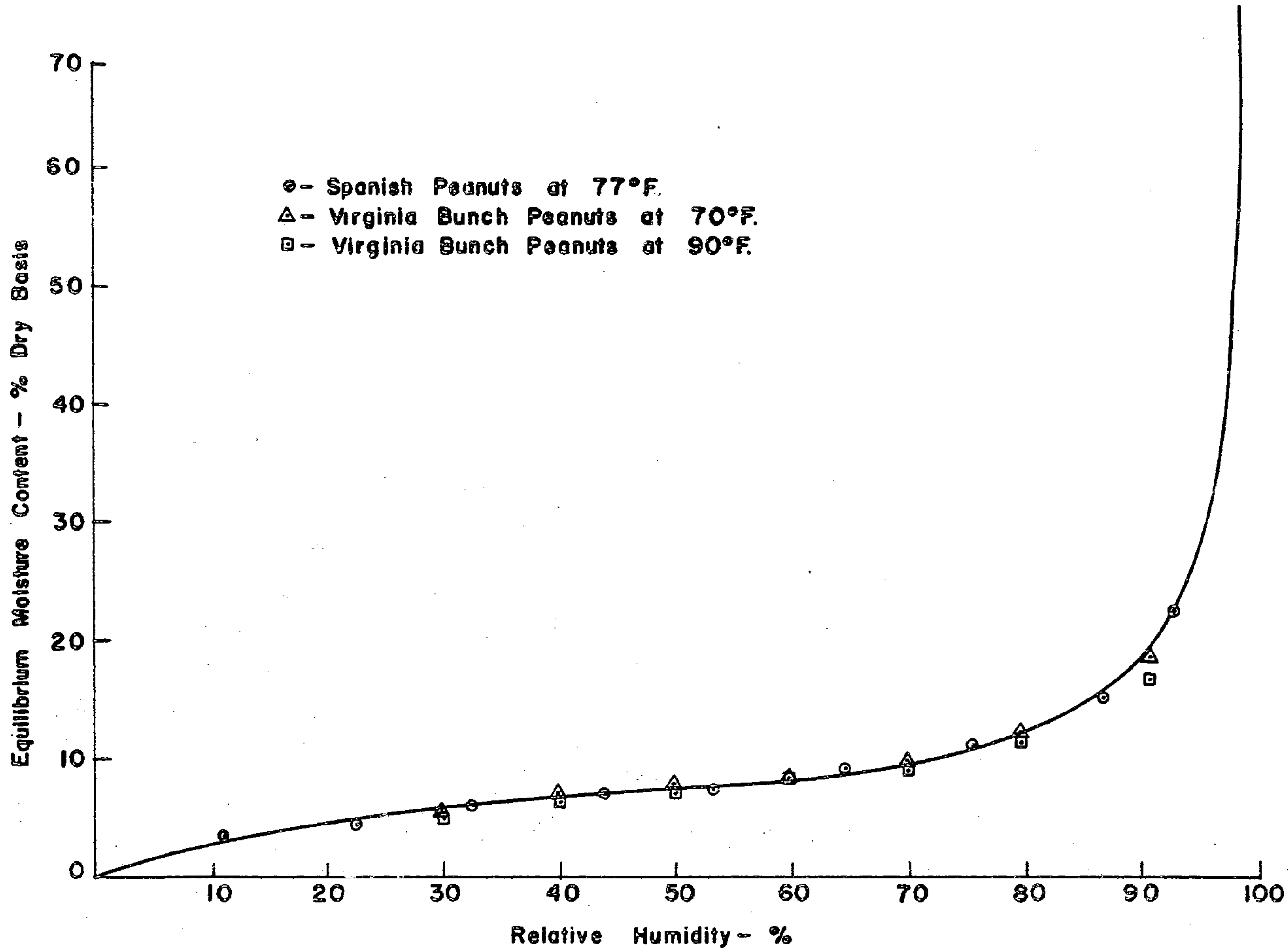

Figure 6. Equilibrium Moisture Content of Peanuts Versus Relative Humidity.

to vary. Part II of the plan required three levels of the power term, Π_5, to be tested against three levels of the moisture term, Π_2, and four levels of the velocity term, Π_4. All the tests in this part of the plan were to be run at 66 °F and 60 % relative humidity. The levels of Π_5 were those equivalent to 0, 50, and 75 % of the maximum output of the available radio-frequency generator, the zero power level to be taken from those tests in Part I with similar incoming air conditions. The levels of the factors in the test plan are shown in Table III. All test runs were to be replicated.

TABLE III

LEVELS OF FACTORS FOR DETERMINING THE RATE OF DRYING OF PEANUTS BY FORCED CONVECTION IN A RADIO-FREQUENCY FIELD

Part I:

Π_2	Π_3	$\Pi_4 X10^{-4}$	Π_2	Π_3	$\Pi_4 X10^{-4}$
0.453	0.121	1.650	0.453	0.281	1.650
0.248	0.117	3.360	0.248	0.279	3.360
0.092	0.099	5.204	0.092	0.263	5.204
0.453	0.121	6.886	0.453	0.281	6.886
0.248	0.117	1.650	0.248	0.279	1.650
0.092	0.099	3.360	0.092	0.263	3.360
0.453	0.121	5.204	0.453	0.281	5.204
0.248	0.117	6.886	0.248	0.279	6.886
0.092	0.099	1.650	0.092	0.263	1.650
0.453	0.121	3.360	0.453	0.281	3.360
0.248	0.117	5.204	0.248	0.279	5.204
0.092	0.099	6.886	0.092	0.263	6.886
0.453	0.121	1.650	0.453	0.281	1.650
0.248	0.117	3.360	0.248	0.279	3.360
0.092	0.099	5.204	0.092	0.263	5.204
0.453	0.121	6.886	0.453	0.281	6.886
0.248	0.117	1.650	0.248	0.279	1.650
0.092	0.099	3.360	0.092	0.263	3.360
0.453	0.121	5.204	0.453	0.281	5.204
0.248	0.117	6.886	0.248	0.279	6.886
0.092	0.099	1.650	0.092	0.263	1.650
0.453	0.121	3.360	0.453	0.281	3.360
0.248	0.117	5.204	0.248	0.279	5.204
0.092	0.099	6.886	0.092	0.263	6.886
Entering air conditions: 66 °F and 60% relative humidity.			Entering air conditions: 95 °F and 23% relative humidity.		

TABLE III (Continued)

Part II:

Π_2	$\Pi_4 X10^{-4}$	Π_5	Π_2	$\Pi_4 X10^{-4}$	Π_5
0.453	1.650	0.50	0.453	1.650	0.75
0.248	3.360	0.50	0.248	3.360	0.75
0.092	5.204	0.50	0.092	5.204	0.75
0.453	6.886	0.50	0.453	6.886	0.75
0.248	1.650	0.50	0.248	1.650	0.75
0.092	3.360	0.50	0.092	3.360	0.75
0.453	5.204	0.50	0.453	5.204	0.75
0.248	6.886	0.50	0.248	6.886	0.75
0.092	1.650	0.50	0.092	1.650	0.75
0.453	3.360	0.50	0.453	3.360	0.75
0.248	5.204	0.50	0.248	5.240	0.75
0.092	6.886	0.50	0.092	6.886	0.75
0.453	1.650	0.50	0.453	1.650	0.75
0.248	3.360	0.50	0.248	3.360	0.75
0.092	5.204	0.50	0.092	5.204	0.75
0.453	6.886	0.50	0.453	6.886	0.75
0.248	1.650	0.50	0.248	1.650	0.75
0.092	3.360	0.50	0.092	3.360	0.75
0.453	5.204	0.50	0.453	5.204	0.75
0.248	6.886	0.50	0.248	6.886	0.75
0.092	1.650	0.50	0.092	1.650	0.75
0.453	3.360	0.50	0.453	3.360	0.75
0.248	5.204	0.50	0.248	5.204	0.75
0.092	6.886	0.50	0.092	6.886	0.75

Quantities under Π_5 represent 50 and 75 % of the power available from the radio-frequency heater - not the actual value of the term. Values of Π_3 are the same in these tests as the corresponding values in Part I of the table for entering air conditions of 66 °F and 60 % relative humidity.

CHAPTER IV

PROCEDURES AND EQUIPMENT

Peanut Characteristic Length

The characteristic length was previously defined for these tests as the average maximum dimension of the peanuts parallel to the electric field or the direction of air flow. The majority of the power absorption tests were to be conducted with the long axis of the peanuts perpendicular to the electric field. All of the drying tests were to be conducted with the long axis of the peanuts perpendicular to the electric field and direction of air flow. The average maximum diameter would then be the characteristic length for these tests.

Maximum length is the only dimension of a peanut that is convenient to measure with a degree of accuracy and repeatability. The technique developed here relates all dimensions in terms of ratios to the maximum length. Thus the shape of any size peanut can be described if its maximum length is determined.

Twelve peanuts were randomly selected from a batch of Spanish peanuts of approximately 20 pounds. The batch had previously been sorted to remove immature, damaged and single kernel nuts. The maximum length of each nut was measured using the device with a dial gage shown in Figure 7. The anvils that held the peanuts had a

1/2 inch radius cup so that each peanut could be oriented with its longest dimension in line with the centerline of the device. A

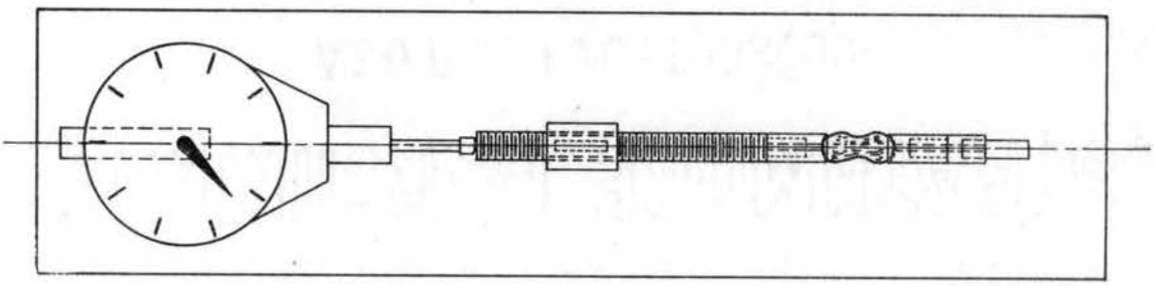

Figure 7. Schematic of Device Used for Measuring Peanut Length

longitudinal hole through the centerline of the anvils allowed this device to serve also as a jig for drilling 1/16 inch diameter holes through the long axes of the peanuts.

After the peanuts were measured and drilled they were mounted on 1/16 inch diameter rods in molds made of one inch square aluminum tubing. All peanuts were oriented in the same manner within each mold. The molds were filled with a liquid acrylic plastic containing a small amount of catalyic hardener. The plastic used was the kind that is commonly available in hobby shops for making paper weights and novelties. The mold was allowed to stand for about eight hours until the plastic was completely hardened.

Each encapsulated peanut was then put in a holder made of one inch square aluminum tubing and sectioned with a band saw. The band saw blade had been filed to remove the set. The holder was equipped with a screw adjustment to advance the sample a predetermined amount after each cut. Average saw kerf thickness for each peanut was determined by subtracting the length of the sample after cutting from the initial length of the peanut and dividing by the number of cuts. Average kerf per cut for all twelve peanuts was 0.0242 inches. Average section thickness for all sections was 0.0485 inches. The number of sections per peanut varied from 10 to 16 depending on the length of the peanuts.

The kernel portion was removed from each section and the section photographed with the aid of a Wilder Micro-Projector (Figure 8). The lens used on the projector had a 10X magnification and the image was projected on to a number 17 clear glass grid chart with 0.01 inch increments manufactured by the Scherr-Tumico Co., Inc. Each section was photographed using a double exposure technique in a dark room. An eight by ten inch sheet of Kodabromide F. 5 contact print paper was laid emulsion side down on the grid chart. The section to be photographed was placed in a holder on the sample table of the projector. The projector light was turned on for 2.0 seconds. The peanut shell ring was then removed from the plastic section without moving the section or the photographic paper. The light was again turned on for approximately 3/4 of a second. Figure 9 is a typical example of a photograph of a section. The grey area represents the hull in the section and the dark area is the kernel cavity.

A circle divided into 20° increments was placed over each photograph as shown in the diagram, Figure 10. The horizontal and vertical dimensions at the inner and outer points where each radius crossed the shell ring were recorded.

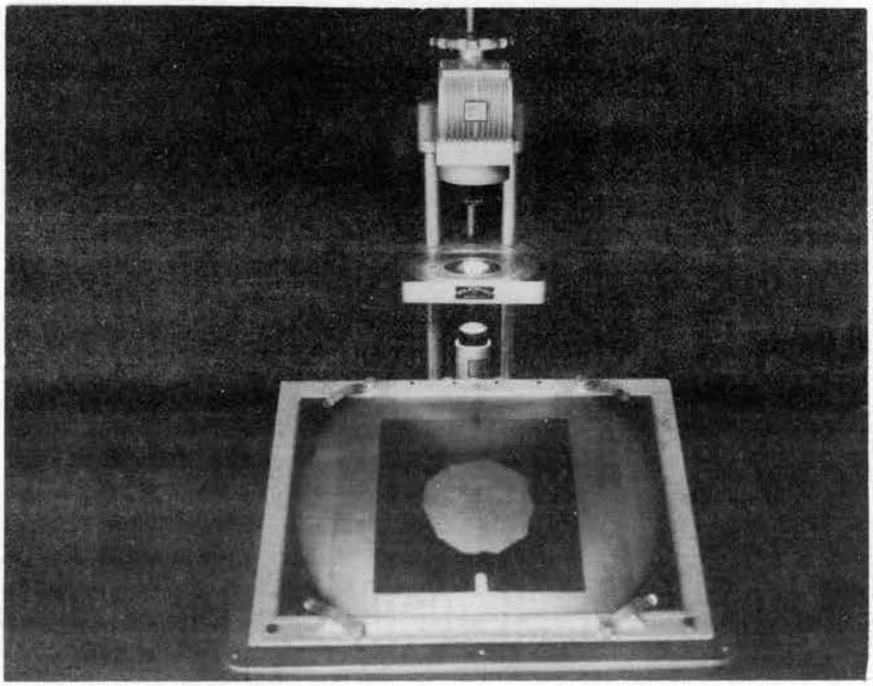

Figure 8. Enlarging Projector Used to Photograph Peanut Sections with Typical Section Showing on Grid Screen

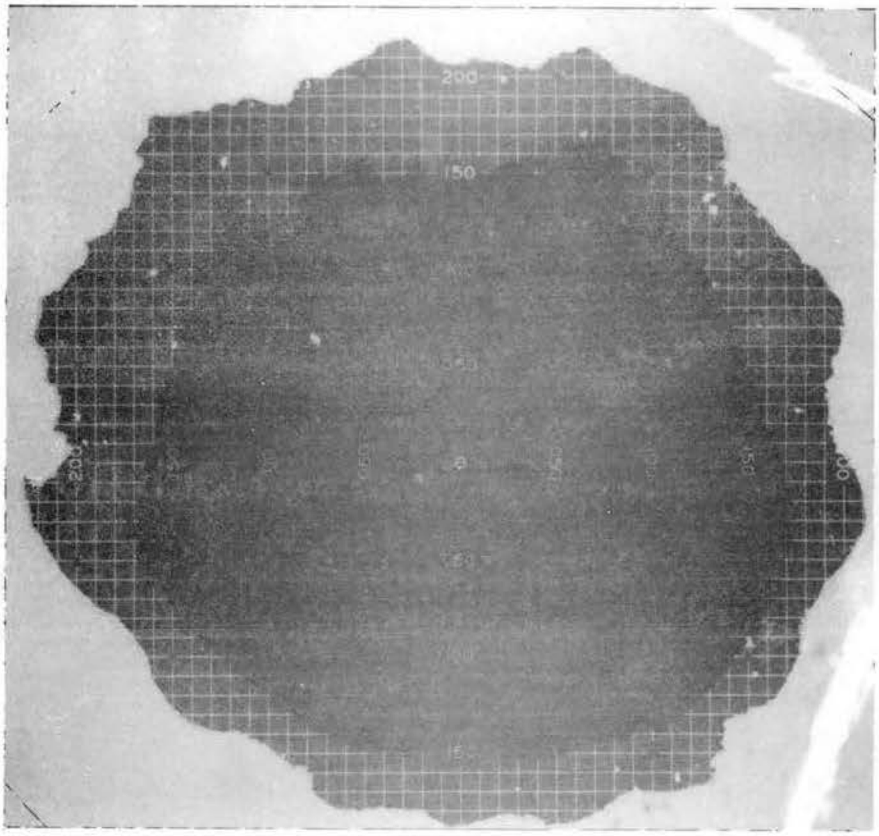

Figure 9. Photograph of Typical Peanut Cross Section

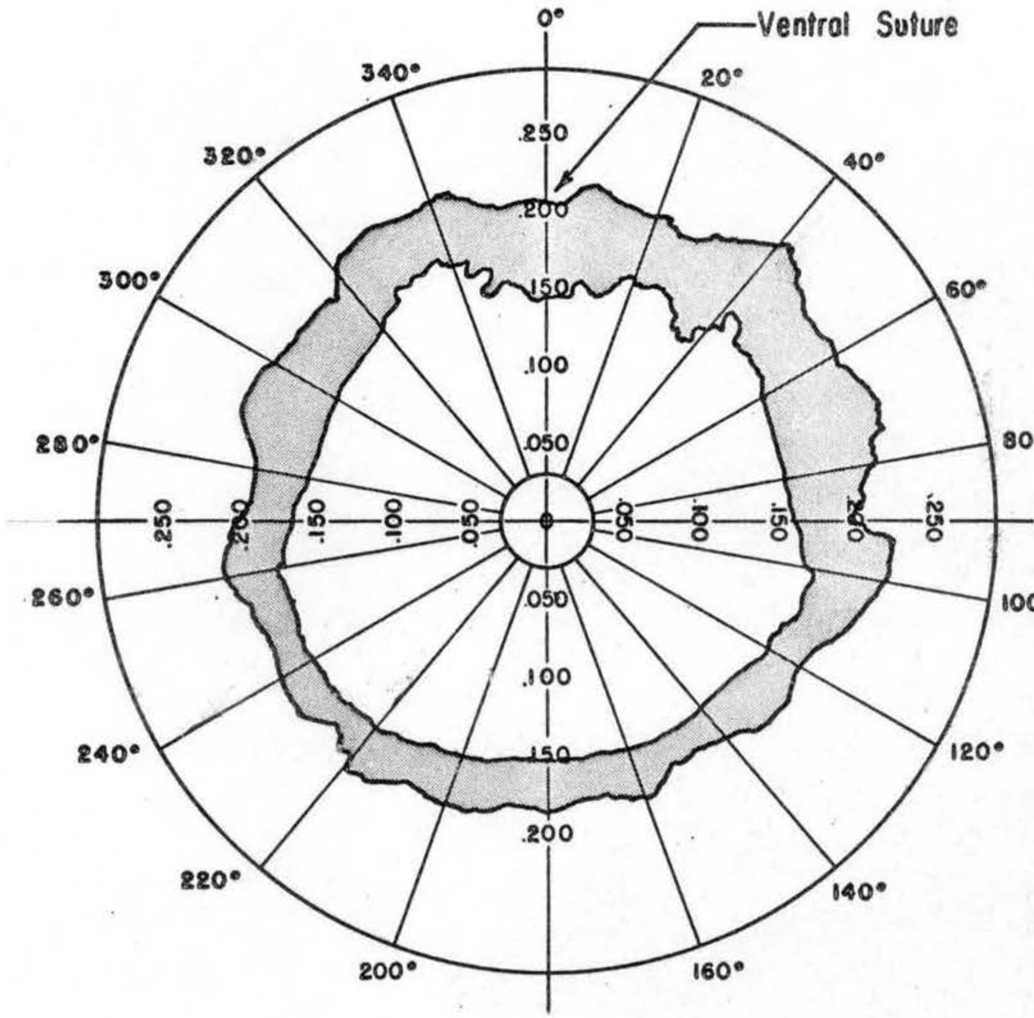

Figure 10. Diagram Illustrating Method of Taking Dimensions from Peanut Cross Sections

A computer program was written to analyze the dimensional data from the photographs. The program adjusted the data from the number of cut sections for each peanut to twelve equally spaced sections per peanut, (See Figure 11). The following dimensional data was then obtained from the adjusted segments for each peanut:

(1) Radii/L

(2) Average outside diameter/L

(3) Maximum outside diameter/L

(4) Average inside diameter/L

(5) Maximum inside diameter/L

(6) Outside surface area/L^2

(7) Total volume/L^3

(8) Kernel cavity volume/L^3

(9) Average hull thickness

where:

L = the length of the peanut.

These data were then averaged for the twelve peanuts tested. Surface areas and volumes were obtained by averaging adjacent radii for each pie-shaped segment of each interior section, determining the end area and volume of each segment and summing these for the whole peanut. The end sections were treated as cones.

The hull thickness was assumed to be independent of the peanut length and was averaged over all interior sections for the twelve peanuts. The hull thickness at a point P in Figure 12 was estimated by averaging two perpendiculars — dotted lines t and t' — erected from P to the straight line segments a a' and b b'. These line segments connect the end of radius R_j with the ends of adjacent

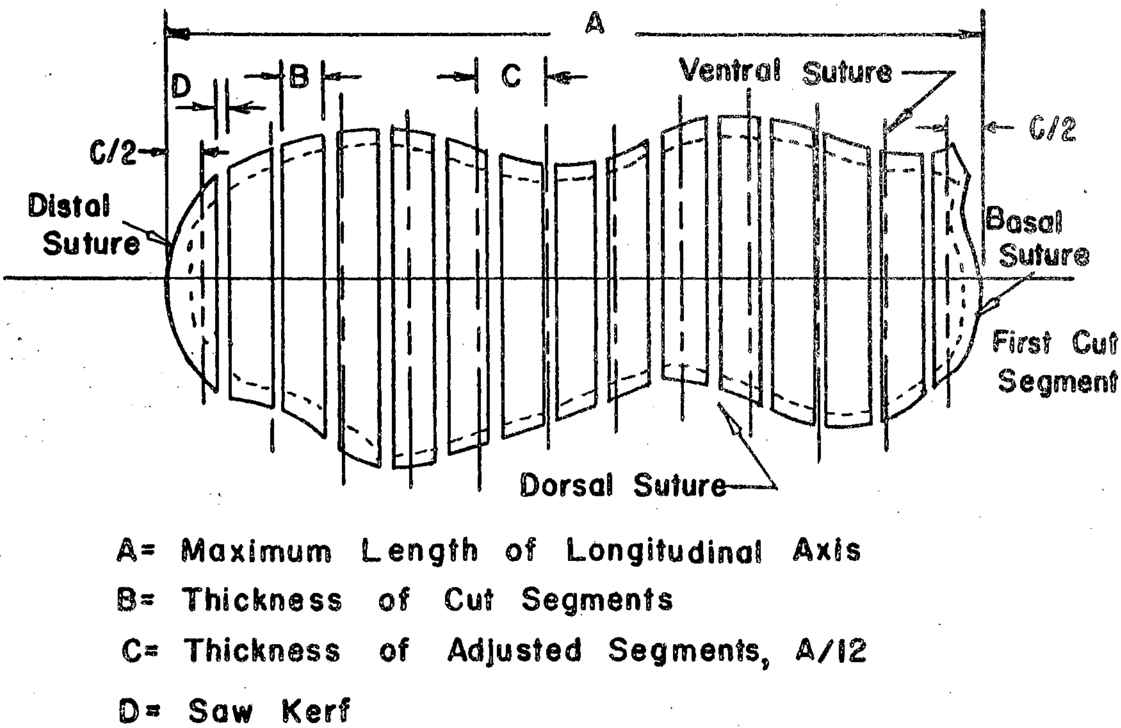

Figure 11. Diagram of Typical Peanut Showing Cut Sections and Adjusted Sections

radii, R_{j-1} and R_{j+1}. These three radii, R_{j-1}, R_j, and R_{j+1} are measured outward from the long axis of the peanut, ℄, at respective distances of X_{j-1}, X_j, and X_{j+1} from the basal end.

Sample Preparation and Volume Determination

Samples of peanuts for the power absorption and drying tests were obtained from a 1000 pound lot of the Spanish variety grown on the Oklahoma State University Experiment Station at Fort Cobb, Oklahoma. The peanuts were washed to remove adhering soil, and the excess surface moisture removed by forced air ventilation. Samples weighing approximately 1000 grams were sorted by hand from the lot.

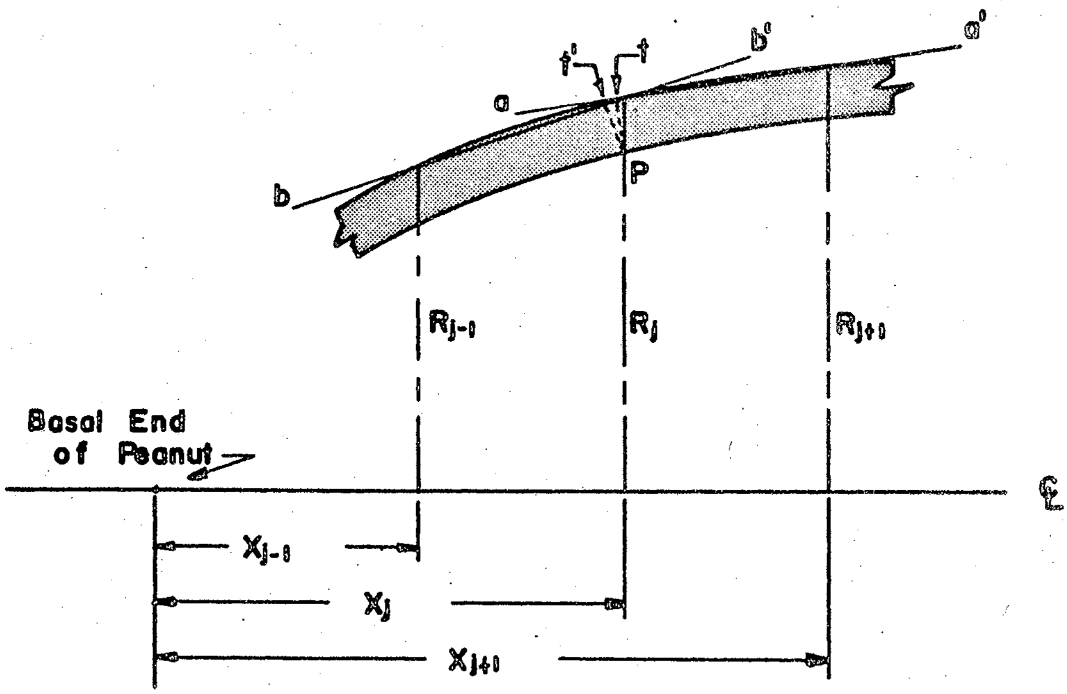

Figure 12. Diagram for Determining the Thickness of a Peanut Hull at a Point

These samples contained only mature, undamaged nuts with two kernels. The sorted samples were dryed at 190°F in a forced draft oven for 8 hours. Several samples were weighed after 7 hours and again after 8 hours. Weight loss between these two weighings averaged less than one gram in a thousand. Eight hours of drying under these conditions was therefore assumed to produce zero moisture content. The dry samples were sealed in gallon containers until needed for testing.

Samples to be tested at 13.62 % dry basis moisture content were imbibed by soaking in water until the wet weight was correct for the desired moisture content. This took approximately 5 minutes per sample. The time required, however, for higher moisture samples to imbibe the correct amount of moisture was considerably longer — up to 25 hours for samples of 56.3 %. Some peanuts in the samples soaked for long periods also appeared to be much wetter than others.

A rapid inbibition rate for the high moisture samples was achieved by partially evacuating the space in the container above the mixture of peanuts and water with a vacuum pump. A typical sample would be held under vacuum for a few minutes, then drained and weighed. This process was repeated until the correct weight for the desired moisture content was achieved. With practice this technique produced samples within ± 1 % of the desired moisture content and of apparently uniform wetness.

A powdered fungicide, Captan 50W manufactured by the Staufer Co., was added to the water used to imbibe the samples to suppress mold growth during the subsequent equilibration period. All wetted samples were allowed to equilibrate seven days before testing.

The above sample procedures were necessary because freshly dug high moisture peanuts begin to deteriorate very rapidly, (often within three days), and they also contain a wide range of moisture contents. There were no obvious indications that the structure of the peanuts was materially changed by the conditioning procedures.

The volume of each sample used in the heating and drying tests was determined by a liquid displacement method. The liquid used was ethylene glycol, (anti-freeze), because it wet the surface of the peanuts thoroughly yet had little tendency to soak in. The ratio of the volume of the sample to the volume of the dielectric heating chamber was determined by the following equation.

$$\nu = \frac{W_f + W_c + W_{nf} - W_t}{S_f\ v} \qquad (42)$$

where:

W_f = Weight of fluid the container could hold, gms.

W_c = Weight of the container, gms.

W_{nf} = Final weight of the peanuts after the volume determination, gms.

W_t = Total weight of container with a mixture of fluid and peanuts, gms.

S_f = Specific gravity of the fluid, 1.212 gms/cm^3.

v = Volume of the dielectric heating chamber, cm^3.

The final weight of the peanuts, W_{nf}, was obtained after draining the antifreeze from the peanuts, rinsing them with acetone, and allowing a few minutes for the acetone to dry from the peanut surface.

Power Absorption Equipment and Procedures

The radio-frequency generator used in the heating and drying tests was a Burdick X-85 medical diathermy machine that operated on a crystal controlled frequency of 13.56 MHz. The generator was connected to the series resonant circuit schematically shown in Figure 13. In this circuit the capacitor C_1, represents the area between the electrodes that contained the sample of peanuts and C_2 represents the annulus of insulation between the electrodes that surrounded the sample. The coil L was wound experimentally so that the adjustable capacitor within the generator could balance the circuit to resonance for all electrode spacings, d, and peanut moisture contents used. The resistor, R, was a "Cantenna" manufactured by the Heath Kit Company. This "Cantenna" is a dummy antenna used by amateur radio operators and consists of a high wattage, low reactive carbon resistor

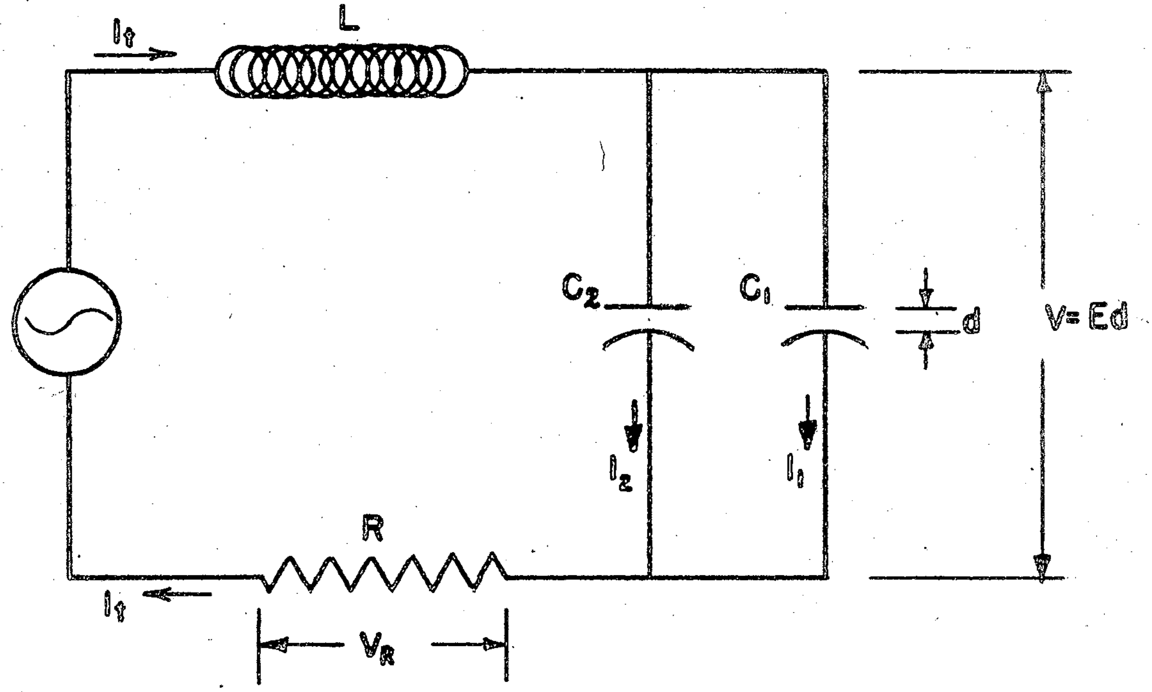

Figure 13. Electrical Diagram of Radio-Frequency Heater.

of 50 Ω immersed in oil for cooling.

Hammond (19) and other electrical engineering texts described the impedance, Z, of a series circuit as:

$$Z = \sqrt{R^2 + (\omega L - \frac{1}{\omega C})^2} \qquad (43)$$

where:

$\omega = 2\pi f$.

f = Frequency.

R = Resistance, ohms.

L = Inductance, henrys.

C = Capacitance, farads.

At resonance the reactive terms in (43) cancel.

That is:

$$\omega L = \frac{1}{\omega C}$$

and:

$$Z = R$$

Therefore, at resonance the current flow is maximum since the impedance is minimum. This total current flow, $I_t = I_1 + I_2$ can be calculated from the voltage drop, V_R, across the resistor. The voltage drop across the capacitor, $V = Ed$, where E is the field strength, is also a maximum at resonance.

The heating chamber was designed to be used in both the power absorption and rate of drying tests. A view with the top electrode removed is shown in Figure 14. The two electrodes were made of 20 gage perforated aluminum sheet metal 17 inches in diameter. The holes were 1/16 inch in diameter on 1/8 inch centers. Open area was 21 % of the total area. The sample cavity was formed by 11 3/4 inch diameter holes cut in rings of polystyrene foam insulation. The outside diameter of the insulation rings was 24 inches.

The chamber was contained in a 24 inch diameter by 5 inch deep cylinder made of light gage aluminum sheet metal. The electrodes were centered in the cylinder by a masonite ring. The bottom electrode was supported and insulated by a solid circle of foam insulation 7/8 inch thick. The top electrode was insulated by a similar circle of insulation glued to a 3/4 inch thick by 24 inch diameter circle of plywood.

Three holes were drilled through the plywood, insulation and top electrode to allow thermometers to be inserted into the samples. One

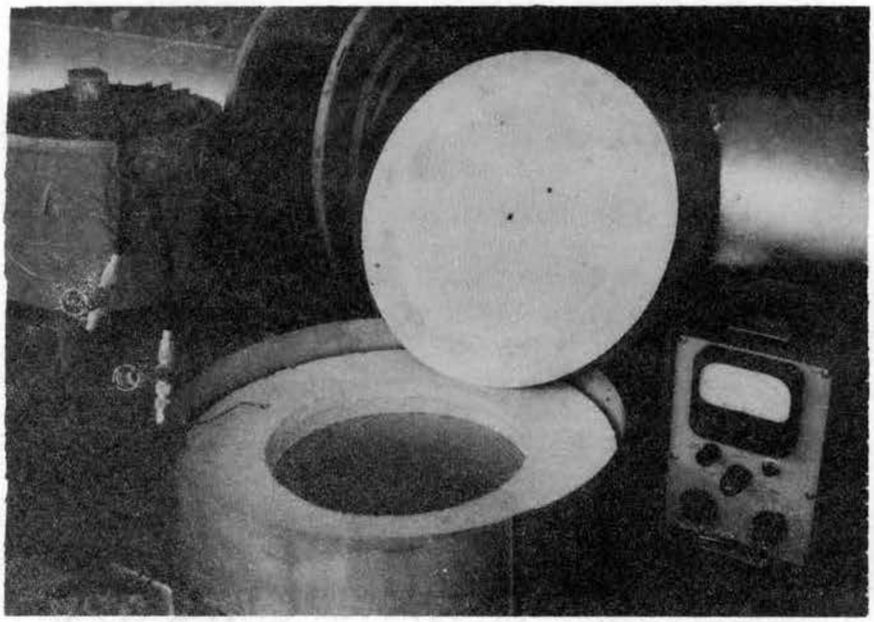

Figure 14. View of Radio-Frequency Heating Chamber with Top Electrode Removed.

hole was centered and the other two were spaced 2 1/2 inches apart along a radius. Laboratory grade mercury in glass thermometers with a range of -2.0 to +80.0 °C in 0.2 °C divisions were used for temperature measurements of the samples. An attempt to use thermocouples with a potentiometer failed because they could not be shielded adequately from the electric field.

The assembled heating chamber and circuit are shown in Figure 15. Fins were soldered to the outside of the container of oil holding the resistor. Small fans were also mounted under both the coil and the resistor to facilitate cooling.

The literature values for the dielectric properties of the insulation used in the heating chamber were nominally the same as

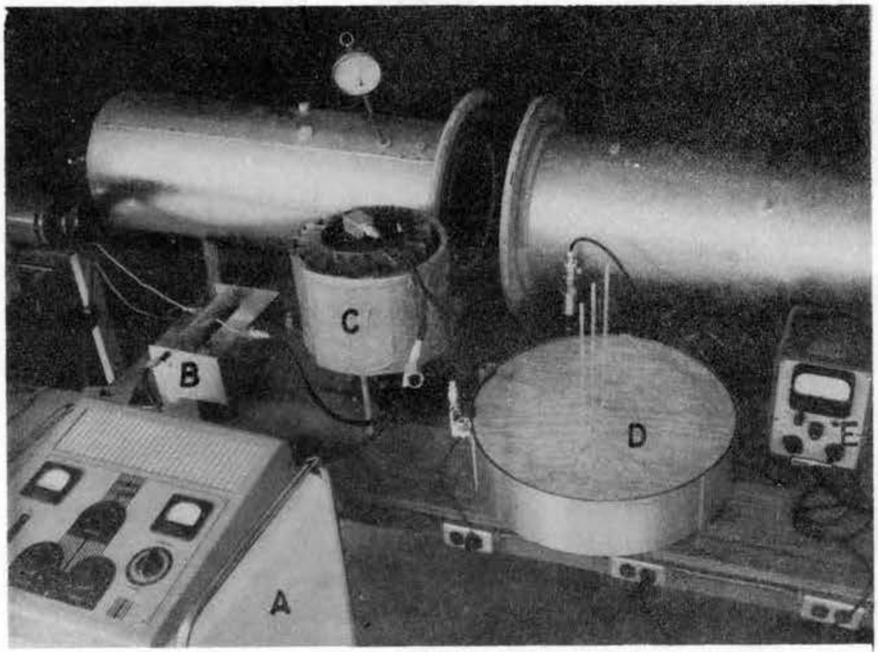

Figure 15. View of Assembled Radio-Frequency Heater. A - Radio-Frequency Generator; B - Coil; C - Resistor; D - Dielectric Heating Chamber with Thermometers; E - Vacuum Tube Volt Meter.

those for air, i.e.: $p = 0.0$ and $\varepsilon = 1.0$. Several tests were made with the cavity of the chamber empty and with it filled with insulation. No difference in total current flow in the circuit between the two situations could be detected for a constant voltage drop across the plates at constant plate spacings. A series of tests were then run to calibrate the voltage drop across the resistor, (R in Figure 13), against the voltage drop across the plates with the chamber empty.

For plate spacing of 1.656 inches:

$$V_{RE} = 0.0108831\ V_p^{1.09942} \tag{44}$$

$R_a = 1.7$ to 11.0, $S = 0.702881$, $R^2 = 0.920970$

For plate spacing of 0.828 inches:

$$V_{RE} = 0.121367\ V_p^{0.969456} \tag{45}$$

$R_a = 12.5$ to 36.0, $S = 0.355553$, $R^2 = 0.998278$

For plate spacing of 0.531 inches:

$$V_{RE} = 0.315845\ V_p^{0.840524} \tag{46}$$

$R_a = 15.0$ to 43.0, $S = 1.171091$, $R^2 = 0.981686$

where:

V_{RE} = Voltage drop across the resistor, R, volts.

V_p = Voltage drop across the plates, volts.

R_a = Range of V_{RE} in tests.

S, R^2 = Standard deviation and goodness of fit ratio, respectively, for the regression of the observed values of V_{RE} versus the values calculated by equations, (44), (45), and (46).

Now for the case of the chamber filled with peanuts:

$$V_R = V_t - (A_1\ V_{RE})/A_2 \tag{47}$$

where:

V_R = Voltage drop across the resistor, R, due to current flow through peanuts, volts.

V_t = Total voltage drop across the resistor, volts.

A_1 = Area of plates covering the peanut filled cavity, in^2.

A_2 = Total area of plates, in^2.

Finally:

$$I_t = \frac{V_R}{R} \tag{48}$$

where:

I_t = Current flowing through peanut sample, amps.

R = Resistance in circuit, (Figure 13), 50 Ω.

The following method was used to determine the heat capacity of the chamber. A very fine insulated iron wire was woven in and out of the perforations of the electrodes to serve as a heating element. The ends of the wire were connected to a Variac variable transformer. A Simpson ammeter was connected in series in the circuit and a Hickok voltmeter in parallel with the resistance wire. Thirteen tests were made using various settings of the variable transformer and recording the voltage, amperage and temperature rise of the chamber in 20 minute periods. The chamber was allowed to cool 6 to 12 hours between tests. Analysis of these data yielded the following equation:

$$Q_c = 0.84914\ \Delta T^{0.983088} \tag{49}$$

$$S = 0.0268067,\ R^2 = 0.997100$$

where:

Q_c = Energy required to raise the temperature of the chamber ΔT °F, Btu.

ΔT = Change in chamber temperature during the heating time, °F.

S, R^2 = Standard deviation and goodness of fit ratio, respectively, for the regression of the observed values of Q_c versus the values calculated by equation (49).

Electrical connections were made to the components in the circuit with coaxial cable for the radio-frequency heating tests.

The center of the cable carried the total load since both sides of the radio-frequency generator operated above ground potential. The shield of the cable was not in the circuit but connected to the ground for safety. Voltage measurements with reference to ground were made at the connection to the high potential electrode, V_1, between the low potential electrode and the resistor, V_2, and between the resistor and the generator, V_3. Thus the voltage drop across the capacitor was $V = V_1 - V_2$, and across the resistor $V_R = V_2 - V_3$.

Voltage measurements were made with a Hewlett-Packard 410 B Vacuum Tube Voltmeter with a range of 0 to 300 volts in 6 scales. Connections were made into the line for the voltmeter with Hewlett-Packard 11043A Coaxial Type "N" Connectors. A Hewlett-Packard 11040A 100:1 capacitive voltage divider was used with the meter probe to measure voltages in excess of 300 volts on the high potential electrode. The entire apparatus was operated in a double walled grounded room 8 feet wide by twelve feet long by 6 feet high made of aluminum screen. This precaution was taken to avoid interference with local radio communications.

The peanuts were arranged in the chamber for each test run according to the test plan. They were put in layers for the tests requiring the long axis of the peanut to be perpendicular to the field, were placed on end for those tests requiring the long axis to be parallel to the field, and poured in loosely for the random orientation tests. Each test ran for 20.0 minutes. Voltages and temperatures were recorded at initiation of the test and every 5.0 minutes thereafter. One to two minutes were required to balance the circuit at the beginning of each test. Therefore, only the last 15 minutes of heating were used in analyzing the data.

Drying Equipment and Procedures

Figure 16 is a photograph of the assembled apparatus and Figure 17 a schematic of the same equipment. The right end of the system was the air inlet. On the inlet end were two heat exchangers in series to control the temperature of the incoming air. A 15 gallon insulated tank of water to which ice could be added if necessary furnished the cooling fluid for the exchangers. Inlet air temperature could be held at 66 °F $\pm$ 2.0° with this arrangement.

A humidity control chamber containing 13 shallow trays filled with a saturated salt solution was located between the two heat exchangers. The trays were 11 x 12 inches in size and 1/2 inch deep. They were mounted on a rack with 1/2 inch vertical spacings between each tray. Sodium bromide was used to prepare the saturated salt solution. The equilibrium relative humidity for this solution was estimated to be 59.5 % at 66 °F by extrapolating data given by Hall (18).

The air conditioning portion of the apparatus was connected to a circular duct by a transition section. Exposed areas of the humidity control chamber, the sides of the second heat exchanger and the transistion section were covered with 7/8 inch thick polystrene foam insulation. A heater made of coiled resistance wire was placed in the opening to the circular duct at the end of the transition section. This heater was controlled externally by a Variac variable transformer and was used to add heat to the air for those tests run at 95°F.

The circular duct was double walled and made of 22 gage sheet metal. The inside diameter was 12 3/4 inches and the outside 14 1/4

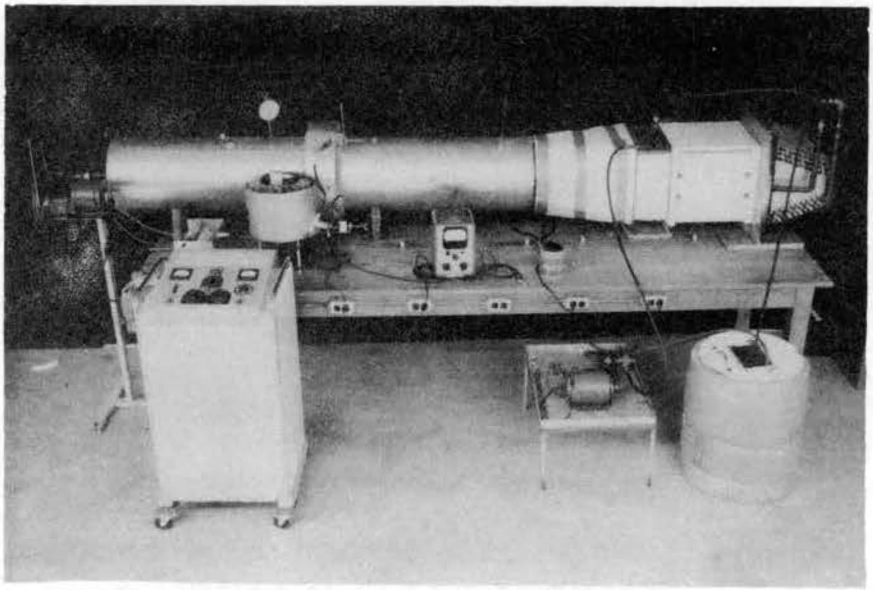

Figure 16. Overall View of Radio-Frequency Heating and Drying Apparatus

inches. The intra-annular space was filled with polystyrene foam insulation. The duct was made in two 3 foot sections. One end of each section had a 24 inch diameter flange made of plywood. The sections were joined by mounting the dielectric heating chamber on the flanges and clamping them together with three adjustable clamps.

Air was drawn through the system by an eight blade vane-type fan in the exit end of the duct. The fan was driven by a V-belt and pulley arrangement from an Zero-Max variable speed drive electric motor.

Electronic devices could not be used in the system to measure air velocity, humidity, or temperature because of the electric field. The thermometers used previously in the power absorption tests were

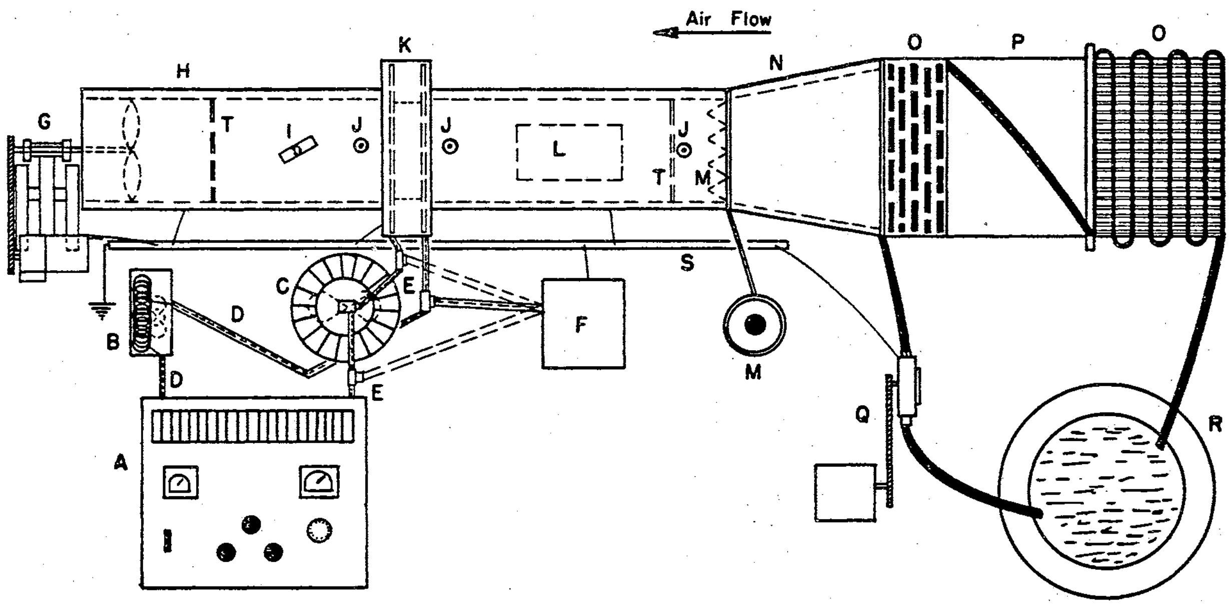

A – Radio-Frequency Transmitter
B – Circuit Balancing Coil with Cooling Fan
C – 50 Ohm Resistor in Oil Bath with Cooling Fan
D – Coaxial Cables
E – Voltmeter Connections
F – Vacuum Tube Voltmeter
G – Fan with Variable Speed Drive Electric Motor
H – Circular Duct
I – Hygrometer
J – Thermometers
K – Peanut Heating Chamber with Perforated Capacitor Plates
L – Hygrothermograph
M – Resistance Heater and Variable Transformer
N – Duct Transition Section
O – Heat Exchangers in Series
P – Humidity Control Chamber Containing Salt Solution Trays
Q – Water Pump and Electric Motor Drive
R – 15 Gallon Water Tank
S – Grounding Buss Bar
T – Radio Wave Grounding Shields

Figure 17. Top View Schematic of Radio-Frequency Heating and Drying Apparatus.

mounted in the duct with their bulbs at the duct centerline. One thermometer was located near the transition section and one was mounted on either side of the dielectric heating chamber. A Green recording hygrothermograph was placed in the duct near the transition section to measure the relative humidity of the incoming air. A Quicktest hygrometer was mounted in the duct downstream from the heating chamber to measure exit air humidity.

Air flow rates for the tests were determined by developing a calibration curve for the fan versus the setting on the adjustable drive motor. A Biram wind-vane anemometer was installed in the inlet end of the circular duct. Flow rates were recorded for four convenient fan settings using peanuts of three different moisture contents. There were a total of 32 tests. The four average flow rates obtained were 11.45, 23.32, 36.12, and 47.80 cfm per square foot of heating chamber crossectional area. Moisture content of the peanuts had no apparent effect on the air velocities. Maximum variation from the averages was less than $\pm$ 4.0 % at the lowest velocity decreasing to less than $\pm$ 1.0 % at the highest.

Test runs for drying peanuts were 60 minutes in length. Inlet and outlet dry bulb temperatures and outlet relative humidity were recorded initially and at 5 minute intervals during all tests. Voltages were recorded similarly for those tests where dielectric heating was used. Inlet relative humidity was recorded by the hygrothermograph.

The hygrothermograph was removed from the duct at the end of each day's testing and the chart replaced. The calibration of both the hygrometer and hygrothermograph were checked at the beginning of each day's testing with a Bendix sling psychrometer.

The ratio of the initial nut temperature to the inlet air temperature, $T_e/T_n = \Pi_6$, was to be held constant. During the testing period the air temperature in the laboratory was maintained as close to 66°F as possible and varied approximately $\pm$ 3°F from this at floor level where the samples were stored. The samples to be tested at 95°F were warmed for six to eight hours in sealed containers in a forced draft oven prior to testing.

A maximum differential of 9.16°F between the incoming and exit air for the dielectric drying tests indicated that the cooling effect of the evaporating moisture was greater than expected. It also indicated that the maximum temperature within the peanuts was probably much less than the maximum recommended drying temperature of 95°F. A series of tests with the electrodes spaced 0.828 inches apart, (half the spacing used in the original test plan), was added. This series was similar to the two series shown in Part II of Table III with two exceptions. First, the radio-frequency heater was operated at approximately 90 % of its capacity. Secondly, the length of the test runs was reduced to 30 minutes to prevent overheating of the resistor in the circuit. This resulted in equivalent Π_4 values equal to 1/2 of those in Table III.

CHAPTER V

RESULTS

Peanut Characteristic Length

The previously defined characteristic length was the average maximum dimension parallel to the electric field and direction of air flow. The characteristic length, then, was the average maximum diameter for peanuts oriented with their long axes perpendicular to the electric field and direction of air flow. Analysis of the data taken from the photographs of the cut sections of twelve peanuts yielded a ratio of 0.532512 average maximum diameter to length.

The length of 120 peanuts selected at random from the power absorption and drying tests was measured. The range of their moisture contents was 0.0 to 54.5 % dry basis. No effect on length due to moisture content was observed and the average length was 0.938400 inches. The characteristic length for the peanuts used in the power absorption and rate of drying tests therefore was:

$\zeta = 0.532572 \times 0.938400 = 0.499765$ inches.

The characteristic length for the power absorption tests where the peanuts were oriented with their long axes parallel to the electric field was taken as the average length. A characteristic length for the case of randomly oriented peanuts was assumed to have a value between 0.499765 and 0.938400 inches. An estimate was an average of these two dimensions, 0.719033 inches.

Power Absorption Tests

Equation (37) developed in Chapter III formed the basis for analyzing the data from the heating tests. The data from these tests are tabulated in Appendix C.

$$\cos\Theta = \frac{K_2 \, (C_p \, W_w \, \Delta T + Q_c)}{K_1 \, E \, I_t \, v \, t} \tag{37}$$

where:

$\cos\Theta$ = Power factor of peanuts.

K_1 = A constant, 16.93 cm^3/in^3.

K_2 = A constant, 17.57 watt-min/Btu.

C_p = Specific heat of the peanuts from equation (41), Btu/lb. °F.

W_w = Wet weight of peanuts, lbs.

Q_c = Heat required to raise the temperature of the chamber ΔT degrees from equation (49), Btu.

E = Electric field strength between the heating chamber plates, volts/in.

I_t = Total current flow in the circuit from equation (48), amps.

v = Volume of heating chamber, in^3.

t = Heating time, min.

ΔT = Change in temperature of the peanuts during the heating time, °F.

A theoretical basis for assuming that the dielectric properties of a biological material would vary with the electric field strength could not be found, although this possibility existed. The experimental plan called for three sets of tests — four moisture contents each at a plate spacing of 1.656 inches — to be run at different field strengths. Both electrodes operated above ground potential and the voltage on each was measured with reference to ground with a single voltmeter. This arrangement made it difficult to maintain an exact field strength for each moisture content within a set of tests. The field strength within each set was therefore estimated by maintaining a constant reading on the power tube plate current ammeter on the generator. This procedure eliminated excessive manipulation of the generator controls and voltmeter probe. The result, however, was three ranges of field strengths instead of exact values, (runs 1-24, table in Appendix C). There was no obvious effect on the power factor or the conductivity due to field strength so it was assumed that equations (36), (37) and (40) would hold for these quantities.

$$\text{Cos}\,\Theta = f(m, d/\zeta, \nu, f) \tag{36}$$

where:

m = Moisture content of the peanuts, decimal per cent dry basis.

d = Distance between the electrode plates, in.

ζ = Characteristic length of peanuts perpendicular to the electric field, in.

ν = Ratio of volume of peanuts in the heating chamber to the total volume of the chamber.

f = Frequency, MHz.

Frequency is the only term above that was not varied in the tests due to equipment limitations. The following model for $\cos\Theta$ as a function of moisture content was assumed based on the shape of loss factor curves for other biological materials (1):

$$\text{Cos}\Theta = C_1 + C_2\, m^{n_1} \tag{50}$$

where:

C_1, C_2, n_1 = Constants.

The power factor, $\cos\Theta$, could be assumed to vary with the filled fraction of the heating chamber. The filled fraction, ν, would affect both terms on the right hand side of equation (50), such that $\cos\Theta$ would be a maximum at $\nu = 1.0$ and equal to zero at $\nu = 0.0$.

The d/ζ ratio is an index of the electric field distortion. It was assumed to have very little effect on the power factor at zero moisture content. This assumption is based on the fact that electric field distortion increases as the dielectric constant increases, (Figure 3) and the dielectric constant could be expected to be low for zero moisture content. Further, the effect of the d/ζ ratio on the power factor could be expected to decrease asymptotically to some constant value as d/ζ increased.

The following equation form was taken to include all of the effects noted above:

$$\text{Cos}\Theta = C_1\, \nu^{n_2} + C_2(1.0 + e^{-C_3 d/\zeta})\, \nu^{n_3}\, m^{n_1} \tag{51}$$

Analysis of the data for the tests with peanuts arranged with their long axes perpendicular to the electric field yielded the following equation:

$$\text{Cos}\,\Theta = 0.185874\, \nu^{1.44355} + 1.655745\, \nu^{1.63001}$$

$$X(1.0 + e^{-0.37328\, d/\zeta})\, m^{1.36113} \tag{52}$$

$R_a = 0.028$ to 0.630, $S = 0.048090$, $R^2 = 0.882423$

where:

R_a = Range of $\cos\Theta$.

S, R^2 = Standard deviation and goodness of fit ratio, respectively, for the regression of the observed values of $\cos\Theta$ versus the values calculated by equation (52).

(Note: Statistics for subsequent prediction equations will be given in the preceding manner.)

The results of these tests are presented graphically in Figure 18. Several other equation forms were tried but none gave a correlation as high as equation (51).

A small amount of data was taken for the two cases of random orientation of the peanuts in the heating chamber and orientation of the peanuts with their long axes parallel to the electric field. The intent of these tests was to determine if an equation form similar to equation (51) could adequately describe the power factor for these arrangements. The results of these limited tests were not satisfactory. An equation for $\cos\Theta$ as a function of moisture content alone was obtained, (equation (53)), for the case of random orientation but it is not considered useful except to show that the power factor increases with increasing moisture content. Attempts to include the effects of the filled fraction, ν, and several different estimates of d/ζ, resulted in a marked loss of correlation. The data for the case of parallel orientation were too erratic to yield any acceptable equation.

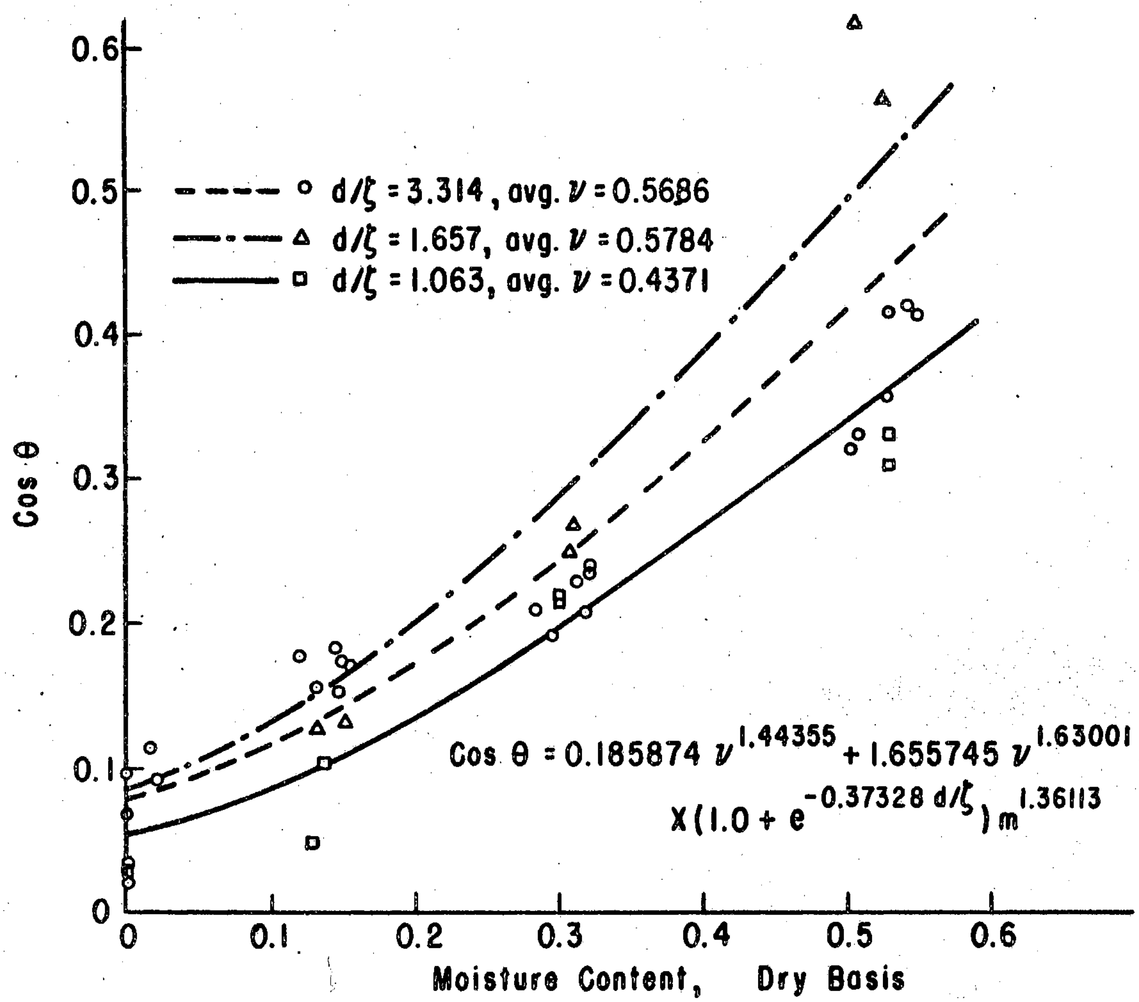

Figure 18. Power Factor, Cosθ, for Peanuts in a Radio-Frequency Field of 13.56 MHz with Their Long Axes Perpendicular to the Field.
ν = Volume of Peanuts per Volume of Chamber.
d/ζ = Electrode Spacing/Peanut Characteristic Length.
m = Moisture Content, Dry Basis.

Several possibilities exist for the lack of reasonable results in the random and parallel orientation tests. One, of course, is experimental error. A second is that the number of samples, (eight in each case), was too small to indicate the effects of the variables. A third possibility is that the development of the problem in terms of the variables chosen and their assumed relationships is not general enough to include all possible arrangements of peanuts in the heating chamber. More work needs to be done, in any case, to determine if the model chosen for peanuts oriented with their long axes perpendicular to the electric field can be generalized for other orientations.

For the random arrangement:

$$\text{Cos}\,\Theta = 0.127338 + 0.470289\ m^{1.38841} \tag{53}$$

$R_a = 0.10$ to 0.37, $S = 0.038183$, $R^2 = 0.811176$

Power absorption may also be calculated by equation (39) if the current flow in a circuit is not known.

$$P = \sigma E^2 \tag{39}$$

where:

P = Power absorbed, watts/in^3.

σ = Conductivity, mhos/in.

E = Electrical field strength, volts/in.

Now from equation (38):

$$\text{Cos}\,\Theta\ I_t = \sigma\ E \tag{38}$$

Or:

$$\sigma = E/\cos\Theta\ I_t$$

where:

I_t = Total current flow in circuit per unit area of chamber, amps/in^2.

Values of σ for the data in the heating tests were obtained by using Equation (37) to obtain $\cos\Theta$. The functional relationship of σ was previously expressed similarly to that for $\cos\Theta$, i.e.:

$$\sigma = f(m, d/\zeta, \nu, f) \qquad (40)$$

Frequency, again, was not a variable in these tests. Several trial attempts were made without success to determine an experimental equation that would include the d/ζ ratio. It was assumed then that the conductivity of the samples was only a function of the moisture content and filled fraction of the chamber. The d/ζ effects may have been masked by the fact that σ is expressed in terms of unit length.

The results were:

$$\sigma = 1.96880\ \nu^{1.62484} + 631.5663\ \nu^{3.38104}\ m^{1.70454} \qquad (54)$$

R_a = 0.39 to 33.22, S = 2.564201, R^2 = 0.954882

where:

σ = Conductivity, micro-mhos/in.

These data and equation (54) are depicted graphically in Figure 19.

Equations (51) and (54) may be used to determine the bulk dielectric constant, (refer to Figure 2), since:

$$\tan\Theta = \frac{2\Pi\varepsilon\varepsilon_o f}{\sigma} \qquad (55)$$

where:

ε = Bulk dielectric constant, dimensionless.

ε_o = Dielectric constant of free space, $22.479\mathrm{X}10^{-14}$ farads/in.

An example of the bulk dielectric constant at 13.56 MHz for

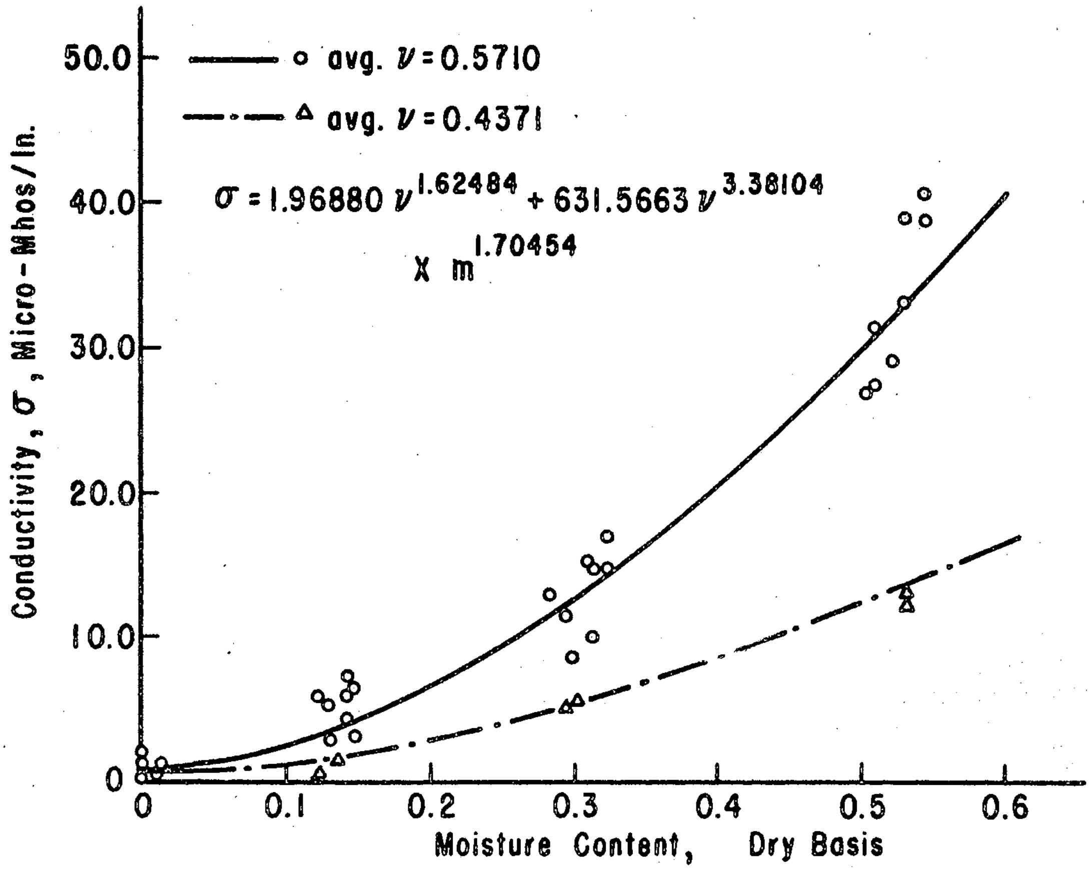

Figure 19. Conductivity, σ, for Peanuts in a Radio-Frequency Field of 13.56 MHz with Their Long Axes Perpendicular to the Field. ν = Volume of Peanuts per Volume of Chamber. m = Moisture Content, Dry Basis.

peanuts oriented with their long axes perpendicular to the electric field is calculated here by assuming the following typical quantities:

$m = 0.43$ moisture content, dry basis, (30.0 % wet basis).

$\nu = 0.571$, filled fraction of chamber.

$d/\zeta = 3.314$

Using these values in equation (51), (54), and (55) yields:

$\varepsilon_1 = 3.20$

Using Whitney and Porterfield's (52) equation (13) for bulk dielectric constant of whole peanuts as a function of frequency and moisture content only yields:

$\varepsilon_2 = 3.50$

Using a moisture content of 0.11, (10.0 % wet basis), with the other factors held constant yields: $\varepsilon_1 = 1.91$ and $\varepsilon_2 = 1.78$. The close agreement between the two methods of calculating the bulk dielectric constant indicates the possibility of relating dielectric properties as measured by a standardized test — the Q-meter test as used by Whitney and Porterfield for example — to the actual power absorption rates under dissimilar conditions.

Rate of Drying Tests

The variables associated with the peanut drying process were developed in terms of dismensionless numbers or Π terms in Chapter III. The terms considered to be the most important and used in the drying tests were:

$\Pi_1 = M_R$, Moisture loss during drying time, t, decimal % dry basis; the dependent variable.

$\Pi_2 = \Delta M$, Initial moisture content minus the moisture content at equilibrium with the incoming air, decimal per cent dry basis.

$\Pi_3 = (T_e - T_1)/T_e$, Where: T_e = entering dry bulb air temperature, °F, and T_1 = an ideal leaving air temperature following a wet bulb drying process, °F, (See Figure 5).

$\Pi_4 = A_v\, t/\zeta$, Where: A_v = air flow rate, cfm per square feet of sample crossectional area, t = drying time, min, and ζ= a characteristic length of the peanut perpendicular to the air flow, ft.

$\Pi_5 = \Delta P\ t/C_a T_e$, Where: ΔP = Power input to the peanuts from the radio-frequency field minus the power input at the same field strength to dry peanuts, Btu/min-in^3, and C_a = volumetric specific heat of entering air, Btu/in^3°F.

The data for all of the drying tests is tabulated in Appendix D. The first phase of the tests were conducted without dielectric heating, ($\Pi_5 = 0$), to establish a relationship for forced convective drying. Two entering air conditions were to be used: (1) dry bulb temperature = 66°F at 60 % relative humidity and (2) 95°F at 23 % relative humidity. Actual conditions during the tests were: (1) average temperature = 65.49°F, + 3.57, - 1.63 with an average relative humidity of 53.25 %, + 10.0, - 7.25 and (2) average temperature = 93.37°F + 1.75, - 2.33 with an average relative humidity of 16.88 %

+ 5.12, - 2.88. Temperature control in the apparatus was adequate but humidity control was not as good as desired.

Previous investigators (17), (30), and (37) assumed that the effects of the drying potential terms, Π_2 and Π_3 could be expressed as:

$$\Pi_1 = C_1 \ (\Pi_2 \ \Pi_3)^{n1} \tag{56}$$

Figure 20, a plot of Π_1 versus Π_2 Π_3 on log-log coordinates, demonstrates that this assumption was essentially correct for the present case. The plot indicated that the exponents of Π_2 and Π_3 if treated separately should be about equal. The computer program used allowed for computing individual exponents for these two terms and they were approximately equal in magnitude as shown in equation (58). Interestingly the values of these exponents for peanuts compare very closely with the value of $n_1 = 0.774$ in equation (56) determined for sorghum, wheat and rye by Nelson, Mahoney and Fryrear (30).

Another requirement of the prediction equation is that the dependent term, Π_1, approach zero as the velocity term, Π_4, approaches zero and also that Π_1 approach a maximum value as Π_4 becomes very large. The following equation for Π_1 was assumed to meet these requirements:

$$\Pi_1 = C_1 \ \Pi_2^{n1} \ \Pi_3^{n2} \ (1.0 - e^{-C_2 \ \Pi_4}) \tag{57}$$

Analysis of the data yielded the following equation:

$$\Pi_1 = 0.662930 \ \Pi_2^{0.782806} \ \Pi_3^{0.701823}$$
$$\times(1.0 - e^{-6.8689\times10^{-5}\Pi_4}) \tag{58}$$

$R_a = 0.023$ to 0.153, $S = 0.006234$, $R^2 = 0.97355$

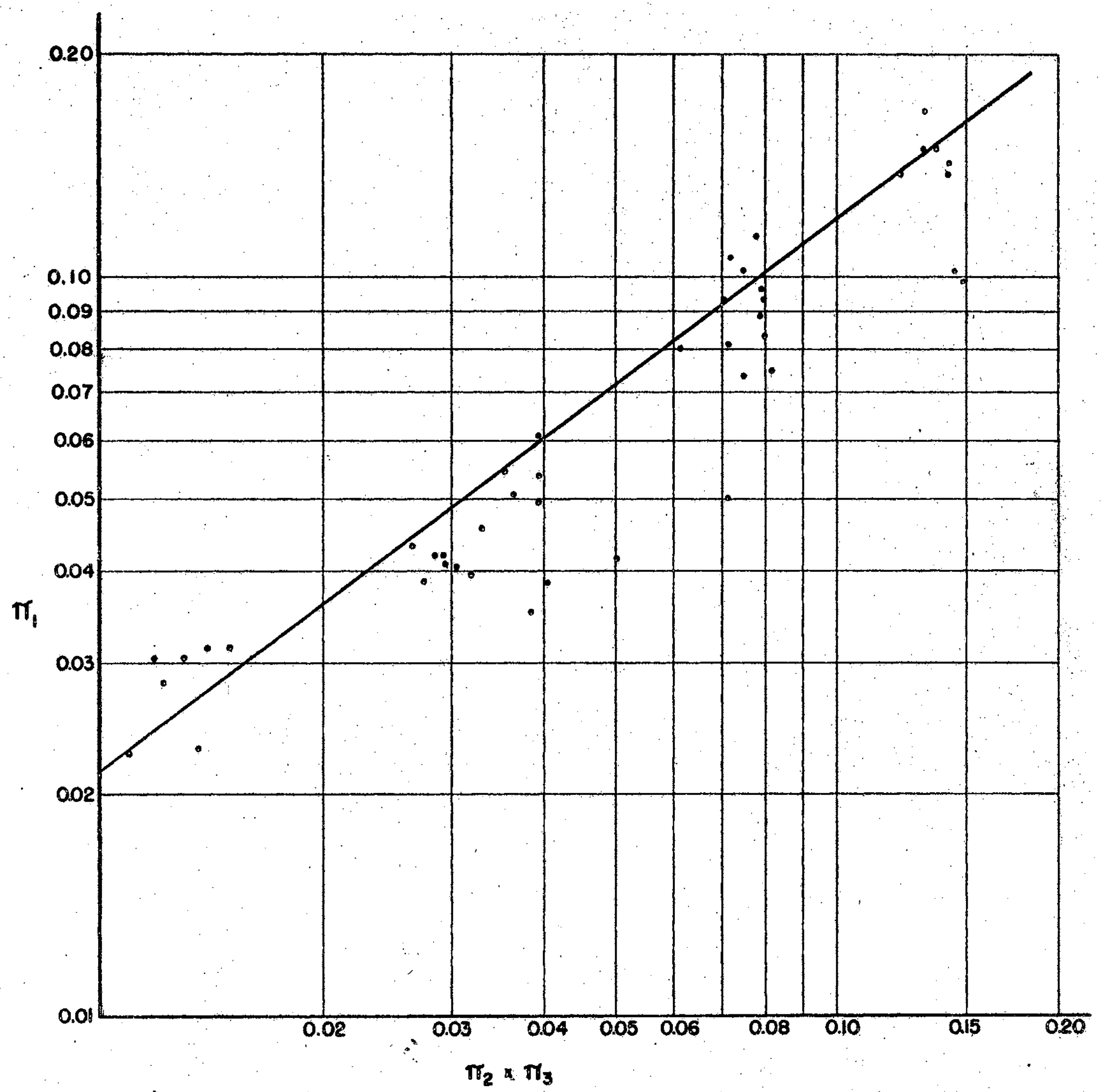

Figure 20. Dependent Drying Term Π_1 Versus the Product of the Drying Potential Terms Π_2 and Π_3.

The effects of the velocity term, Π_4, shown in Figure 21 indicate that the equation form selected met the requirements above.

The index for the effect of the length of time the air was in contact with the peanuts was $\Pi_7 = d/\zeta$, the ratio of the depth of the sample parallel to air flow to the characteristic length. This term was held constant at $\Pi_7 = 3.314$ in the tests above. The depth of the peanut samples was decreased by one-half, $\Pi_7 = 1.657$, in one series of the tests using radio-frequency heating. This was done to maximize the electric field strength and power absorption by the sample without overloading the radio-frequency generator. It also required that some means of estimating the effects of Π_7 be devised so that the data from these runs could be included in the analysis.

Five successive layers of peanuts, $\Pi_7 = 3.314$ for each, were assumed. The average amount of moisture removed per minute from the first layer in a 60 minute drying period was calculated by using equation (58) and an average sample weight. New values for relative humidity and temperature for the exiting air were calculated from the amount of moisture added to each pound of air flowing through the sample. Brooker's (8) equations for the psychrometric chart were used in these calculations. Values of Π_2 and Π_3 were then calculated for the second layer using the values of relative humidity and temperature of the air exiting from the first layer. This process was repeated for each successive layer.

The following values of the variables in the terms were assumed to calculate the $\Pi_7 = d/\zeta$ effect:

$M_i = 0.36$, initial peanut moisture content,

dry basis, average.

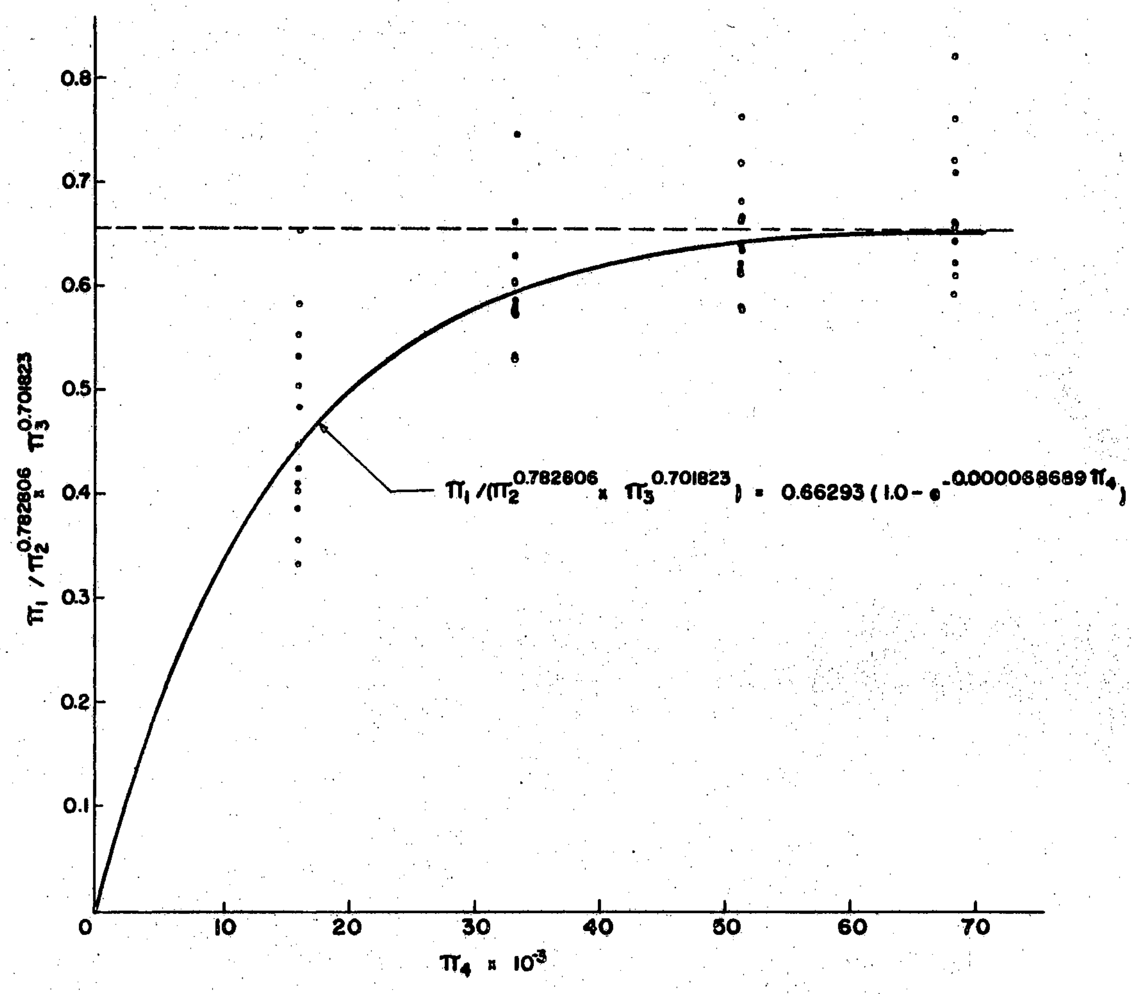

Figure 21. Equation of Forced Convective Drying of Peanuts, in Terms of Dimensionless Parameters.

$T_e = 66^\circ F$, entering air temperature.

$R_h = 50.0$ %, entering air relative humidity, average.

$A_v = 30$ fpm, air velocity, average.

$t = 60$ min., drying time.

$\zeta = 0.500$ in., peanut characteristic length.

$W_d = 1.982$ lb., dry weight of all samples, average.

$T_d = 0.00133$ lb. $H_2O/\text{min}^\circ F$, average.

The quantity, T_d, is an average ratio of the pounds of water per minute to the drop in air temperature as measured in all of the Part I drying tests. The heat to evaporate moisture from the peanuts would come from both the air and the peanuts. Calculation of T_d was a means of estimating the heat loss from the air. This ratio was assumed to hold for the second and successive layers. Other average conditions in the list were averages of the conditions for those tests in Part I with 66°F and 50.0 % relative humidity entering air.

Adding successive layers together gave Π_7 values of 3.314, 6.628, 9.943, 13.257, 16.571. Π_1 was determined for each value of Π_7 by averaging the percent moisture loss over the number of layers within each Π_7 value. The values of Π_1 versus Π_7 were plotted on semi-log coordinates as shown in Figure 22. This plot shows that the drying effectiveness decreased in an exponential manner with increasing sample depth, as expected. The equation obtained was:

$$\Pi_1 = 0.073300/1.04238^{\Pi_7} \tag{59}$$

The first constant in equation (58) was $C_1 = 0.662930$. This constant was obtained for samples with a depth to peanut characteristic

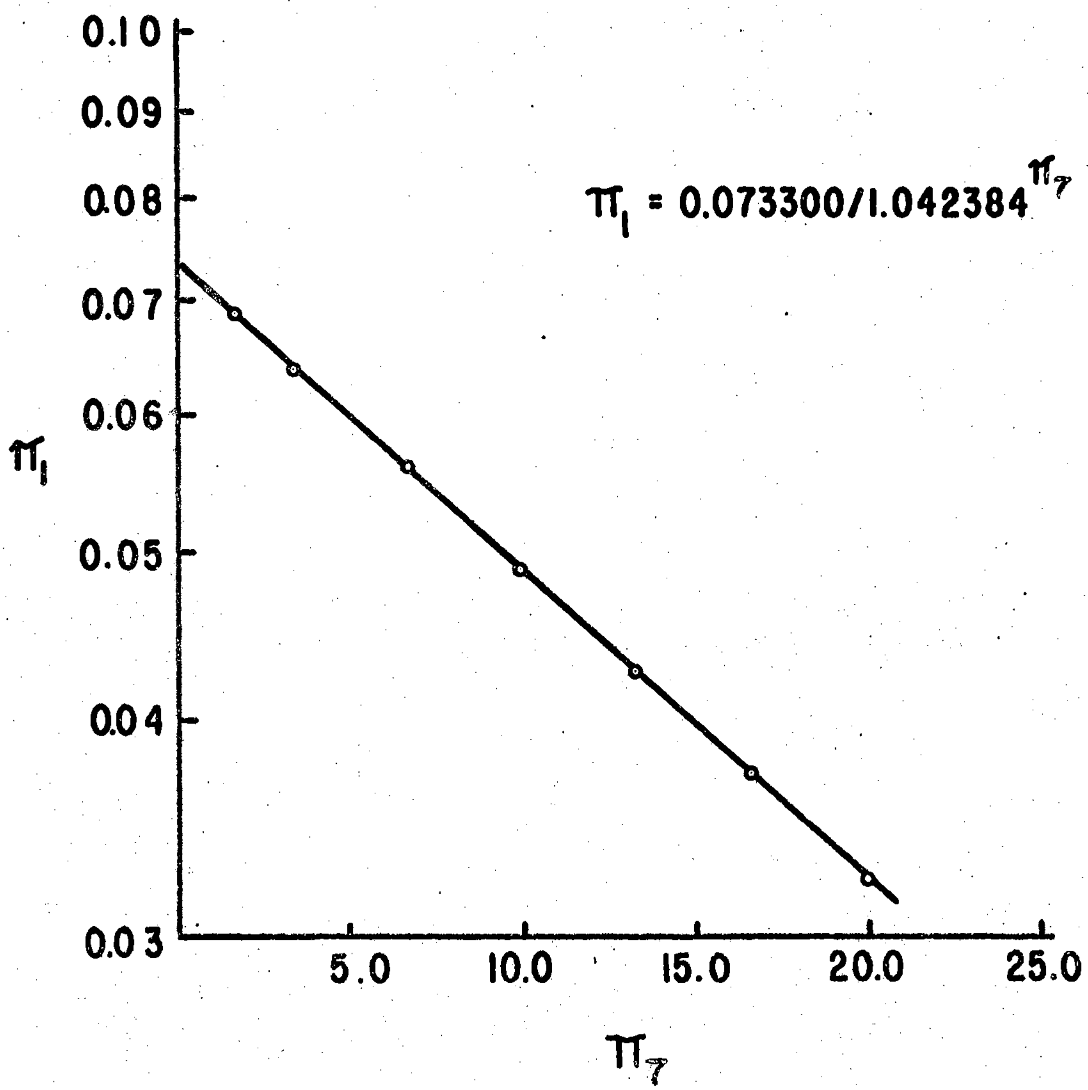

Figure 22. Effect of the Ratio of Sample Depth to Characteristic Length, Π_7, on the Percentage of Moisture Removed from Peanuts in a Given Time by Forced Convection, Π_1.

length ratio of $\Pi_7 = 3.314$. To include the effect of Π_7 in equation (58) then:

$$0.662930 = C_1/(1.04238)^{3.314}$$

$$C_1 = 0.760693$$

Modifying equation (58) to include the effect of Π_7 yields:

$$\Pi_1 = 0.760693(1.04238)^{-\Pi_7} \quad \Pi_2^{0.782806} \quad \Pi_3^{0.701823} \times (1.0 - e^{-6.8689X10^{-5}\Pi_4}) \tag{60}$$

The term that expressed the effects of adding heat to the peanuts from the radio-frequency field was $\Pi_6 = \Delta P\ t/C_a\ T_e$. Δ P is the average electrical power per unit volume applied to the sample during the drying time minus the electrical power per unit volume that would be applied at the same electrical field strength if the sample were dry. Equations (5) and (52) were used with the average values of the voltages taken during each test run and the average moisture content of the sample to determine the average power applied. Equations (39) and (54) were used to calculate the power that would have been applied to a similar dry sample with the same average field strength. The volumetric specific heat C_a was calculated by using the entering air temperature, T_e, and entering relative humidity in Brooker's (8) equations.

The requirements for selecting a model for drying that would include the power term, Π_5, were: (1) the drying effects would be the same as those predicted by equation (57) when $\Pi_5 = 0.0$ and (2) the drying effects would equal zero for any value of Π_5 when one of the other independent Π terms became zero. Several such models were tried and the following gave the best results:

$$\Pi_1 = 0.760693(1.04238)^{-\Pi_7} \ \Pi_2^{0.782806} \ \Pi_3^{0.701823}$$
$$(1.0 - e^{-6.8689X10^{-5}\Pi_4}) \ (1.0 + 0.0223669\Pi_5^{0.37760}) \quad (61)$$

$R_a = 0.02230$ to 0.1536, $S = 0.016278$, $R^2 = 0.781024$.

Equation (61) is depicted graphically in Figure 23. Other models that did not correlate as well with the experimental data included a multiplicative term, $ce^{n\Pi}$, and terms that were additive to the drying potential terms, i.e. $(\Pi_2 + C\Pi_5^n)^{0.782806}$ and $(\Pi_3 + C\ \Pi_5^n)^{0.701823}$.

An example using typical conditions will serve to compare the effects of drying peanuts with and without the use of radio-frequency heating. The following conditions are assumed for drying with heated air and without using radio-frequency heating:

$M_i = 0.36$, initial peanut moisture content, dry basis.

$T_e = 95.0°F$, entering air temperature.

$R_h = 23.0$ %, entering air relative humidity.

$B_d = 1.103 \ X \ 10^{-2}$ lb/in^3, bulk density of dry peanuts.

$\nu = 0.571$, filled fraction of sample container.

$d = 1.6563$ in., depth of sample.

$\zeta = 0.500$ in., peanut characteristic length.

$t = 60.0$ min., drying time.

$A_v = 30$ cfm/ft^2, air flow rate.

Using Figure 6 and thepsychrometric chart, (in the manner of Figure 5), and the quantities above the following values are obtained:

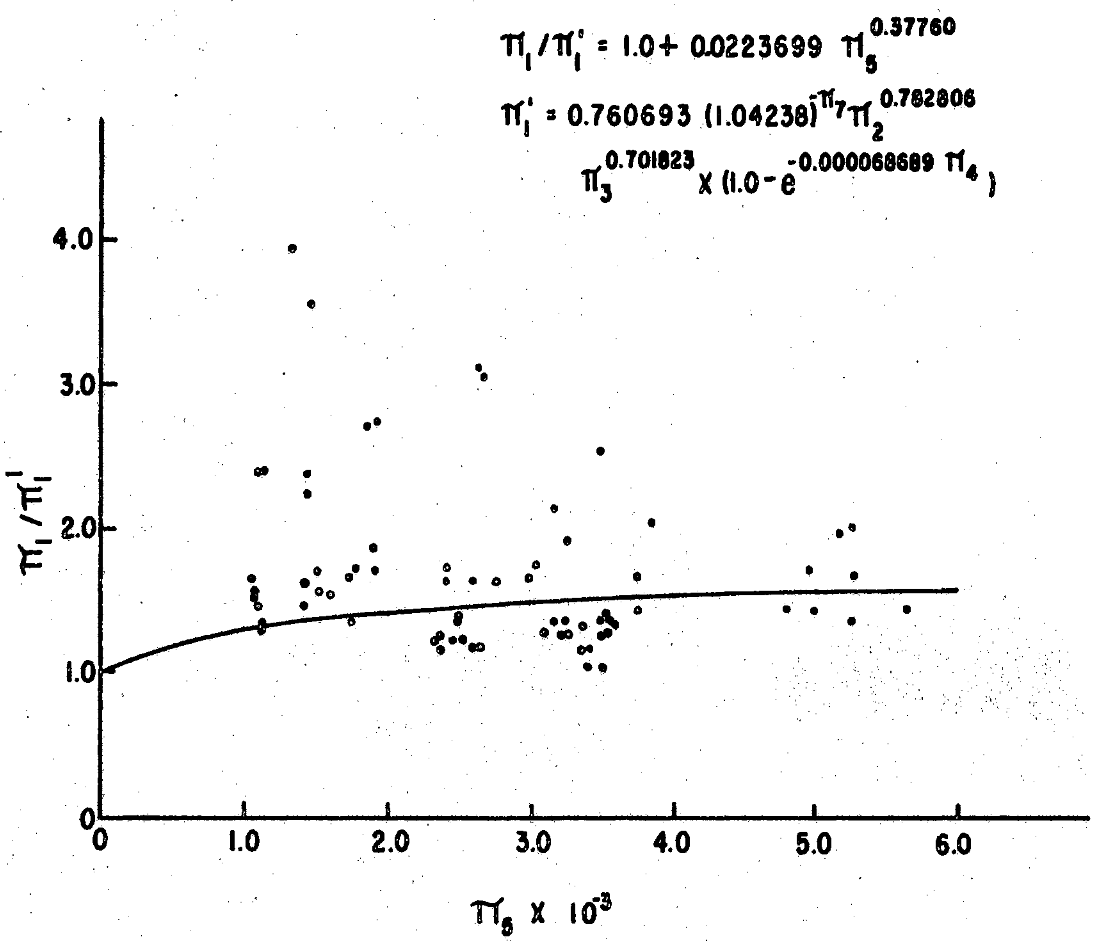

Figure 23. Drying Effect Due to Radio-Frequency Heating of Peanuts in Forced Convective Drying Versus a Dimensionless Power Input Term, Π_5

$$\Pi_2 = 0.360 - 0.055 = 0.305$$

$$\Pi_3 = \frac{95.0 - 68.3}{95.0} = 0.281$$

$$\Pi_4 = \frac{30 \text{ X } 60 \text{ X } 12}{0.500} = 43{,}220$$

$$\Pi_7 = \frac{1.6563}{0.500} = 3.314$$

Substituting these values in equation (60) yields:

$$\Pi_1 = 0.10184$$

To dry the peanuts using radio-frequency heating the following ambient air conditions are assumed:

$$T_e = 66\,^\circ F$$

$$R_h = 60.0\ \%$$

With these new conditions:

$$\Pi_2 = 0.360 - 0.084 = 0.276$$

$$\Pi_3 = \frac{66.0 - 58.2}{66.0} = 0.118$$

Substituting these values in equation (60) yields the drying effect from forced convection alone:

$$\Pi_1' = 0.04991$$

Referring to equation (61) the difference between Π_1 and Π_1' must be equal to the effect of the power term for an equivalent drying effect between the two systems, i.e.:

$$\Pi_1 - \Pi_1' = 0.05193 = \Pi_1' \quad 0.0223669 \quad \Pi_5^{\,0.377760} \tag{62}$$

Now:

$$\Pi_5 = \Delta P\ t/C_a\ T_e$$

For the incoming air conditions:

$$C_a = 1.03686 \text{ X } 10^{-5} \text{ Btu/in}^3\text{-}^\circ F$$

Solving equation (62) for ΔP yields:

$$\Delta P = 0.392267 \text{ watts/in}^3 = 0.022325 \text{ Btu/min-in}^3$$

Now:

$$\Delta P = \sigma_1 E^2 - \sigma_2 E^2 = (\sigma_1 - \sigma_2) E^2 \quad (63)$$

where:

σ_1, σ_2 = Conductivity of the wet and dry peanuts respectively, mhos/in.

E = Electrical field strength, volts/in.

Equation (54) may be used to compute σ_1 and σ_2 using the filled fraction value $\nu = 0.571$ and an average moisture content during drying of $m = 0.308$.

And:

$$P_i = \sigma_1 E^2 \quad (64)$$

where:

P_i = Average power input per unit volume during drying, Btu/min-in^3.

Solving equations (54), (63), and (64) yields:

$$P_i = 0.023712 \text{ Btu/min-in}^3 \text{ at } E = 175.4 \text{ volts/in.}$$

The amount of electrical energy required to evaporate a pound of water based on the total moisture loss in the one hour drying period is:

$$\text{Btu/lb. } H_2O = 60.0\ P_i/B_d\ \Pi_1 = 1266.6$$

A conservative estimate for the efficiency of a radio-frequency generator is 0.60. Using this figure 2111 Btu electrical power input would be required to remove a pound of water from the peanuts.

Beasley and Dickens (4) estimate an average of 2500 Btu are required to remove a pound of water from peanuts with a conventional heated air system. The exact conditions under which this estimate was obtained were not stated, however.

The average temperature rise in the air after flowing through the sample in the radio-frequency heating tests was 3.67°F. The maximum was 9.16°F. Although the peanut temperatures were not measured it was apparent that they did not increase greatly during the tests. The power applied in the tests ranged from 0.0135 to 0.903 Btu/min-in^3. A much greater increase in drying rate could be obtained without heating the peanuts above 95°F with a radio-frequency generator of greater capacity than the one available for these tests.

CHAPTER VI

CONCLUSIONS AND SUGGESTIONS FOR FURTHER WORK

Conclusions

The following conclusions are drawn from the results of the rate of heating study of peanuts in a radio-frequency field of constant frequency:

1. The power factor for peanuts oriented such that their long axes are perpendicular to the field is a function of their moisture content, m, the filled fraction of the space occupied by the peanuts, ν , and the ratio of the distance between the electrodes to a characteristic length of the peanuts parallel to the field, d/ζ.
2. The conductivity for peanuts oriented as above is also a function of moisture content and filled fraction of the space occupied by the peanuts. No effect of the d/ζ ratio could be detected.
3. The power factor and conductivity of peanuts oriented as above increases with increasing moisture content and with an increase in the filled fraction of the space occupied by the peanuts.
4. The power factor for peanuts oriented as above is

a maximum at a d/ζ ratio of 1.0 and decreases asymptotic to a constant value as the d/ζ ratio increases.

5. The dielectric properties of peanuts were not affected by electric field strength within the range of field strengths tested.

6. The power factor of randomly oriented peanuts increases as the moisture content increases.

The following conclusions are drawn from the results of peanut drying studies:

1. Equation (58) adequately predicts the drying effect, Π_1, for forced convective drying with a constant d/ζ ratio = 3.835, (Π_7).

2. The effects of the drying potential parameters — $\Pi_2 = \Delta M$ and $\Pi_3 = (T_e - T_1)/T_e$ — are similar. Π_1 increases as they increase.

3. Drying effect increases asymptotically from zero to a given value as the velocity term, $\Pi_4 = A_V\ t/\zeta$, increases from zero.

4. A reasonable estimate of the effect of the d/ζ ratio, Π_7, on the drying effect, (Equation (59)), is obtained by estimating the change in entering air conditions between successive layers from the amount of moisture added by each preceding layer. The drying effect decreases as the d/ζ ratio increases.

5. The effect of the radio-frequency heating term, $\Pi_5 = \Delta Pt/C_a T_e$, on the drying effect is best represented by a multiplicative term, $(1 + C\Pi_5^n)$, on to the convective drying equation, (Equation (61)).

6. A knowledge of the internal heat and mass transfer coefficients used in Π_{12} and Π_{13} would increase the accuracy of the prediction equations for drying, especially when internal energy generation is used.

Suggestions for Further Study

A comprehensive study, based on electric field theory, of power absorption of dielectric particles in a radio-frequency field would be very useful. This study could include the effects of frequency and particle size and orientation. A means of predicting rates of heating from dielectric properties as measured by some standardized test could also be developed.

Further work needs to be done in developing means of predicting the internal and surface heat and mass transfer coefficients of small hygroscopic particles. Knowledge of these variables combined with classical heat and mass transfer theory and numerical analysis could provide better estimates of drying rates than dimensional analysis. The classical approach to heat and mass transfer, however, requires a knowledge of particle shape. Standardized methods of obtaining and analyzing the large amount of data necessary to describe the shape of irregular objects would be useful.

The results of these drying studies with radio-frequency heating indicate a practical potential for this drying technique. Further work to develop design criteria for a commercial or on-the-farm dielectric dryer appears warranted. The most efficient electrode configuration, (coaxial, stacked plates), for batch drying could be determined. Methods could also be developed for continuous flow processes in which the material was heated intermittently by a radio-frequency field. Maximum heating rates and temperatures for quality control would also have to be determined.

BIBLIOGRAPHY

(1) Agricultural Engineers Yearbook, 16th ed., St. Joseph, Mich.: ASAE, 1969.

(2) Aristizabal, L., E. E. Burns, and O. R. Kunze, "Physical, Chemical and Organoleptic Properties of Peanuts Separated in a Controlled Air Stream," ASAE Paper No. 68-381.

(3) Arpaci, V. S., Conduction Heat Transfer, Reading Mass: Addison-Wesley, 1966.

(4) Beasley, E. O. and J. W. Dickens, "Engineering Research in Peanut Curing," North Carolina, Agricultural Experiment Station, Bulletin No. 155, Raleigh, N. C., 1963.

(5) Beasley, E. O. and J. W. Dickens, "Some Peanut Properties Which are Influenced by Harvesting and Curing Methods," Proceedings of the Peanut Improvement Working Group, Oklahoma State University, pp. 68-85, July, 1963.

(6) Beavers, John, "Some Physical Characteristics of the Spanish Peanut Pod and Kernel," Unpublished M.S. Thesis, Oklahoma State University, May, 1959.

(7) Borg, J. Z., "Non-Linear Damped Taylor Series Curve Filter" - A computer program written for the Louisiana State University Computer Research Center.

(8) Brooker, D. B., "Mathematical Model of the Psychrometric Chart," Trans. of the Am. Soc. of Agri. Engr. 10: 558-560, 563, No. 4, 1967.

(9) Brown, G. H., C. N. Hoyler and R. A. Bierwirth, Theory and Application of Radio-Frequency Heating, New York: D. Van Nostrand Co., 1947.

(10) Buckham, J. A. and T. R. Stuelpnagel, "A Correlation of Theoretical and Experimental Temperature Distribution in High Frequency Dielectric Heating," Unpublished M. S. Thesis, University of Washington, 1948.

(11) Carslaw, H. S. and J. C. Jaeger, Conduction of Heat in Solids, London: Oxford University Press, 1959.

(12) Cecil, S. R., "Relation of Certain Environmental and Cultural Factors to Peanut Quality," Proceedings of the Peanut Improvement Working Group, Oklahoma State University, pp. 16-25, July, 1963.

(13) Chaffin, W., "Peanut Production in Oklahoma," Oklahoma State University, Agricultural Extension Service, Circular E-410, pp. 21-22.

(14) Chemical Engineers Handbook, New York: McGraw-Hill, 1963.

(15) Chen, C. S. and W. H. Johnson, "Kinetics of Moisture Movement in Hygroscopic Materials: I. An Application to Foliar Materials," Paper No. 68-305, Am. Soc. of Agri. Engr., St. Joseph, Mich., July, 1968.

(16) Chen, C. S. and W. H. Johnson, "Kinetics of Moisture Movement in Hygroscopic Materials: I. Theoretical Considerations of Drying Phenomena," Trans. of the Am. Soc. of Agri. Engr., 11: 109-113, No. 1, 1969.

(17) Day, D. L., "Experimental Analysis of Cross-Flow Grain Drying in Deep Cylindrical Bins," Unpublished Ph.D. Thesis, Oklahoma State University, August, 1962.

(18) Hall, C. W., Drying Farm Crops, pp. 33-34, Reynoldsburg, Ohio: Agricultural Consulting Associates, 1957.

(19) Hammond, S. B., Electrical Engineering, New York: McGraw-Hill, 1961.

(20) Henderson, S. M. and R. L. Perry, Agricultural Process Engineering, pp. 282, 283, New York: John Wiley and Sons, 1955.

(21) Hutchinson, R. S., "Research Studies on Drying Farmers Stock Peanuts," Proceedings of the Fourth National Peanut Research Conference, University of Georgia, 1966.

(22) Karon, M. L. and B. E. Hillery, "Hygroscopic Equilibrium of Peanuts," Jour. of Am. Oil Chemistry Soc., 26: 16-19, No. 1, 1949.

(23) Kazarin, E. A. and C. W. Hall, "The Thermal Properties of Grain," Trans. of the Am. Soc. of Agri. Engr., 8: 33-37, 48, No. 1, 1965.

(24) Kinch, D. M. and C. C. Stoutenberg, "Predicting Internal Temperatures of Fruit During Thermal Processing," Paper No. 68-383, American Soc. of Agri. Engr., St. Joseph, Mich., 1968.

(25) Kramer, H. A., et al., "Spectrophotometric Investigations on Peanuts with Particular Reference to Estimation of Maturity." Food Technology, 17: 90-92, No. 7, 1963.

(26) Langhaar, H. L., Dimensional Analysis and Theory of Models, New York: John Wiley and Sons, 1951.

(27) Mann, C. A., N. H. Ceaglske and A. C. Olson, "Mechanism of Dielectric Drying," Industrial and Engineering Chemistry, 41: 1686-1694, 1949.

(28) Matthes, R. K., Jr. and H. D. Bowen, "Steady-State Heat and Moisture Transfer in an Unsaturated Soil," Paper No. 68-354, Am. Soc. of Agri. Engr., St. Joseph, Mich., 1968.

(29) Mills, W. T. and J. W. Dickens, "Harvesting and Curing the Windrow Way," North Carolina State University Agricultural Experiment Station Bulletin 405, 1958.

(30) Nelson, G. L., G. W. A. Mahoney and J. I. Fryrear, "Grain Drying and Conditioning Investigations," Oklahoma State University Agricultural Experiment Station Bulletin B-520, July, 1959.

(31) Nelson, S. O., "A Method for Determining the Dielectric Properties of Grain," Unpublished M. S. Thesis, University of Nebraska, June, 1952.

(32) Nelson, S. O., L. H. Soderholm and F. D. Yung, "Determining the Dielectric Properties of Grain," Agricultural Engineering, 34: 608-610, No. 9, 1953.

(33) Nelson, S. O. and E. R. Walker, "Effects of Radio-Frequency Electrical Seed Treatment," Agricultural Engineering, 42: 688-691, No. 12, 1961.

(34) Nelson, S. O. and W. K. Whitney, "Radio-Frequency Electric Fields for Stored Grain Insect Control," Trans. of ASAE, 3: 133-137, 144, No. 2, 1960.

(35) Parker, R. E. and J. A. Friesen, "Thermal Properties of Seed Cotton," Paper No. 68-301, Am. Soc. of Agri. Engr., St. Joseph, Mich., 1968.

(36) Pattee, H. E., E. O. Beasley and J. A. Singleton, "Isolation and Identification of Off-Flavor Components from High Temperature Cured Peanuts," Proceedings of the Third National Peanut Research Conference, Auburn University, pp. 66-68, July, 1964.

(37) RamaRao, V. V., F. T. Wratten and M. D. Faulkner, "Development of a Generalized Prediction Equation for Drying Rice in a Continuous Flow Intermittent Type Dryer," Paper presented at the Southwest Regional Meeting of the ASAE, Tyler, Texas, March, 1969.

(38) Schenk, Roy U., "Effects of Curing Temperature on Gas Permeability and Moisture Equilibrium of Stored Peanuts," Food Technology, 13: 667-669, 1959.

(39) Schenk, Roy U., "Source of Inner Brown Color of the Peanut Shell," Botanical Gazette, 121: 191-192, 1960.

(40) Schneider, P. J., Conduction Heat Transfer, Reading, Mass., Addison-Wesley, 1955.

(41) Schutz, P. W. and E. I. McMahon, "Dielectric Heating of Granular Materials," Industrial and Engineering Chemistry, 38: 179-184, 1946.

(42) Sharon, David, "Measurement of Peanut Quality and Factors Influencing It," Proceedings of the Peanut Improvement Working Group, Oklahoma State University, pp. 1-15, July, 1965.

(43) Smith, R. E., G. L. Nelson and R. L. Henrickson, "Analysis of Transient Heat from Anomalous Shapes," Transactions of the ASAE, 10: 236-245, No. 2, 1967.

(44) Smith, R. E., G. L. Nelson and R. L. Henrickson, "Applications of Geometry Analysis of Anomalous Shapes to Problems in Transient Heat Transfer," Transactions of ASAE, 11: 296-302, No. 2, 1968.

(45) Soderholm, L. H., "An Application of 40 Megacycle Radio-Frequency Energy for the Destruction of Rice Weevil in Wheat," Unpublished M. S. Thesis, University of Nebraska, June, 1953.

(46) Soderholm, L. H., "Effect of Dielectric Heating and Cathode Rays on Germination and Early Growth of Wheat," Agricultural Engineering, 38: 302-307, No. 5, May, 1957.

(47) Spath, H., "The Damped Taylor's Series Method for Minimizing a Sum of Squares," Communications of the Association of Computing Machinery, 10: 726-728, No. 11, Nov., 1967.

(48) Stetson, L. E., R. L. Ogden, and S. O. Nelson, "Effects of Radio-Frequency Electric Fields on Drying and Carotene Retention of Chopped Alfalfa," Paper No. 68-114, ASAE, St. Joseph, Mich., 1968.

(49) Thompson, D. R. and G. L. Zachariah, "Dielectric Properties of Apples," Paper No. 68-332, ASAE, St. Joseph, Mich., 1968.

(50) Whitaker, T. B. and J. W. Dickens, "The Effects of Curing on Respiration and Off-Flavor in Peanuts," Proceedings of the Third National Peanut Research Conference, Auburn University, pp. 71-86, July, 1964.

(51) Whitney, J. D., "Moisture Transfer in a Porous, Hygroscopic Solid," Unpublished Ph.D. Thesis, Oklahoma State University, May, 1966.

(52) Whitney, J. D. and J. G. Porterfield, "Dielectric Properties of Peanuts," Paper Presented at the Joint Meeting of the Southeast and Southwest Regions of the ASAE, Dallas, Texas, February, 1965.

(53) Whitney, J. D. and J. G. Porterfield, Unpublished data from research on the dielectric properties of peanuts.

(54) Whitney, J. D. and J. G. Porterfield, "Moisture Movement in a Porous, Hygroscopic Solid," Transactions of the ASAE, 11: 716-719, 723, No. 5, 1968.

(55) Woodward, J. D., R. S. Hutchinson and J. I. Davidson, Jr., "Drying Farmers Stock Peanuts with Low Temperature Air," Paper No. 69-345, ASAE, St. Joseph, Mich., 1969.

(56) Wratten, F. T., "The Application of Dielectric Heat to the Processing of Rice," Unpublished M. S. Thesis, Louisiana State University, May, 1948.

(57) Wratten, F. T., et al., "Physical and Thermal Properties of Rough Rice," Paper No. 68-809, ASAE, St. Joseph, Mich., 1968.

(58) Wright, M. E. and J. G. Porterfield, "Specific Heat of Spanish Peanuts," Paper presented at the Southwest Resional meeting of the ASAE, Tyler, Texas, March, 1969.

(59) Young, J. H., "Simultaneous Heat and Mass Transfer in a Porous, Hygroscopic Solid," Paper No. 68-353, ASAE, St. Joseph, Mich., 1968.

(60) Young, J. H., "A Study of the Sorption and Desorption Equilibrium Moisture Content Isotherms of Biological Materials," Unpublished Ph.D. Thesis, Oklahoma State University, May 1966.

(61) Young, J. H. and G. L. Nelson, "Theory of Sorption Isotherm Hysteresis in Biological Materials," Transactions of the Am. Soc. of Agri. Engr., 10: 260-263, No. 2, 1967.

APPENDIX A

SPECIFIC HEAT OF SPANISH PEANUTS

Expressions for the specific heat of Spanish peanuts were developed by Wright and Porterfield (58) using two methods. In the first method individual peanuts were heated in a small chamber surrounded by a resistance heating element. The second method was the commonly used method of mixtures for small batches of peanuts. The results were presented as quadratic multivariate equations. A non-linear curve fit computer program was used to simplify these expressions.

For the dry heated peanuts:

$$C_p = 0.704014 + 0.803355\ T^{-3.82133}\ m^{0.307002} \tag{65}$$

$$S = 0.102870\ ;\ R^2 = 0.556166$$

or:

$$C_p = 0.750828 + 0.481290\ m^{0.559337} \tag{66}$$

$$S = 0.112091\ ;\ R^2 = 0.473029$$

For the batch tests using the method of mixtures:

$$C_p = 0.365120 + 0.317126\ T^{-0.996}\ m^{0.652133} \tag{67}$$

$$S = 0.022114\ ;\ R^2 = 0.925108$$

or:

$$C_p = 0.402630 + 0.424561\ m^{0.880457} \tag{68}$$

$$S = 0.021784\ ;\ R^2 = 0.874349$$

where:

C_p = Specific heat, Btu/lb-°F

T = Temperature divided by 100, °F

m = Moisture content, decimal percent, dry basis.

S = Standard deviation for regression of the observed values versus the values calculated by the equation.

R^2 = Goodness of fit ratio for the observed versus the calculated values.

Figures 24 and 25 are graphic representations of the data from the tests and equations (65), (66), (67), and (68). The range of temperatures in the single peanut tests was 100°F to 150°F and equation (65) should not be extrapolated outside this range. Equation (66), however, is considered to be a good estimate of the effect of moisture content on specific heat or more precisely the "thermal absorption" of peanuts warmed by dry heat from an external source. The low correlation in both equations (65) and (66) is not surprising when the variability of individual peanuts is considered. The apparatus and techniques used in this experiment were tested by determining the specific heat of peanut size lumps of crystalline suplhur. Variations were within ± 6.0 % from values in the literature (14).

Equations (67) and (68) are considered to be the best estimates of the true heat capacity or specific heat of peanuts. Equation (67), again, should not be extropolated outside the temperature range used in the tests, 65 to 85 °F.

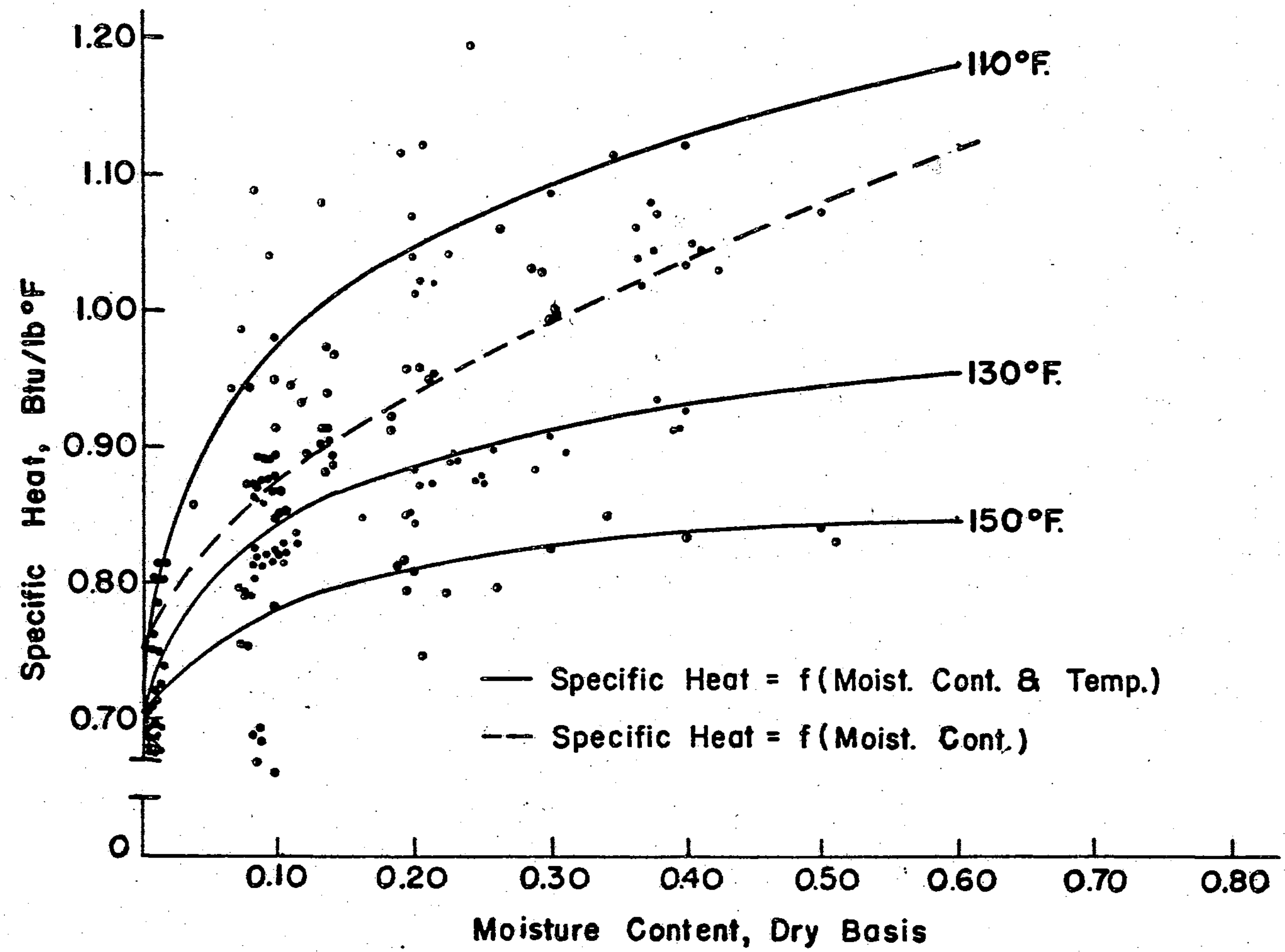

Figure 24. Specific Heat Versus Moisture Content for Spanish Peanuts Determined from Single Peanut Tests with Dry Heat.

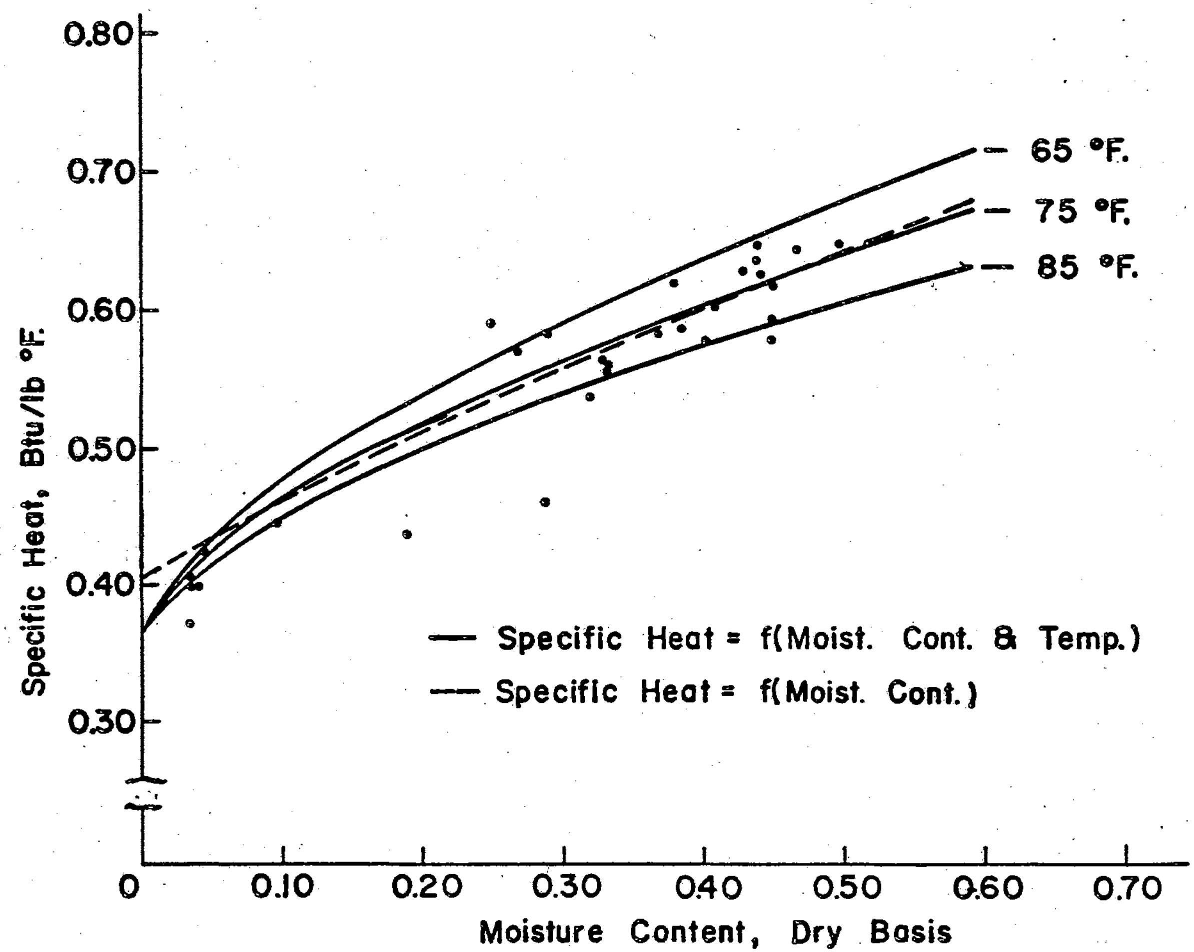

Figure 25. Specific Heat Versus Moisture Content for Spanish Peanuts Determined from Batch Tests by Method of Mixtures.

APPENDIX B

DIMENSIONAL DATA FOR A TYPICAL PEANUT

Dimensions were taken from twelve peanuts and analyzed as described in Chapter IV. The results of this investigation are listed below and in the following Table. All quantities are expressed as average dimensionless ratios, excepting hull thickness. Figures 26 and 27 are longitudinal cross sections drawn from the tablulated data on the following two pages. Figure 26 is the crossection at the suture, (0° in Figure 10), and Figure 27 is at 60° from the suture.

Average outside diameter/L	= 0.423312
Maximum outside diameter/L	= 0.532572
Average inside diameter/L	= 0.330199
Maximum inside diameter/L	= 0.456973
Outside surface area/L^2	= 1.213286
Total volume/L^3	= 0.138678
Kernel cavity volume/L^3	= 0.089898
Average hull thickness	= 0.036888 inches.

where:

L = the length of the peanut.

APPENDIX B

DIMENSIONAL DATA FOR A TYPICAL PEANUT

OUTSIDE HULL RATIOS (R*1000/L)

DEGREES ROTATION FROM VENTRAL SUTURE

D	0	20	40	60	80	100	120	140	160	180	200	220	240	260	280	300	320	340
1	105.	108.	115.	121.	131.	136.	134.	132.	125.	119.	119.	124.	131.	139.	137.	127.	119.	108.
3	196.	200.	206.	212.	212.	212.	206.	200.	199.	195.	196.	203.	213.	220.	221.	215.	208.	196.
5	242.	245.	247.	245.	240.	237.	230.	226.	222.	218.	218.	226.	230.	240.	242.	241.	244.	239.
7	264.	257.	258.	260.	246.	241.	236.	232.	228.	222.	223.	232.	229.	241.	248.	249.	256.	257.
9	260.	252.	249.	247.	239.	236.	242.	232.	234.	230.	227.	231.	230.	233.	237.	247.	245.	248.
11	236.	231.	229.	226.	230.	237.	243.	249.	249.	247.	244.	243.	242.	234.	221.	232.	224.	225.
13	210.	207.	214.	224.	235.	246.	258.	263.	259.	260.	258.	256.	250.	237.	226.	222.	211.	207.
15	208.	208.	219.	221.	242.	258.	263.	266.	266.	263.	259.	257.	253.	243.	232.	233.	220.	205.
17	215.	218.	223.	225.	243.	256.	260.	259.	257.	253.	251.	249.	247.	242.	239.	234.	227.	207.
19	218.	217.	220.	223.	231.	241.	242.	237.	230.	225.	224.	226.	227.	233.	232.	225.	221.	207.
21	202.	199.	197.	197.	198.	196.	203.	191.	183.	182.	180.	184.	187.	189.	191.	193.	200.	196.
23	134.	133.	128.	127.	126.	128.	128.	118.	116.	117.	116.	112.	113.	113.	115.	118.	127.	132.

APPENDIX B (CONTINUED)

INSIDE HULL RATIOS (R*1000/L)

DEGREES ROTATION FROM VENTRAL SUTURE

D	0	20	40	60	80	100	120	140	160	180	200	220	240	260	280	300	320	340
1	54.	56.	58.	66.	68.	70.	67.	67.	65.	64.	67.	69.	72.	74.	75.	96.	64.	56.
3	138.	146.	152.	165.	165.	168.	165.	162.	156.	153.	159.	163.	172.	178.	179.	191.	161.	146.
5	186.	198.	198.	200.	199.	195.	193.	186.	181.	179.	181.	187.	196.	201.	204.	199.	205.	195.
7	213.	215.	212.	212.	204.	198.	199.	193.	186.	185.	185.	192.	199.	204.	206.	210.	213.	210.
9	206.	203.	197.	202.	193.	190.	193.	190.	186.	185.	184.	186.	188.	192.	191.	200.	198.	198.
11	170.	174.	172.	171.	177.	183.	195.	203.	204.	204.	203.	201.	199.	186.	175.	174.	171.	170.
13	153.	154.	159.	166.	177.	191.	208.	220.	222.	219.	218.	215.	202.	188.	175.	168.	157.	150.
15	154.	160.	165.	180.	185.	200.	218.	228.	227.	222.	217.	221.	212.	198.	190.	187.	170.	160.
17	170.	168.	174.	188.	195.	206.	222.	225.	220.	214.	206.	215.	210.	201.	196.	188.	180.	168.
19	170.	170.	176.	192.	191.	200.	214.	204.	193.	188.	189.	192.	193.	192.	191.	183.	176.	171.
21	147.	148.	150.	155.	155.	160.	159.	150.	143.	141.	145.	147.	150.	149.	152.	147.	143.	144.
23	63.	64.	67.	68.	67.	68.	65.	60.	60.	63.	69.	64.	64.	61.	61.	62.	60.	62.

RADII*1000/LENGTH ARE GIVEN FOR 20 DEGREE ROTATIONAL INCREMENTS AROUND LONG AXIS MEASURED FROM THE VENTRAL SUTURE FOR EACH OF 12 CROSS SECTIONS, (SEE FIGURES 10 AND 11).

L = LENGTH OF LONG AXIS OF PEANUT.

D = DISTANCE OF CROSS SECTION FROM BASAL END OF PEANUT IN 24THS OF THE LENGTH OF THE LONG AXIS, (I.E. THE SECOND SECTION IS 3/24 OF THE LENGTH OF THE PEANUT FROM THE BASAL END).

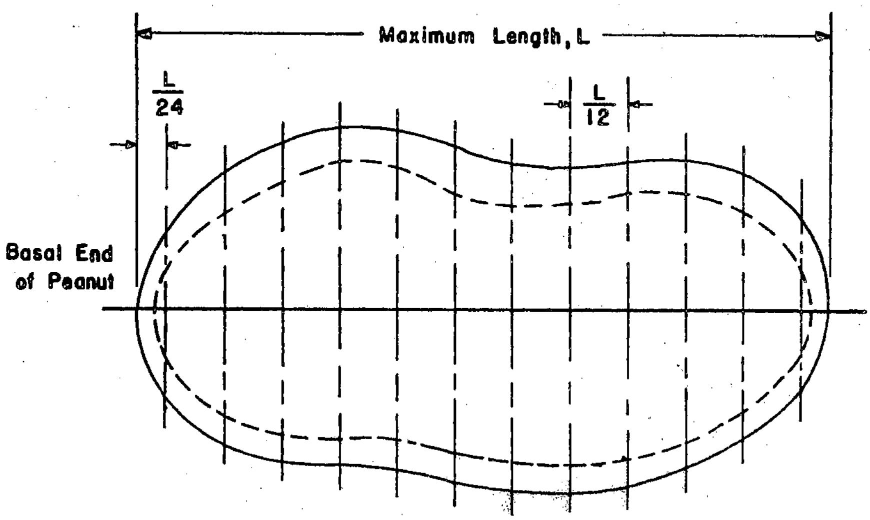

Figure 26. Longitudinal Crossection at the Suture of a Typical Spanish Peanut Drawn from Dimensional Data.

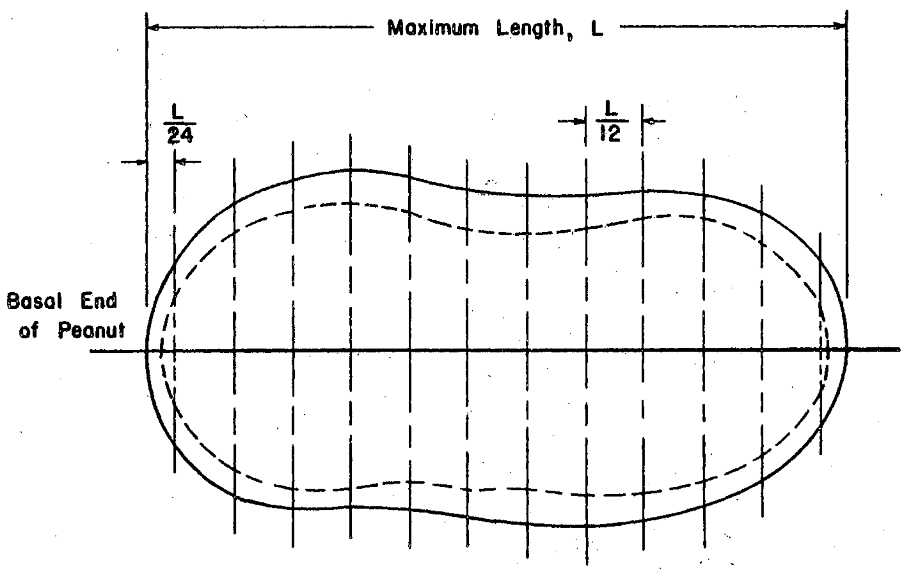

Figure 27. Longitudinal Crossection at 60° from the Suture of a Typical Spanish Peanut Drawn from Dimensional Data.

APPENDIX C

POWER ABSORPTION DATA FOR PEANUTS IN A RADIO-FREQUENCY FIELD OF 13.56 MEGAHERTZ

APPENDIX C

POWER ABSORPTION DATA FOR PEANUTS IN A RADIO-FREQUENCY FIELD OF 13.56 MHZ

RUN	ARR	WW	MC	ΔT	AMPS	VOLTS	D	L	ν	COSθ	σ
1	$\perp$	3.049	0.53	27.7	1.23	202.9	1.656	0.499	0.564	0.358	33.22
2	$\perp$	3.036	0.55	32.7	1.25	204.4	1.656	0.499	0.567	0.415	38.72
3	$\perp$	2.615	0.31	22.8	1.15	247.9	1.656	0.499	0.568	0.210	14.89
4	$\perp$	2.612	0.32	25.6	1.16	244.3	1.656	0.499	0.575	0.238	17.24
5	$\perp$	2.414	0.14	14.1	0.73	254.8	1.656	0.499	0.568	0.173	7.60
6	$\perp$	2.196	0.15	12.1	0.61	253.0	1.656	0.499	0.550	0.170	6.29
7	$\perp$	2.205	0.02	1.9	0.17	241.1	1.656	0.499	0.576	0.094	1.03
8	$\perp$	2.205	0.0	1.6	0.19	242.0	1.656	0.499	0.578	0.068	0.82
9	$\perp$	3.071	0.54	12.7	0.79	125.0	1.656	0.499	0.567	0.420	40.79
10	$\perp$	3.005	0.53	12.7	0.77	126.8	1.656	0.499	0.563	0.417	38.81
11	$\perp$	2.632	0.32	8.2	0.61	149.8	1.656	0.499	0.571	0.239	14.80
12	$\perp$	2.595	0.31	8.2	0.62	150.1	1.656	0.499	0.573	0.230	14.55
13	$\perp$	2.416	0.15	3.9	0.33	150.9	1.656	0.499	0.598	0.182	6.06
14	$\perp$	2.189	0.15	2.8	0.26	149.4	1.656	0.499	0.549	0.154	4.14
15	$\perp$	2.205	0.02	0.7	0.08	144.5	1.656	0.499	0.576	0.115	1.00
16	$\perp$	2.205	0.0	0.5	0.08	144.4	1.656	0.499	0.578	0.096	0.80
17	$\perp$	3.056	0.50	20.0	1.03	190.8	1.656	0.499	0.568	0.326	26.87
18	$\perp$	3.058	0.51	20.1	1.03	188.6	1.656	0.499	0.566	0.332	27.74
19	$\perp$	2.621	0.30	14.8	0.89	223.8	1.656	0.499	0.574	0.193	11.78
20	$\perp$	2.621	0.28	16.4	0.91	222.2	1.656	0.499	0.577	0.211	13.21
21	$\perp$	2.194	0.13	8.3	0.50	226.8	1.656	0.499	0.548	0.159	5.35
22	$\perp$	2.194	0.12	9.4	0.50	226.9	1.656	0.499	0.544	0.178	5.97
23	$\perp$	2.205	0.0	1.9	0.16	218.6	1.656	0.499	0.569	0.109	1.19
24	$\perp$	2.205	0.0	3.0	0.15	217.9	1.656	0.499	0.577	0.178	1.90
25	$\perp$	1.519	0.52	14.2	0.60	87.5	0.828	0.499	0.581	0.562	29.33
26	$\perp$	1.526	0.51	15.6	0.58	88.0	0.828	0.499	0.574	0.630	31.86
27	$\perp$	1.303	0.31	9.9	0.55	117.4	0.828	0.499	0.569	0.273	9.80
28	$\perp$	1.314	0.30	9.1	0.55	120.0	0.828	0.499	0.581	0.248	8.65
29	$\perp$	1.202	0.14	4.2	0.40	134.3	0.828	0.499	0.601	0.128	2.88
30	$\perp$	1.102	0.15	4.3	0.39	134.9	0.828	0.499	0.553	0.130	2.86
31	$\perp$	1.102	0.01	0.8	0.30	141.5	0.828	0.499	0.595	0.028	0.45
32	$\perp$	1.102	0.0	0.9	0.30	141.3	0.828	0.499	0.573	0.032	0.52
33	$\perp$	0.763	0.53	3.2	0.36	44.5	0.531	0.499	0.431	0.306	12.31
34	$\perp$	0.763	0.53	3.6	0.37	45.5	0.531	0.499	0.438	0.330	13.10
35	$\perp$	0.653	0.30	2.5	0.29	55.5	0.531	0.499	0.433	0.217	5.54
36	$\perp$	0.655	0.30	2.6	0.30	55.6	0.531	0.499	0.448	0.215	5.64
37	$\perp$	0.545	0.14	1.3	0.24	64.9	0.531	0.499	0.414	0.105	1.87
38	$\perp$	0.547	0.13	0.6	0.25	64.0	0.531	0.499	0.431	0.049	0.92
39	$\perp$	0.551	0.01	0.3	0.20	69.9	0.531	0.499	0.454	0.028	0.39
40	$\perp$	0.551	0.0	0.4	0.20	70.0	0.531	0.499	0.446	0.033	0.46

APPENDIX C (CONTINUED)

RUN	ARR	WW	MC	ΔT	AMPS	VOLTS	D	L	ν	$\cos\theta$	σ
41	R	2.690	0.52	25.6	1.18	221.0	1.656	0.719*	0.503	0.290	23.63
42	R	2.610	0.52	33.0	1.22	212.1	1.656	0.719	0.493	0.369	32.28
43	R	2.112	0.29	19.4	0.98	254.7	1.656	0.719	0.465	0.177	10.42
44	R	2.176	0.30	18.8	1.01	254.9	1.656	0.719	0.511	0.169	10.25
45	R	1.971	0.13	12.2	0.58	252.0	1.656	0.719	0.494	0.171	5.98
46	R	1.918	0.12	14.9	0.58	251.9	1.656	0.719	0.485	0.204	7.14
47	R	1.894	0.0	2.4	0.18	242.0	1.656	0.719	0.495	0.101	1.16
48	R	1.883	0.0	2.8	0.17	241.6	1.656	0.719	0.496	0.127	1.37
49	∥	0.456	0.52	10.3	0.35	192.3	1.094	0.938	0.526	0.197	10.79
50	∥	0.459	0.52	11.6	0.39	193.1	1.094	0.938	0.533	0.197	12.01
51	∥	0.392	0.30	10.7	0.27	196.6	1.094	0.938	0.518	0.238	9.98
52	∥	0.395	0.30	10.9	0.26	196.7	1.094	0.938	0.526	0.252	10.13
53	∥	0.351	0.13	10.6	0.18	196.9	1.094	0.938	0.532	0.331	9.38
54	∥	0.337	0.13	8.2	0.18	197.0	1.094	0.938	0.521	0.259	7.24
55	∥	0.313	0.01	0.9	0.10	196.0	1.094	0.938	0.486	0.054	0.81
56	∥	0.328	0.01	0.5	0.10	196.1	1.094	0.938	0.523	0.031	0.48

ARR = ARRANGEMENT OF PEANUTS IN HEATING CHAMBER − ⊥ = LONG AXES PERPENDICULAR TO ELECTRIC FIELD, R = RANDOM ORIENTATION, ∥ = LONG AXES PARALELL TO ELECTRIC FIELD.

WW = SAMPLE WET WEIGHT, LBS.

MC = SAMPLE MOISTURE CONTENT, DRY BASIS.

ΔT = CHANGE IN SAMPLE TEMPERATURE DURING RUN, (15 MINUTES), °F.

AMPS = TOTAL CURRENT FLOW, AMPS.

VOLTS = VOLTAGE DROP ACROSS HEATING CHAMBER ELECTRODES.

D = DISTANCE BETWEEN ELECTRODES, IN.

L = PEANUT CHARACTERISTIC LENGTH PARALELL WITH THE ELECTRIC FIELD, IN. * = AVERAGE L FOR RANDOM ORIENTATION.

ν = FRACTION OF HEATING CHAMBER OCCUPPIED BY PEANUTS.

$\cos\theta$ = POWER FACTOR OF SAMPLE.

σ = CONDUCTIVITY OF SAMPLE, MICRO-MHOS PER IN.

APPENDIX D

D-1 DATA FOR RATE OF DRYING PEANUTS WITHOUT RADIO-FREQUENCY HEATING

D-2 DATA FOR RATE OF DRYING PEANUTS WITH RADIO-FREQUENCY HEATING

D-3 Π TERM DATA FOR RATE OF DRYING PEANUTS

Description of Quantities in Appendix D Tables

In Tables D-1 and D-2:

WW1 = Sample wet weight before test, lbs.

WW2 = Sample wet weight after test, lbs.

WD = Sample dry weight, lbs.

VEL = Air flow rate - cubic feet of air per minute per square foot of sample cros sectional area perpendicular to the air flow direction, ft./min.

TE = Entering air temperature, °F.

RH = Relative humidity of entering air, decimal.

TIME = Drying time of test, min.

VDP = Voltage drop across the electrodes of the radio-frequency heating chamber, volts.

ν = Volume of peanuts per volume of radio-frequency heating chamber, decimal.

D = Distances between the electrodes of the radio-frequency heating chamber, in.

AMPS = Total current flow through the circuit to the radio-frequency heating chamber, amps.

For a description of the Π terms in Appendix D-3, see page 38 and Table II, (page 36).

APPENDIX D-1

DATA FOR RATE OF DRYING PEANUTS WITHOUT RADIO-FREQUENCY HEATING

RUN	WW1	WW2	WD	VEL	TE	RH	TIME
1	3.042	2.943	1.980	11.45	65.84	0.484	60.0
2	3.042	2.960	1.980	11.45	66.09	0.633	60.0
3	2.674	2.575	2.007	23.32	64.90	0.476	60.0
4	2.676	2.575	2.007	23.32	65.62	0.522	60.0
5	2.311	2.249	1.960	36.12	66.33	0.472	60.0
6	2.302	2.242	1.960	36.12	65.68	0.509	60.0
7	3.046	2.822	1.980	47.80	66.16	0.468	60.0
8	3.048	2.839	1.980	47.80	66.49	0.506	60.0
9	2.672	2.595	2.007	11.45	66.31	0.481	60.0
10	2.678	2.608	2.007	11.45	64.99	0.516	60.0
11	2.313	2.256	1.960	23.32	65.93	0.476	60.0
12	2.311	2.256	1.960	23.32	64.74	0.533	60.0
13	3.040	2.839	1.980	36.12	66.51	0.483	60.0
14	3.044	2.859	1.980	36.12	65.79	0.520	60.0
15	2.663	2.540	2.007	47.80	65.97	0.482	60.0
16	2.678	2.555	2.007	47.80	66.74	0.512	60.0
17	2.306	2.262	1.960	11.45	65.97	0.498	60.0
18	2.308	2.264	1.960	11.45	66.25	0.564	60.0
19	3.040	2.881	1.980	23.32	66.20	0.498	60.0
20	3.040	2.883	1.980	23.32	66.47	0.544	60.0
21	2.667	2.559	2.007	36.12	66.20	0.495	60.0
22	2.674	2.564	2.007	36.12	66.51	0.533	60.0
23	2.308	2.247	1.960	47.80	66.27	0.494	60.0
24	2.304	2.244	1.960	47.80	66.60	0.526	60.0
25	2.956	2.751	1.993	11.45	93.79	0.147	60.0
26	2.969	2.773	1.993	11.45	93.46	0.150	60.0
27	2.595	2.419	2.007	23.32	91.21	0.153	60.0
28	2.604	2.434	2.007	23.32	91.23	0.160	60.0
29	2.236	2.156	1.945	36.12	94.62	0.169	60.0
30	2.231	2.150	1.945	36.12	94.55	0.180	60.0
31	2.963	2.665	1.993	47.80	92.71	0.187	60.0
32	2.958	2.661	1.993	47.80	94.19	0.181	60.0
33	2.599	2.452	2.007	11.45	93.79	0.159	60.0
34	2.595	2.449	2.007	11.45	94.06	0.184	60.0
35	2.225	2.150	1.945	23.32	91.36	0.177	60.0
36	2.231	2.150	1.945	23.32	91.18	0.172	60.0
37	2.965	2.670	1.993	36.12	94.27	0.165	60.0
38	2.974	2.667	1.993	36.12	94.98	0.150	60.0
39	2.599	2.410	2.007	47.80	94.17	0.160	60.0
40	2.599	2.414	2.007	47.80	93.12	0.163	60.0

APPENDIX D-1 (CONTINUED)

RUN	WW1	WW2	WD	VEL	TE	RH	TIME
41	2.238	2.161	1.945	11.45	93.97	0.159	60.0
42	2.229	2.150	1.945	11.45	94.08	0.170	60.0
43	2.976	2.703	1.993	23.32	91.21	0.168	60.0
44	2.963	2.692	1.993	23.32	91.04	0.220	60.0
45	2.604	2.421	2.007	36.12	94.51	0.145	60.0
46	2.597	2.421	2.007	36.12	94.62	0.192	60.0
47	2.231	2.143	1.945	47.80	93.55	0.140	60.0
48	2.233	2.150	1.945	47.80	95.12	0.200	60.0

APPENDIX D-2

DATA FOR RATE OF DRYING PEANUTS WITH RADIO-FREQUENCY HEATING

RUN	WW1	WW2	WD	VEL	TE	RH	TIME	VDP	ν	D	AMPS
49	3.037	2.786	1.980	11.45	65.70	0.526	60.0	310.4	0.5709	1.656	1.369
50	3.046	2.806	1.980	11.45	63.86	0.544	60.0	300.9	0.5667	1.656	1.354
51	2.678	2.529	2.007	23.32	64.08	0.519	60.0	379.4	0.5746	1.656	1.228
52	2.681	2.526	2.007	23.32	64.62	0.592	60.0	377.9	0.5719	1.656	1.307
53	2.306	2.220	1.960	36.12	65.77	0.464	60.0	394.0	0.5594	1.656	1.027
54	2.308	2.231	1.960	36.12	65.91	0.555	60.0	423.0	0.5582	1.656	1.071
55	3.031	2.778	1.980	47.80	65.41	0.520	60.0	320.0	0.5767	1.656	1.308
56	3.046	2.789	1.980	47.80	66.49	0.553	60.0	321.3	0.5861	1.656	1.356
57	2.672	2.515	2.007	11.45	66.47	0.510	60.0	369.4	0.5746	1.656	1.205
58	2.678	2.513	2.007	11.45	66.51	0.548	60.0	378.5	0.5852	1.656	1.332
59	2.306	2.227	1.960	23.32	64.98	0.510	60.0	403.2	0.5591	1.656	1.072
60	2.311	2.227	1.960	23.32	65.97	0.528	60.0	425.9	0.5625	1.656	1.107
61	3.033	2.762	1.980	36.12	65.59	0.503	60.0	305.0	0.5676	1.656	1.338
62	3.051	2.780	1.980	36.12	66.09	0.597	60.0	301.4	0.5640	1.656	1.341
63	2.672	2.526	2.007	47.80	65.73	0.531	60.0	368.3	0.5703	1.656	1.214
64	2.634	2.507	2.007	47.80	66.34	0.518	60.0	391.5	0.5782	1.656	1.220
65	2.308	2.216	1.960	11.45	66.83	0.522	60.0	420.1	0.5676	1.656	1.114
66	2.311	2.222	1.960	11.45	67.35	0.550	60.0	426.3	0.5634	1.656	1.125
67	3.031	2.773	1.980	23.32	64.76	0.498	60.0	294.9	0.5737	1.656	1.298
68	3.048	2.782	1.980	23.32	66.07	0.553	60.0	309.7	0.5755	1.656	1.347
69	2.676	2.524	2.007	36.12	66.04	0.498	60.0	363.6	0.5649	1.656	1.221
70	2.678	2.529	2.007	36.12	66.06	0.570	60.0	383.5	0.5646	1.656	1.271
71	2.302	2.225	1.960	47.80	64.87	0.460	60.0	420.1	0.5600	1.656	1.045
72	2.311	2.229	1.960	47.80	65.82	0.542	60.0	427.9	0.5570	1.656	1.122

APPENDIX D-2 (CONTINUED)

RUN	WW1	WW2	WD	VEL	TE	RH	TIME	VDP	ν	D	AMPS
73	3.055	2.830	1.980	11.45	66.49	0.541	60.0	214.2	0.5749	1.656	1.110
74	3.031	2.835	1.980	11.45	66.42	0.560	60.0	221.9	0.5740	1.656	1.090
75	2.681	2.535	2.007	23.32	66.15	0.523	60.0	296.8	0.5725	1.656	1.126
76	2.674	2.537	2.007	23.32	66.36	0.551	60.0	292.8	0.5725	1.656	1.108
77	2.308	2.233	1.960	36.12	65.55	0.508	60.0	320.8	0.5537	1.656	0.871
78	2.304	2.233	1.960	36.12	65.62	0.532	60.0	316.7	0.5606	1.656	0.853
79	3.048	2.782	1.980	47.80	66.02	0.474	60.0	243.5	0.5691	1.656	1.188
80	3.042	2.795	1.980	47.80	66.33	0.535	60.0	230.7	0.5737	1.656	1.102
81	2.674	2.544	2.007	11.45	66.09	0.533	60.0	286.7	0.5706	1.656	1.115
82	2.674	2.544	2.007	11.45	65.57	0.542	60.0	286.7	0.5694	1.656	1.118
83	2.308	2.233	1.960	23.32	65.70	0.506	60.0	322.1	0.5615	1.656	0.843
84	2.311	2.240	1.960	23.32	66.49	0.546	60.0	321.1	0.5625	1.656	0.820
85	3.057	2.815	1.980	36.12	65.95	0.515	60.0	229.7	0.5800	1.656	1.175
86	3.044	2.811	1.980	36.12	66.11	0.530	60.0	238.2	0.5682	1.656	1.137
87	2.674	2.533	2.007	47.80	66.45	0.507	60.0	292.5	0.5679	1.656	1.120
88	2.681	2.537	2.007	47.80	66.29	0.543	60.0	292.8	0.5758	1.656	1.077
89	2.308	2.231	1.960	11.45	66.49	0.541	60.0	320.4	0.5606	1.656	0.895
90	2.308	2.236	1.960	11.45	66.56	0.570	60.0	324.3	0.5631	1.656	0.857
91	3.051	2.817	1.980	23.32	65.71	0.526	60.0	231.7	0.5697	1.656	1.114
92	3.029	2.811	1.980	23.32	66.31	0.522	60.0	227.8	0.5706	1.656	1.113
93	2.674	2.529	2.007	36.12	66.45	0.509	60.0	286.6	0.5691	1.656	1.112
94	2.672	2.529	2.007	36.12	66.16	0.505	60.0	293.8	0.5728	1.656	1.120
95	2.306	2.231	1.960	47.80	66.33	0.469	60.0	321.3	0.5597	1.656	0.879
96	2.306	2.231	1.960	47.80	66.25	0.486	60.0	322.2	0.5576	1.656	0.885

APPENDIX D-2 (CONTINUED)

RUN	WW1	WW2	WD	VEL	TE	RH	TIME	VDP	ν	D	AMPS
97	1.524	1.427	0.991	11.45	67.46	0.581	30.0	206.3	0.5715	0.828	1.206
98	1.524	1.436	0.991	11.45	66.58	0.552	30.0	187.6	0.5722	0.828	1.189
99	1.344	1.275	1.004	23.32	65.68	0.549	30.0	286.3	0.5794	0.828	1.130
100	1.346	1.280	1.004	23.32	67.05	0.571	30.0	268.0	0.5903	0.828	1.098
101	1.159	1.121	0.980	36.12	65.05	0.544	30.0	331.5	0.5661	0.828	1.060
102	1.161	1.126	0.980	36.12	65.66	0.589	30.0	328.8	0.5685	0.828	1.005
103	1.524	1.434	0.991	47.80	65.97	0.603	30.0	191.5	0.5812	0.828	1.203
104	1.526	1.421	0.991	47.80	65.91	0.601	30.0	201.4	0.5849	0.828	1.161
105	1.348	1.275	1.004	11.45	69.06	0.594	30.0	270.6	0.5855	0.828	1.177
106	1.344	1.269	1.004	11.45	67.84	0.595	30.0	276.6	0.5946	0.828	1.113
107	1.159	1.121	0.980	23.32	68.97	0.570	30.0	327.2	0.5788	0.828	1.043
108	1.161	1.123	0.980	23.32	67.62	0.596	30.0	328.5	0.5819	0.828	1.012
109	1.522	1.449	0.991	36.12	66.99	0.609	30.0	201.9	0.5873	0.828	1.186
110	1.520	1.432	0.991	36.12	66.49	0.566	30.0	206.1	0.5922	0.828	1.140
111	1.339	1.273	1.004	47.80	67.05	0.531	30.0	278.2	0.5849	0.828	1.128
112	1.344	1.282	1.004	47.80	66.04	0.585	30.0	267.7	0.5758	0.828	1.108
113	1.159	1.115	0.980	11.45	68.25	0.542	30.0	328.2	0.5643	0.828	1.095
114	1.161	1.119	0.980	11.45	68.05	0.569	30.0	334.3	0.5673	0.828	0.997
115	1.524	1.430	0.991	23.32	67.33	0.543	30.0	220.1	0.5946	0.828	1.163
116	1.522	1.434	0.991	23.32	67.26	0.549	30.0	206.0	0.5879	0.828	1.132
117	1.339	1.275	1.004	36.12	65.48	0.506	30.0	273.0	0.5885	0.828	1.122
118	1.344	1.282	1.004	36.12	66.04	0.557	30.0	268.2	0.5831	0.828	1.108
119	1.156	1.121	0.980	47.80	65.61	0.561	30.0	343.4	0.5728	0.828	1.051
120	1.161	1.126	0.980	47.80	66.25	0.549	30.0	328.4	0.5740	0.828	0.998

APPENDIX D-3

π TERM DATA FOR DRYING PEANUTS

RUN	π_1	π_2	π_3	π_4	π_5	π_7
1	0.050	0.459	0.160	16496.6	0.0	3.314
2	0.041	0.448	0.113	16496.6	0.0	3.314
3	0.049	0.257	0.153	33578.1	0.0	3.314
4	0.050	0.256	0.144	33578.1	0.0	3.314
5	0.031	0.104	0.145	52027.6	0.0	3.314
6	0.030	0.097	0.135	52027.6	0.0	3.314
7	0.113	0.463	0.169	68901.4	0.0	3.314
8	0.106	0.462	0.156	68901.4	0.0	3.314
9	0.038	0.255	0.157	16496.6	0.0	3.314
10	0.035	0.257	0.149	16496.6	0.0	3.314
11	0.029	0.105	0.145	33578.1	0.0	3.314
12	0.028	0.099	0.124	33578.1	0.0	3.314
13	0.101	0.459	0.163	52027.6	0.0	3.314
14	0.093	0.459	0.153	52027.6	0.0	3.314
15	0.061	0.251	0.159	68901.4	0.0	3.314
16	0.061	0.258	0.152	68901.4	0.0	3.314
17	0.022	0.099	0.137	16496.6	0.0	3.314
18	0.022	0.096	0.112	16496.6	0.0	3.314
19	0.080	0.458	0.160	33578.1	0.0	3.314
20	0.079	0.455	0.138	33578.1	0.0	3.314
21	0.054	0.252	0.157	52027.6	0.0	3.314
22	0.055	0.253	0.141	52027.6	0.0	3.314
23	0.031	0.100	0.138	68901.4	0.0	3.314
24	0.030	0.096	0.123	68901.4	0.0	3.314
25	0.103	0.443	0.327	16496.6	0.0	3.314
26	0.098	0.448	0.325	16496.6	0.0	3.314
27	0.088	0.251	0.318	33578.1	0.0	3.314
28	0.084	0.254	0.314	33578.1	0.0	3.314
29	0.041	0.105	0.289	52027.6	0.0	3.314
30	0.042	0.101	0.281	52027.6	0.0	3.314
31	0.149	0.438	0.303	68901.4	0.0	3.314
32	0.149	0.438	0.310	68901.4	0.0	3.314
33	0.074	0.252	0.318	16496.6	0.0	3.314
34	0.072	0.246	0.302	16496.6	0.0	3.314
35	0.038	0.098	0.279	33578.1	0.0	3.314
36	0.042	0.103	0.284	33578.1	0.0	3.314
37	0.148	0.443	0.319	52027.6	0.0	3.314
38	0.154	0.406	0.326	52027.6	0.0	3.314
39	0.094	0.252	0.313	68901.4	0.0	3.314
40	0.092	0.252	0.312	68901.4	0.0	3.314

APPENDIX D-3 (CONTINUED)

RUN	π_1	π_2	π_3	π_4	π_5	π_7
41	0.040	0.109	0.294	16496.6	0.0	3.314
42	0.041	0.102	0.288	16496.6	0.0	3.314
43	0.137	0.449	0.314	33578.1	0.0	3.314
44	0.136	0.433	0.286	33578.1	0.0	3.314
45	0.091	0.257	0.325	52027.6	0.0	3.314
46	0.088	0.246	0.296	52027.6	0.0	3.314
47	0.045	0.108	0.304	68901.4	0.0	3.314
48	0.043	0.098	0.269	68901.4	0.0	3.314
49	0.127	0.456	0.146	16496.6	5277.0	3.314
50	0.121	0.458	0.140	16496.6	5177.7	3.314
51	0.075	0.257	0.148	33578.1	3560.3	3.314
52	0.077	0.253	0.119	33578.1	3755.6	3.314
53	0.044	0.101	0.150	52027.6	1602.9	3.314
54	0.039	0.097	0.114	52027.6	1790.4	3.314
55	0.128	0.453	0.148	68901.4	5255.1	3.314
56	0.130	0.458	0.138	68901.4	5635.9	3.314
57	0.078	0.254	0.151	16496.6	3268.0	3.314
58	0.082	0.255	0.146	16496.6	3825.6	3.314
59	0.040	0.099	0.134	33578.1	1734.2	3.314
60	0.043	0.100	0.124	33578.1	1899.4	3.314
61	0.137	0.455	0.157	52027.6	5000.1	3.314
62	0.137	0.458	0.122	52027.6	4978.1	3.314
63	0.072	0.252	0.142	68901.4	3276.5	3.314
64	0.064	0.235	0.147	68901.4	3337.7	3.314
65	0.047	0.099	0.128	16496.6	1885.1	3.314
66	0.045	0.099	0.118	16496.6	1906.7	3.314
67	0.130	0.454	0.158	33578.1	4812.4	3.314
68	0.135	0.459	0.134	33578.1	5285.6	3.314
69	0.076	0.257	0.154	52027.6	3215.1	3.314
70	0.075	0.254	0.130	52027.6	3541.1	3.314
71	0.039	0.099	0.152	68901.4	1732.9	3.314
72	0.042	0.100	0.119	68901.4	1910.9	3.314
73	0.113	0.464	0.141	16496.6	3024.5	3.314
74	0.099	0.450	0.137	16496.6	2991.2	3.314
75	0.072	0.258	0.144	33578.1	2504.6	3.314
76	0.068	0.253	0.132	33578.1	2401.5	3.314
77	0.038	0.100	0.133	52027.6	1104.2	3.314
78	0.036	0.096	0.122	52027.6	1076.7	3.314
79	0.135	0.453	0.165	68901.4	3608.5	3.314
80	0.125	0.457	0.145	68901.4	3178.6	3.314

APPENDIX D-3 (CONTINUED)

RUN	π_1	π_2	π_3	π_4	π_5	π_7
81	0.065	0.254	0.139	16496.6	2363.3	3.314
82	0.065	0.253	0.135	16496.6	2378.8	3.314
83	0.038	0.100	0.134	33578.1	1089.2	3.314
84	0.036	0.099	0.119	33578.1	1050.9	3.314
85	0.122	0.469	0.155	52027.6	3509.5	3.314
86	0.118	0.458	0.145	52027.6	3350.9	3.314
87	0.070	0.256	0.151	68901.4	2389.5	3.314
88	0.071	0.256	0.139	68901.4	2376.2	3.314
89	0.039	0.097	0.120	16496.6	1147.1	3.314
90	0.037	0.095	0.111	16496.6	1110.6	3.314
91	0.118	0.462	0.149	33578.1	3245.4	3.314
92	0.110	0.451	0.151	33578.1	3099.2	3.314
93	0.072	0.256	0.151	52027.6	2334.0	3.314
94	0.071	0.254	0.151	52027.6	2432.9	3.314
95	0.038	0.101	0.151	68901.4	1119.2	3.314
96	0.038	0.105	0.140	68901.4	1124.5	3.314
97	0.098	0.455	0.125	8248.3	3506.2	1.657
98	0.089	0.457	0.139	8248.3	3192.8	1.657
99	0.068	0.258	0.135	16789.0	2735.1	1.657
100	0.066	0.258	0.128	16789.0	2544.8	1.657
101	0.038	0.102	0.119	26013.8	1504.6	1.657
102	0.036	0.101	0.114	26013.8	1416.4	1.657
103	0.091	0.454	0.118	34450.7	3407.7	1.657
104	0.107	0.456	0.118	34450.7	3504.4	1.657
105	0.072	0.259	0.117	8248.3	2686.2	1.657
106	0.075	0.255	0.120	8248.3	2645.2	1.657
107	0.038	0.100	0.113	16789.0	1439.2	1.657
108	0.038	0.100	0.101	16789.0	1443.7	1.657
109	0.091	0.451	0.119	26013.8	3533.2	1.657
110	0.089	0.451	0.138	26013.8	3505.2	1.657
111	0.066	0.254	0.141	34450.7	2614.7	1.657
112	0.061	0.255	0.120	34450.7	2484.3	1.657
113	0.045	0.102	0.136	8248.3	1471.0	1.657
114	0.043	0.102	0.109	8248.3	1372.6	1.657
115	0.096	0.458	0.143	16789.0	3833.9	1.657
116	0.089	0.456	0.141	33578.1	3421.0	1.657
117	0.064	0.256	0.151	26013.8	2631.7	1.657
118	0.061	0.256	0.134	26013.8	2537.9	1.657
119	0.036	0.099	0.113	34450.7	1529.7	1.657
120	0.036	0.104	0.120	34450.7	1411.6	1.657

VITA

Malcolm Edward Wright

Candidate for the Degree of

Doctor of Philosophy

Thesis: HEATING AND DRYING PEANUTS WITH RADIO-FREQUENCY ENERGY

Major Field: Agricultural Engineering

Biographical:

Personal Data: Born in Welsh, Louisiana, March 4, 1934, the son of Ernest and Mabel Wright.

Education: Graduated from Welsh High School Welsh, Louisiana in 1952 as class salutatorian; graduated from the Louisiana State University with a Bachelor of Science in Agricultural Engineering in 1957; received a Master of Science in Agricultural Engineering from the Louisiana State University in 1966; completed the requirements for the Doctor of Philosophy degree at the Oklahoma State University in May, 1970.

Professional Experience: Laboratory Assistant for the Agricultural Engineering Department, Louisiana State University, as an undergraduate; Engineer Officer, United States Marine Corps, 1957 to 1960; Design Engineer, J. I. Case Company, Rockford, Illinois, 1960 to 1961; Research Associate and Instructor, Louisiana State University, 1961 to 1966; Graduate Research Assistant, Oklahoma State University, 1966 to 1969.

Professional and Honorary Societies: Associate Member American Society of Agricultural Engineers, Registered Professional Engineer (Louisiana), Member of Tau Beta Pi, Associate Member of Sigma Xi.